University of Michigan

Moon to Mars eXploration Systems and Habitation (M2M X-Hab) 2026 Academic Innovation Challenge

Project Title:

Lightweight Actuated Tunnels for Crewed Habitation

Recommendations for an Active Pressurized Tunnel System for Functionality on the Martian Surface

University of Michigan Authors:

Nava Abedinpour, Angel Saul Andrade, Elisabeth Bassin, Nicholas DaSilva, Nicholas Demopoulos, Avanti Ganesan, Manan Gupta, Lucas Hamlin, Teagan Hollman, Sophia Kersh, Elizabeth Kooistra, Oleg Korobkov, Vanya Krishna, Olivia Miller, Morgan Taege, Reid Schmaltz, Darren Sheinberg, Katherine Snowdon, Max Swartz, Kaycee Rasch, Lowen Walter, Lukas Zahuranic,

Aasha Patel, Adrian Corrales, Alice Chen, David Jackson Jr., Joban Guron, Joshua Walker, Kalista Kollmansberger, Nguyen Tran, Ronja Stargala, Zachary Gammo

University of Michigan Principal Investigator:

Dr. Nilton Rennó

Project Sponsor (NASA Marshall Space Flight Center):

Dr. Tracie Prater

Table of Contents

List of Figures

List of Tables

1 Introduction

1.1 Project Overview

NASA's Artemis campaign is a critical milestone in long-term human space exploration and it seeks to establish a continuous presence on the lunar surface and prepare for eventual human Mars exploration [1]. Continuous human presence on Mars requires frequent crew transit between localized surface assets, including habitats, rovers, and ascent vehicles. Without anything to facilitate pressurized travel in between these locations, crew movement between locations would demand astronauts conducting Extravehicular Activities (EVAs), an extremely time-consuming and complicated process.

To eliminate the operational burden of repeated EVAs, the Moon to Mars eXploration Systems and Habitation (M2M X-Hab) 2026 Academic Innovation Challenge features a project titled "LATCH: Lightweight Actuated Tunnels for Crewed Habitation" [1]. The project calls for the development of concepts for a "lightweight pressurized tunnel system" which can "provide active positioning and berthing between crewed surface assets on Mars" [1]. The deliverables for the project are full CAD models of the proposed system, as well as a prototype demonstrator of the tunnel and actuation system, along with its control software. The Bioastronautics and Life Support Systems (BLiSS) team at the University of Michigan has worked on this project to develop concepts of a lightweight actuated tunnel adapted to work in a Mars environment.

1.2 Team Breakdown

The LATCH team is organized into three sub-teams: Mechanical, Controls, and Ergonomics. Each is responsible for conducting their own set of literature review, trade studies, tests, and simulations. However, requirement writing, prototype design, and design brainstorming often involved collaboration amongst the teams. The Mechanical subteam is responsible for structural design, actuation mechanisms, and material selection. The Controls subteam develops the system architecture, embedded software, and sensor integration. The Ergonomics subteam evaluates human factors, crew interaction, and accessibility requirements.

The LATCH team is composed of over thirty active members from eleven different science and engineering disciplines, ranging from first-year undergraduate students to graduate students. All members collaborate with one another to ensure each subsystem is physically capable, controllable, and ergonomically safe for crew operations.

2 Problem Definition

2.1 Travel in Space Applications

Extravehicular activity (EVA) is the process of crew members venturing out of a pressurized environment into some uncontrolled space environment. The current process of traveling between habitats in space applications is a lengthy, time-consuming, and risk-inducing process. The entire process, including hours of preparation (pre-breathing oxygen), suiting up, airlock depressurization, and post-EVA cleanup, constitutes a full day's work for the crew. For transit from one crewed location to another, this becomes extremely problematic when the journey itself could take minutes if the locations were connected with a controlled environment.

Additionally, without a pressurized connection between an initial surface asset and the MAV, an EVA suit must be used when entering the MAV. Not only are EVAs time-consuming, but the suits themselves are very massive. This becomes problematic when an astronaut is ascending from the Martian surface using the MAV, as the additional EVA suit adds weight. In fact, preliminary analysis of the Mars Ascent Vehicle (MAV) used by crew to get to and from the Martian surface shows that each EVA suit requires 560 kilograms more propellant than an Intra-Vehicular Activity (IVA) suit would require [2]. Additionally, EVA suits take up volume in the launch vehicle, roughly the size of a person. This would require a larger cabin size, which in turn would require more propellant mass.

This paper seeks to characterize an active tunnel system as a means of replacing EVAs in crew transportation between surface elements, including the MAV, surface habitats, and rovers. Although an active tunnel system takes up mass and volume for launch and landing, it must only be transported to the Martian surface once, and could be reused for multiple missions.

2.2 Customer Needs

The stakeholder objectives are broadly encapsulated by the four top-level requirements listed in Table 1.

ID	Requirement Description
R1	The LATCH mission shall provide the capability to transport at least two crew members wearing IVA suits, carrying cargo, between surface elements on Mars.
R2	The LATCH mission shall provide a controlled, habitable environment between surface elements that is isolated from the Martian environment.
R3	The LATCH mission shall last throughout the duration of crewed surface operations on Mars.
R4	The LATCH mission shall reduce power consumption, mass, and crew operation time compared to previous mission designs.

Table 1: Top-level System Requirements

Further system requirements are outlined in Appendix A.

2.3 Scoping the Project

To create a project that could be executed by a team of about 30 members, mostly undergraduate students, during the 2025-26 academic school year with limited resources available, certain key

aspects of the system and its handling were deemed out of scope. In order to reduce the complexity of our project, the team decided to focus solely on the Martian environment, as opposed to the lunar and Martian environments. The decision to focus on the Martian environment instead of the lunar environment was made with scalability in mind; since Martian gravity is greater, it was assumed that any structure that could hold up in Martian gravity has a high likelihood of being able to hold up in lunar gravity as well.

Due to limited knowledge of NASA habitat specifications, we opted to treat the connection between the tunnel and the habitats as a "black box". Fire suppression and atmospheric regulation were both considered out of scope for this project due to the complicated nature of their control. The method of pressurizing the tunnel was also considered out of scope, but choosing materials that could withstand the pressure difference was not. To limit the use cases of the system, we chose to rule out assembly, storage, transport, system maintenance, and alternate egress options in the event of a failure as out of scope. Finally, thermal and radiation shielding were not verified beyond literature review in an attempt to limit the technical complexity of the project.

3 System Design

3.1 Concept of Operations

A high-level Concept of Operations can be seen in Figure 1. Crew member and Ground interaction with our proposed tunnel is designed for minimal communication. The tunnel, installed on the outside of the hatch of the habitat in which the crew members reside, starts in its compressed state. A crew member within the habitat can select the destination of the tunnel (another surface element) by using the User Interface (UI). Ground has the ability to perform the same operations as a crew member.

Once the destination is selected, the tunnel begins to extend toward the destination hatch. The extension is driven by motors and actuators, which also grant the tunnel the ability to make fine adjustments to its path. Sensor data and ground monitoring provide feedback for alignment and trajectory correction. Once the tunnel is fully extended, and both ends are secured to a hatch, a slow and controlled pressurization process begins with breathable air. Sensors will detect leakage, contamination, or system faults during this process. The UI will allow for crew members and Ground to view the status of the tunnel at any point.

Once pressurized, and after confirmation from Ground and sensor data that the environment is safe, the tunnel is used to allow for as many as two crew members to walk through the tunnel carrying cargo. Sensor data will be used to monitor system status and crew safety during traversal. In the case of an emergency, systems such as lights, handrails, and other needed support systems will help ensure the crew members safely reach the other side of the tunnel.

To reposition or stow the tunnel, depressurization and retraction are performed. This process is similar to deployment, except that air is removed from the tunnel and the structure is compressed.

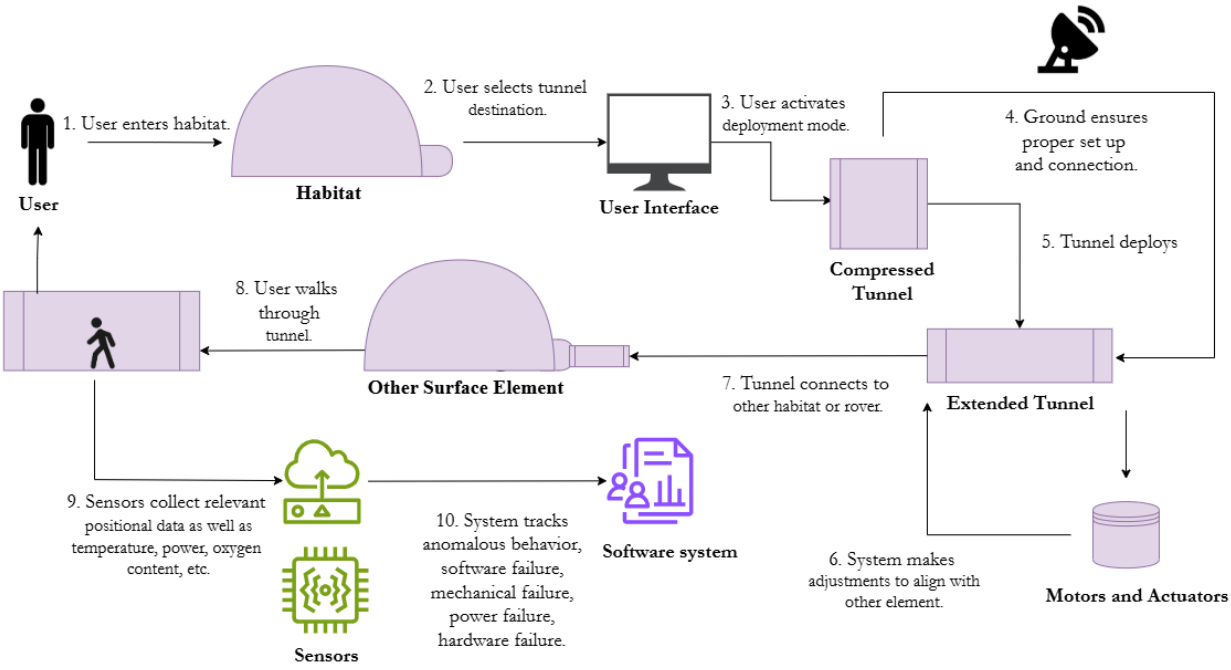

Figure 1: System Concept of Operations

3.2 Proposed System Architecture

3.2.1 Structural Design

The structural design for the tunnel is broken into multiple components: the shell, the rings, the handrails, the scissor mechanism, the rollout floor, the treads, and the positioning mechanisms, which include the linear actuators, suspension, and end positioning mechanism. This section will describe the flight system design in more detail. Figure 2 shows the full tunnel system and its components.

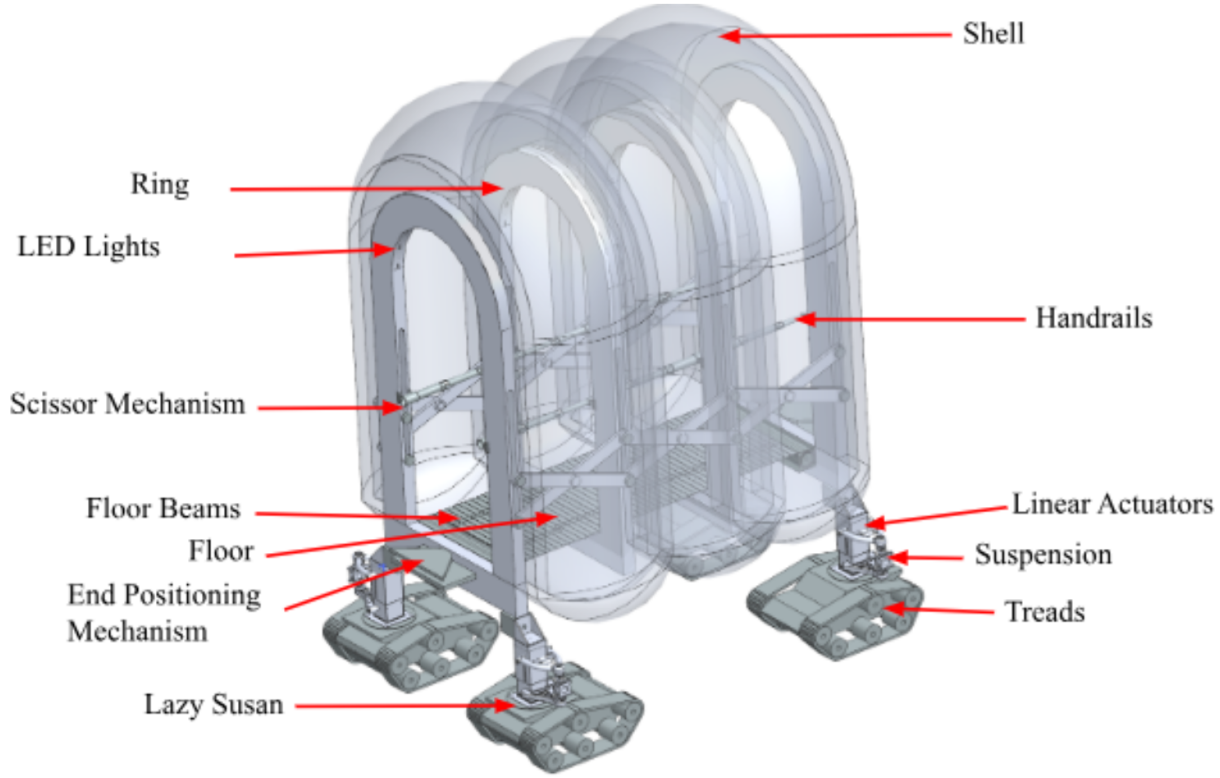

Figure 2: Full Tunnel Extended with Components Labeled

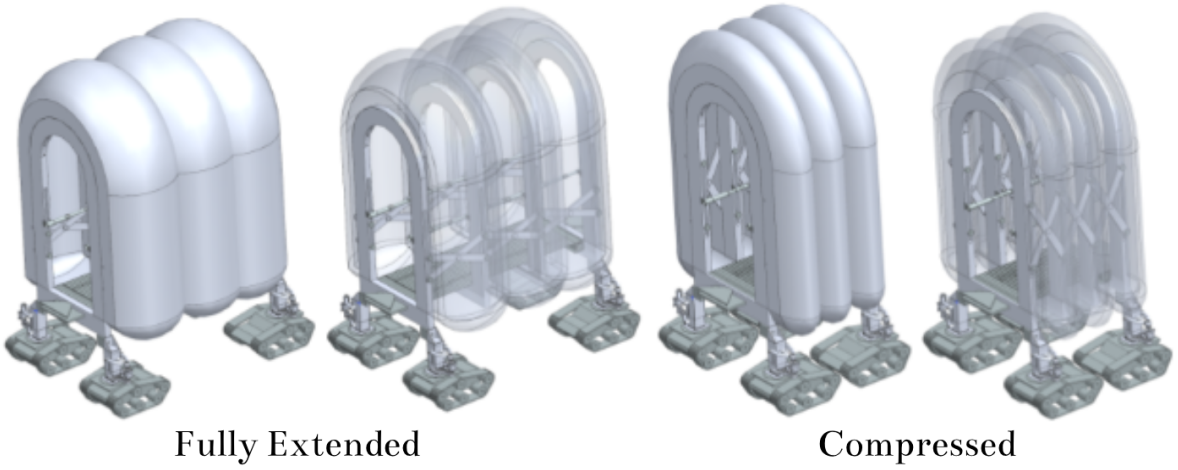

Figure 3: Full Tunnel Model with Different Views

Our design allows for the tunnel to be extended and used at a variety of different lengths, allowing the system to be used in many different scenarios. Additionally, this means that the distance between connection points does not have to be exact. Figure 4 shows the dimensions of the tunnel design at the fully extended and fully compressed lengths. It is important to note that the 1 meter width of the tunnel is measured between the tunnel handrails.

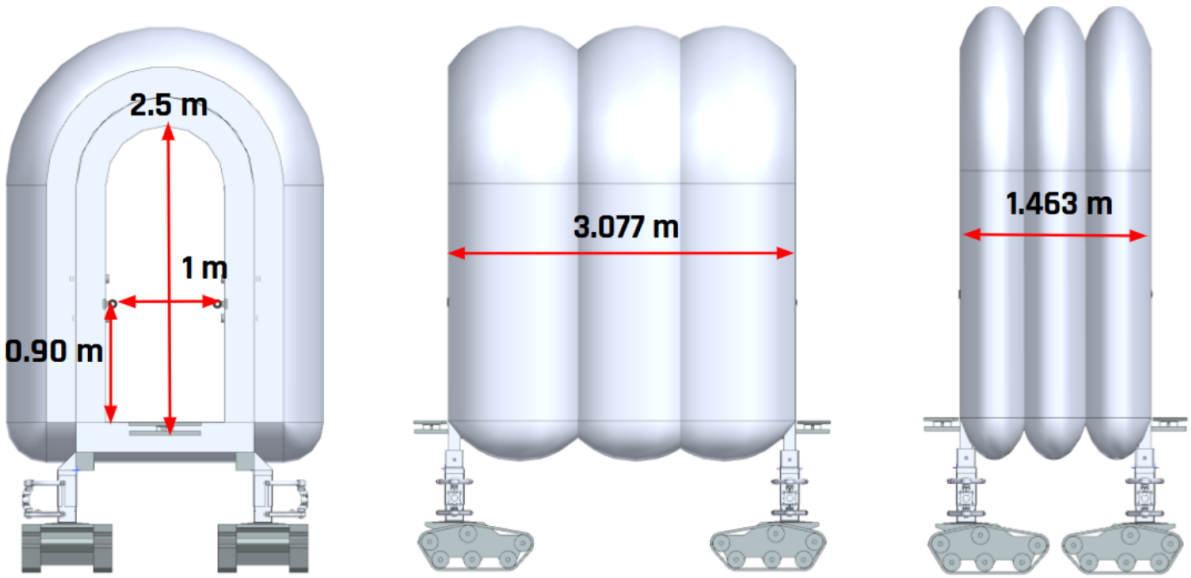

Figure 4: Tunnel with Major Dimensions

Based on our overall system geometry and material selections, a mass estimate seen below was developed for the full tunnel system. The system was broken down into its primary components including the rings, softgoods shell, walkway, passive extension components, active extension and positioning mechanisms (treads, elevation change, end positioning mechanism/rotator platform, and suspension) and electronics. Due to the still limited fidelity of the CAD model, some compo-

nent masses were estimated using hand calculations.

The mass of the rings was estimated by calculating the volume using the height to be 3 meters, the thickness of the ring as 0.25 meters, and the inner radius of 0.5 meters. Then using the density of Aluminum 6061 the mass of a fully solid ring was estimated as 504 kg. This value was reduced by 80% to about 101 kg to account for a mass-saving design such as an inner lattice structure and hollowing while maintaining structural integrity.

The softgoods shell mass was estimated similarly by finding the volume using a fabric width of 3.2 meters and a height of 12 meters and then using the density of Vectran fabric to get the estimate of one layer being 96 kg. To incorporate redundancy, the softgoods shell will have two layers, making the estimated mass total 192 kg. An extra 23 kg was added to account for the silicone coating, giving a shell mass of 215 kg.

For the floor, titanium was the selected material. The initial CAD mass estimate was 261 kg, but this assumed the floor beams were solid. To estimate the floor mass with non-solid beams, the mass was reduced by 25% to get 195 kg. Similarly, the combined mass for the tread, linear actuator, and suspension was reduced from the solid CAD estimate of 433 kg to 105 kg, using a similar reduction approach.

The masses for the rotator platform, scissor mechanism, and handrails were taken from CAD estimations and can be found in Table 2. The electronics mass was approximated based on representative component values.

Summing all of the subsystem contributions results in a total estimated system mass of 1530 kg.

Component	**Unit Mass (kg)**	**Quantity**	**Total Mass (kg)**
Ring	101	4	404
Softgoods Shell	215	1	215
Floor	195	1	195
Rotator Platform	23	2	46
Tread + Linear Actuator + Suspension	105	4	420
Scissor Mechanism + Handrail	65	2	130
Electronics + Misc.	120	1	120
Total	-	-	1,530

Table 2: Full System Mass Estimation

3.2.2 Frame

The purpose of the frame is to provide the main shape and structure of the tunnel. Most of the other subsystems, like the handrails and floor, are connected directly to these rings. Therefore, the rings provide a significant amount of the tunnel's structure and strength.

Key Design Decisions Aluminum 6061 lattice or hollowed-out, arch-shaped rings were chosen for the frame. Aluminum 6061 was selected for the material based on cost, strength, and ease of manufacturing. The shape of the ring was chosen to be an arch based on literature review. The number of rings and how far to space them was determined based on the compression ratio and the handrail dimensions.

Flight Design In flight, the structural rings would be made of 6061 aluminum. In the tunnel, rings are placed one meter apart. Figure 5 shows the extended version of the tunnel, showing the softgoods shell while opaque and transparent to showcase the inner features of the tunnel. Figure 6 shows a single ring of the frame, with slots carved out to accommodate the connection of passive elements of the tunnel.

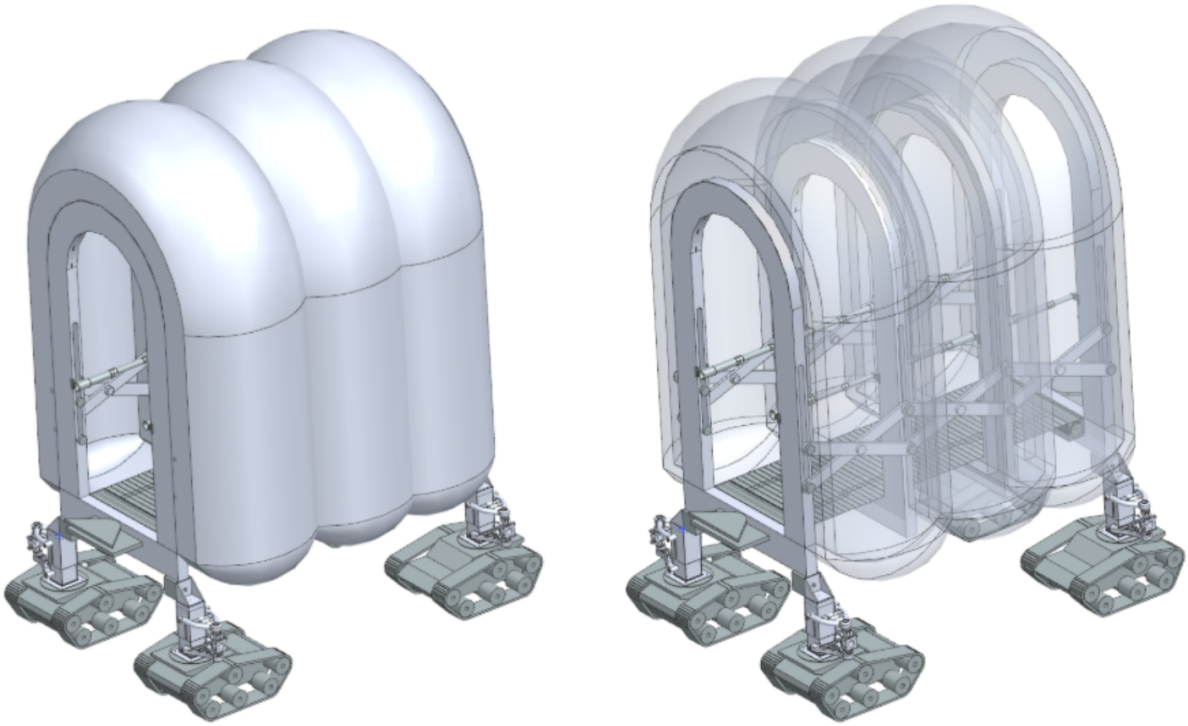

Figure 5: Full Tunnel Extended

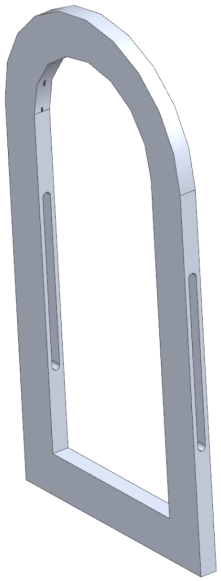

Figure 6: Structural Ring

3.2.3 Shell

The purpose of the softgoods shell is to provide a barrier between the interior of the tunnel and the Martian environment. The shell allows the interior of the tunnel to be pressurized, and also provides thermal, dust, and radiation protection for the system and the crew within. There are two layers of the softgoods shell to allow for redundancy in case of damage. Even small tears or punctures could cause a loss of pressure and therefore pose an extreme hazard to the astronauts inside. The softgoods shell is connected to the structural rings within the tunnel.

Key Design Decisions and Flight Design In flight, the softgoods shell would be made from 2 layers of Vectran fabric with a silicone coating. This was based on NASA softgoods studies that found the Vectran was able to withstand the pressure forces it would endure during multiple pressurization cycles. The silicone coating is meant to help with the radiation the system would endure on Mars.

3.2.4 Passive Extension

The purpose of the passive extension subsystem is to maintain the alignment and equal spacing between the rings of the tunnel during the extension and compression. The passive extension subsystem is responsive to the active extension subsystem, and ensures the rings are aligned, spaced, and stabilized properly at various tunnel lengths. The subsystem should be flexible enough to account for incremental adjustments to the desired length of extension. It is also important that the shell not interfere with the flooring or handrails during extension and contraction, while allowing for a minimum 2:1 extension ratio.

Key Design Decisions Scissor mechanisms were identified as the optimal extension mechanism. However, there were lots of other decisions, including the number of scissor links, the length

of each scissor, the material of each scissor link, and the orientation/position of each scissor mechanism, that were crucial to come to.

Different types of scissor mechanisms were deliberated, as some offer advantages to different kinds of loads and movement patterns. Some scissor mechanisms offered curvilinear motion, which could be advantageous in some instances and may have removed the need for as many degrees of freedom on the ends. However, such a scissor mechanism is complicated and under-researched. The standard scissor mechanism was chosen due to its simplicity, repairability, and known performance capabilities.

Placement and number of scissor mechanisms were further critical design decisions. We decided to use only one cross between each ring in order to minimize the number of joints and separate parts, and thus the complexity of the system.

Flight Design The scissor mechanism is made up of two aluminum arms, which are secured with a loose pin to allow for fluid movement. Each end of the aluminum arms is secured using a pin to a slit on the outside of a ring to allow the arms to move up and down as the tunnel extends and contracts. The pins would be tightened just enough to ensure the arms do not fall while stationary, but loose enough that the arms can move while the tunnel is in motion. Figure 7 showcases this mechanism.

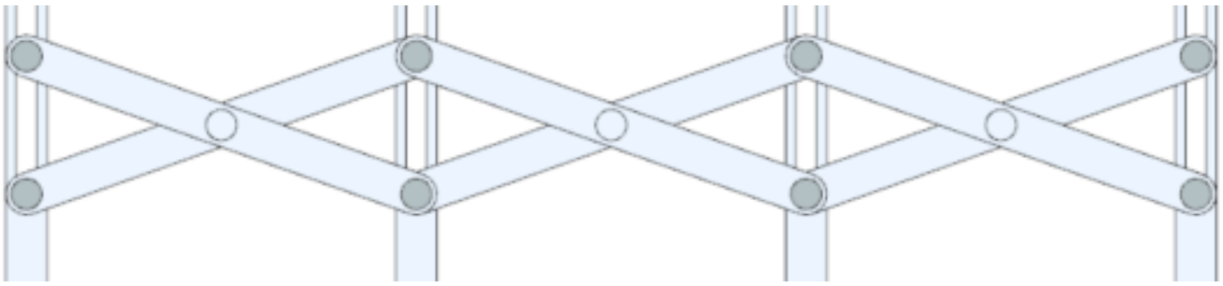

Figure 7: Passive Extension Mechanism

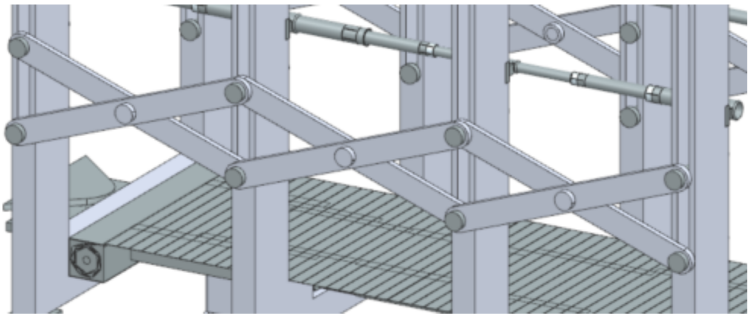

Figure 8: Isometric View of Passive Extension Mechanism

3.2.5 Handrail

The purpose of the subsystem is to provide individuals traveling through the tunnel with adequate physical stability. This support is provided through two horizontally spanning handrails

placed on either side of the tunnel that can be held onto while traversing the tunnel. The handrails are meant to be used as a fallback mechanism or as a means of supplementing stable walking patterns.

Key Design Decisions Three possible handrail systems were explored: horizontal telescoping, vertical, and using a tensioned rope system.

After deciding to pursue the horizontal telescoping tubes, we were able to address other issues that are necessary for designing handrails. One of these concerns was the diameter of the handrail. For the outermost tube, the ergonomics team concluded that a width of about 1.75 inches was the upper diameter possible to still allow for ease of use and comfort. From here, the diameter of the tubes was decreased by a quarter of an inch, meaning the smallest tube would have a diameter of 1.25 inches, which was found to also be within the range of allowable handrail diameters.

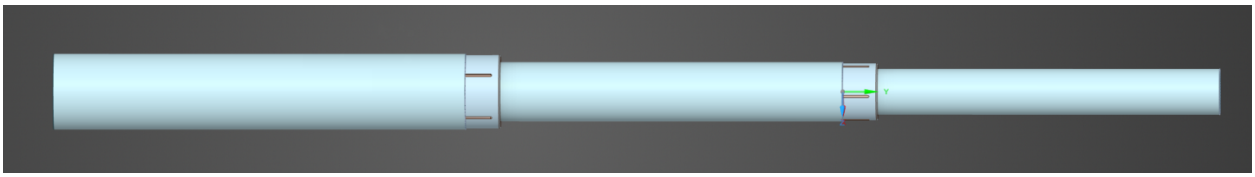

Figure 9: Telescoping Handrail

Flight Design Figure 9 shows a side-on view of the telescoping handrails. Linear ball-bearings are affixed to the ends of the larger sections to allow for smooth extension and retraction of the handrails. Each set of rings has its own pair of handrails spanning between them. Each handrail is affixed to the sides of each ring, providing structural support and minimizing deflection as much as possible. The handrails were chosen to have a 1:3 extension ratio, so that the largest and smallest sections would each remain within the allowable range of handrail diameters. This extension ratio, with the two smaller handrails contracting into the bigger one, results in a compact 0.33 meter long handrail when the tunnel is fully contracted. This handrail design would also be feasibly attached to the rings, which was a large part of choosing it compared to the tensioned rope design. Additionally, horizontal handrails would provide support to astronauts along the whole tunnel compared to the vertical handrails which would only be usable when the astronaut is a reasonable length from each ring.

3.2.6 Active Extension

The drive subsystem acts as the actuator that drives the extension, retraction, and connection of the tunnel between habitats and other structures. Without a drive system capable of supporting the tunnel and providing enough power, the tunnel would not be able to satisfy its main objective.

Key Design Decisions A lot went into the decision to use motorized treads as the active extension component for our system. First we had to decide what part of the tunnel we wanted to be active and passive. We decided the simplest for design and mass purposes was to make the wheels motorized instead of any part of the structure, like the scissor mechanism.

The system had to be able to go over rough terrain easily, so multiple wheel designs were considered including caster wheels, NASA's NiTiNOL wheel, and the rocker-bogie design used for

Mars rovers. In the end, the tread design was chosen because it was the simplest and lightest option to motorize, as each tread would only need one motor for the motion we needed, unlike the rocker-bogie which would need a motor on at least two out of three of the wheels.

Other design decisions included how many wheels and where the wheels would be placed. To make the system as simple as possible while still adding structural support where needed, we decided to have two wheels on each end of the tunnel. At first there were worries that this could mean the middle of the tunnel could sag, but after running simulations, it was found that under the expected loads, this was not a big concern.

Flight Design In flight, there would be two tread systems acting in parallel near both ends of the tunnel, adding up to four total treads. These treads need to be designed strong and large enough to support the weight of the tunnel, but also small enough to permit the tunnel to collapse to its smallest size.

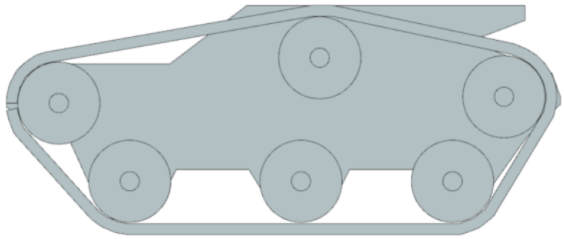

Figure 10: Side View of Tread

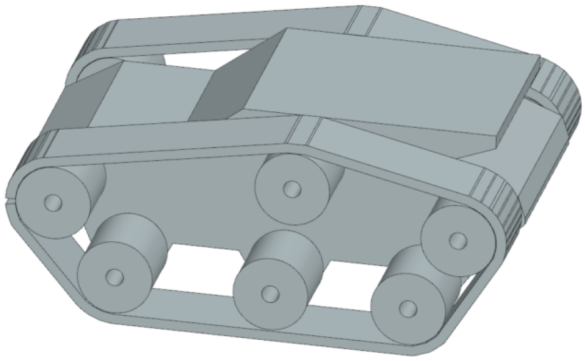

Figure 11: Isometric View of Tread

Not shown in the CAD views on top of each tread is a passive rotating platform that allows the drive system to rotate and change the direction of the tunnel without breaking off from the system.

3.2.7 End Positioning

The purpose of this subsystem is to provide the ability to concentrically align the docking terminal (end) of the tunnel with the hatch of the target surface element. This subsystem also

ensures that the base (start) of the tunnel stays securely connected and airtight at the starting habitat, even while the main body of the tunnel tilts up, down, or sideways during deployment. The end positioning mechanism will provide fine, small scale adjustments as well as additional degrees of freedom to help fulfill our motion requirements.

Key Design Decisions Previously proposed tunnel designs utilize a Stewart platform for end alignment and fine positioning of the system. However, we decided against the use of a Stewart platform due to its complexity, the mass it would add to our system, and its power requirements. Due to the temperature range on the Martian surface, using hydraulics was not a feasible option. In order to design a new system, we used Stewart platforms as an inspiration, as well as jet bridges. This resulted in a design that allows for isolated motion in both the y and z directions, allowing for side-to-side as well as up-and-down motion. This ensures that the end of our tunnel remains parallel to the hatch of the connecting surface element.

Flight Design This design consists of a platform on top of a large bearing. On the underside, a motor drive shaft is connected to the platform to allow for yaw-movement of the platform. At the point nearest the tunnel walkway and at the end of this aforementioned platform there is an axis and hinge at which the platform, bearing, and motor drive shaft system can pivot. This pivoting is driven by a large servo motor that allows for the system to have variable change in pitch. The far end of this platform can then connect with another habitat. Since no hatch design was provided, we left this part of the design open ended. The idea would be to have a short extending platform with a hatch attached to the end of it. This hatch would then connect the tunnel to the hatch of the surface element. It should be noted that it is not expected that the servo motor being used would be required to be strong enough to hold the torque created by a large segment of the tunnel. We assume that the end of this platform would be securely connected to the habitat, thus taking on the load while the crew is walking through it.

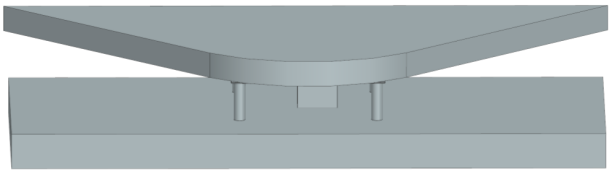

Figure 12: End Positioning Mechanism CAD

3.2.8 Elevation Change

The elevation change subsystem provides the tunnel with the ability to adjust its vertical height so it can mate with habitats at varying heights. It translates the tunnel vertically, holds that height and does so with required the precision to achieve a proper connection at the interface.

Key Design Decisions A lead screw mechanism was selected as the optimal method for vertical translation due to the harsh constraints of the Martian surface. The highly abrasive nature of Martian dust requires moving parts to be strictly isolated; a lead screw architecture naturally lends itself to enclosed, tube-in-tube designs that shield the internal workings from environmental contamination.

Furthermore, this design perfectly balances the tunnel's large mass with the operational timeline. Since the overall time constraint for the docking procedure was 30 minutes, the speed of the elevation change is not a primary limiting factor. This time allowance permitted the selection of a fine-pitch lead screw, which maximizes mechanical advantage and provides the high lifting force necessary to elevate the system's massive payload without requiring excessively large motors.

Flight Design In the Mars-surface system, each elevation change unit consists of four main elements arranged in a nested vertical stack; an outer aluminum extrusion, inner aluminum extrusion, a lead screw, and a stepper motor.

The outer aluminum extrusion is a hollow square tube rigidly mounted to the tunnel chassis. This acts as the structural housing and linear guide for the translating inner tube.

The inner aluminum extrusion is a smaller hollow square tube that slides vertically inside the outer tube. Its top end is the mounting interface for the suspension subsystem below it, while its bottom end carries the lead screw follower nut internally. The square cross-section of both tubes provides anti-rotation without requiring a separate keyway or guide rail.

The lead screw is oriented vertically, rotationally fixed at its lower end to the motor output. Threads into a follower nut mounted inside the inner extrusion. Rotation of the screw drives vertical translation of the inner tube.

The stepper motor is mounted at the base of the outer extrusion assembly, coupled directly to the lead screw. Sized to provide the required lifting torque at the screw pitch and expected load, with a holding capability consistent with the self-locking behavior of the screw.

The outer extrusion mounts to the tunnel structure via ball joints. The inner extrusion's upper end provides the mounting interface to the suspension stack. The lead screw and motor are fully enclosed within the outer extrusion, shielded from direct dust exposure by the extrusion walls and by the nested tube-in-tube geometry.

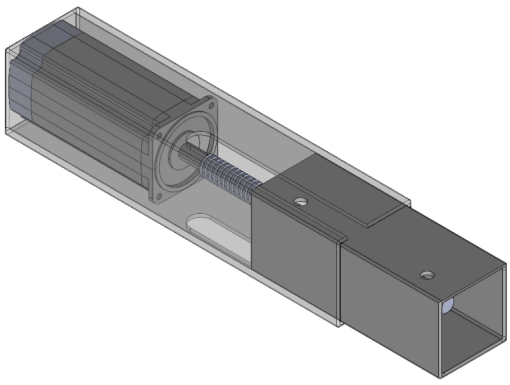

Figure 13: Elevation Change

3.2.9 Suspension

The suspension system connects the treads to the tunnel structure and allows for consistent ground contact as the tunnel moves over uneven terrain, absorbs vibrations, and traverses incline. The entire tread-suspension assembly is connected to the linear actuators which provide the vertical height adjustment capability.

Key Design Decisions Multiple designs were considered for the suspension; double wishbone, MacPherson strut, and trailing arm. In the end the double wishbone suspension was chosen based on what was easiest to adapt to the tunnel design, while still maintaining full functionality.

Flight Design In flight, the suspension system connects the tread assembly to the tunnel structure via a four-part stack; a modified double wishbone, a spiral torsion spring, a linear actuator, and a silicone dust cover.

The modified double wishbone has upper and lower control arms that pivot from mounting points on the actuator output bracket and terminate at a knuckle that carries the tread assembly. This portion handles vertical terrain variation (rocks and dips), allowing each tread to move independently without disturbing the tunnel structure.

The spiral torsion spring is mounted at the knuckle, oriented so its axis of rotation is aligned with the direction of travel. This permits the tread to pitch nose-up or nose-down relative to the suspension, keeping the full tread footprint in contact with the ground when transitioning onto or off of an incline, rather than riding on the leading or trailing edge alone.

The linear actuator is retained from the original design, now acting on the suspension assembly as a whole rather than on the tread directly. Provides commanded vertical height adjustment so the tunnel can mate with habitat or airlock interfaces at different heights.

The silicone dust cover consists of flexible silicone boots enclosing all moving joints in the suspension stack to protect them from Martian dust. Dust mitigation is critical because Martian regolith is abrasive and electrostatically charged, and would significantly reduce lifetime of the system.

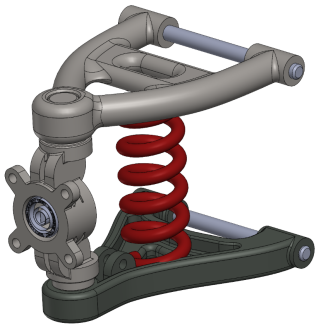

Figure 14: Suspension

3.2.10 Walkway

The purpose of the walkway is to allow the crew to pass easily through the tunnel at any extension length. It is important that the walkway is lightweight and compact, while still being strong enough to withstand the weight of the crew and cargo traversing over it.

Key Design Decisions There were four designs considered: a stacked pull out floor, a tunnel design similar to a jetbridge with a nested pullout structure, a cascading elevator mechanism, and a roll out floor. Ultimately a roll out, sushi-mat-like floor was chosen due to its adaptability for different tunnel lengths. The roll out floor is rolled similar to a two ended scroll, with a rolled up section housed in a box on each end of the tunnel. The system includes a tensioned mechanism to ensure the floor does not shift while an astronaut is passing through. The material chosen was Titanium Ti-6Al-4V due to the loads the floor would endure.

Flight Design In flight, the walkway is made up of numerous thin sheets of titanium connected by two hinge joints on either side. The hinge is used to connect each slat to the next slat in a chain-like fashion. The hinge joints allow the slats to be rolled up and stored in a box at each end of the tunnel. During extension, the system is passively from either side. Once the system has reached full extension, it is held taut using a torsional spring so that as the tunnel compresses, the floor roll will roll tightly back in.

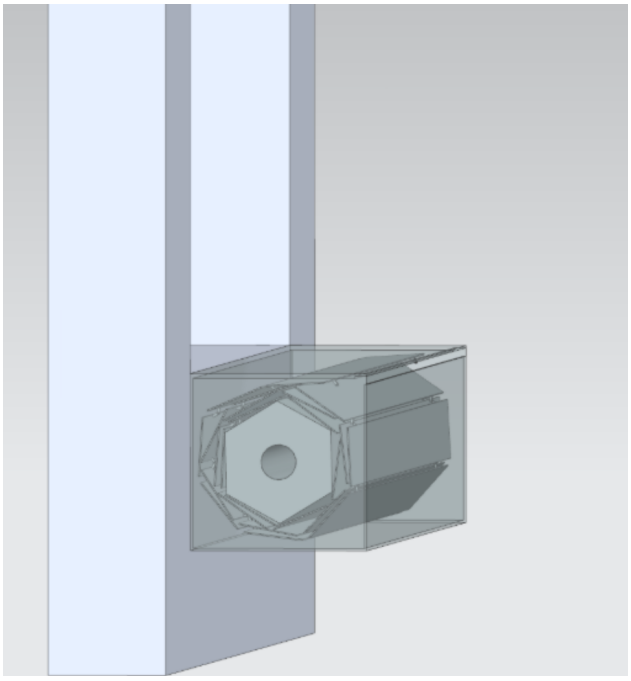

Figure 15: Rolled-Up Floor

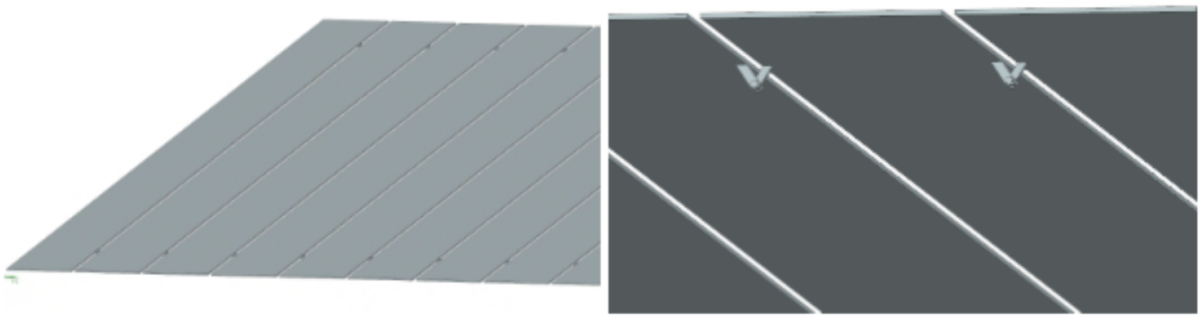

Figure 16: Close-Up View of the Floor Slats and Joints

In order to support the crew members passing through the tunnel, the system includes titanium floor beams that run along the length of the tunnel. The supporting floor beams are telescoping and extend by sliding on a rail system. Using this system, the tops of all of the telescoping floor beams stay aligned and provide a flat surface for the floor slats to lay on. Similar to the floor rolls, there are two sets of telescoping beams placed on either side of the tunnel so that both will extend and contract with the tunnel.

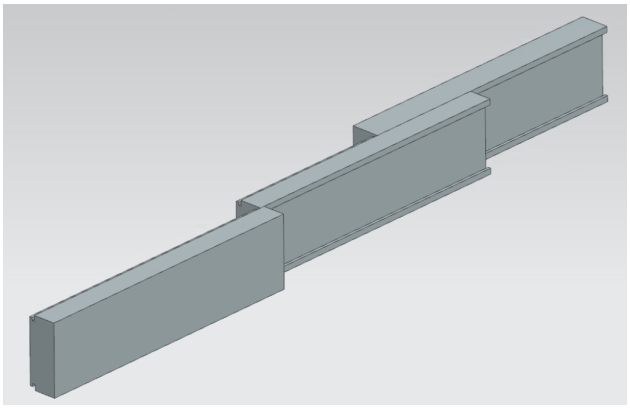

Figure 17: Telescoping Floor Beams

3.2.11 User Interface

In flight, the user interface (UI) system will serve as a critical component of the overall system. Through the UI, astronauts will be able to directly interact with the tunnel's mechanical systems, including controlling tunnel movement and aligning it with the hatches of other habitats. The UI will also enable communication with astronauts in connected habitats to coordinate the logistics of attaching and detaching the tunnel. In addition, it will display essential system metrics and notify users of any tunnel-related alarms or warnings. Astronauts will be able to monitor the tunnel through three distinct display sections: one providing a diagrammatic system-level view of the tunnel's position, and the other two showing interior and exterior camera feeds.

Key Design Decisions At a minimum, the flight UI design should satisfy the following objectives: provide a graphical user interface, allow the crew to control and monitor the docking process, support emergency communication between crew members, and display the internal conditions within the tunnel. The UI should also effectively integrate alert functions so that the crew can

quickly identify any issues that require adjustment or repair for the tunnel to operate as intended.

Flight Design In a realistic configuration, the display screens should be located just outside the tunnel within the connected habitats, allowing astronauts to access the UI before beginning tunnel setup or docking operations. The system should include a clear multi-tiered alarm structure, enabling users to view, distinguish, and respond to alarms based on their severity. Consistent with the trade study findings, the alarm system should use a conventional color-coding scheme to improve crew familiarity, reduce training requirements, and support faster decision-making.

Finally, the design would include video feeds with connected audio controls to help monitor the tunnel interior and alert users to potential hazards during an emergency. This feature would improve situational awareness by providing real-time information about tunnel conditions and reflects another key design decision identified through the trade studies.

3.3 Physical Interfaces

Overall, the ergonomic systems demonstrate strong alignment between design intent, trade study decisions, and experimental validation. The combination of usability testing and full-system verification provides consistent evidence that the selected design parameters support safe, efficient, and intuitive human interaction.

A key takeaway is that handrail design is the dominant factor in user stability and recovery. Across both the Optimal Handrail Height and Fall Recovery tests, a 90 cm handrail height emerged as the most universally effective solution. It balanced accessibility, minimized torso flexion, and reduced perceived exertion while still accommodating a wide anthropometric range. Importantly, this height performed well independent of user stature, suggesting robustness for a diverse astronaut population. The convergence of subjective comfort data and objective performance metrics strengthens confidence in this selection.

The inclination testing further validates overall system usability, showing that slopes up to 15°do not introduce meaningful safety risks. The absence of slips or stumbles, combined with low instability ratings, indicates that the integration of flooring, handrails, and spatial layout effectively mitigates balance challenges. The fact that participants voluntarily used handrails in over half the trials reinforces their intuitive placement and functional value as a stability aid.

From a systems perspective, the interdependency between subsystems (handrails, flooring, geometry) is a major success point. The walkway width, tunnel shape, and material choices all contribute to a cohesive environment that supports both mobility and cargo transfer without compromising safety. The rounded rectangular geometry, in particular, enhances usable space and simplifies integration of ergonomic features.

In an idealized version of the tunnel, we suggest implementing the following:

- Rounded rectangular tunnel shape with internal height of 2.01 meters.
- Roll-out walkway with a width of 1 meter.
- Handrails implemented 90 cm above the walkway with clearance of at least 5.715 cm from the wall.

- Handrails with telescoping sections of diameters 1.25 in, 1.5 in, and 1.75 in.

3.4 Controls

High Level Controls The High Level Controls (HLC) subsystem serves as the decision-making layer of the LATCH tunnel system. Its purpose is to interpret user input, through the graphical user interface (GUI), and sensor data (wheel encoders, IMU, camera), to determine the movements of the wheels and elevation mechanisms that best accomplish the given request.

The subsystem primarily accomplishes five main tasks: perception, localization, autonomous navigation, state machine behavior, and fault monitoring. These tasks are achieved through three main pathways:

- **GUI Pathway:** The user inputs their desired HAB location into the designated GUI, which starts the state machine and HLC process for that specific request. Intermittently, feedback will be provided back to the GUI, and a final result will be displayed, ending the process for that request
- **Sensing Pathway:** The sensing pathway determines where the tunnel is located at the present moment and what constraints may be around the tunnel. LiDAR data (implemented in software but not hardware), camera/AprilTag pose, and odometry data from the wheel encoders and IMU are published to their associated ROS2 topics. AprilTag and odometry information are fused using an Extended Kalman Filter (EKF) to provide a continuous estimated pose
- **Drive Pathway:** The state machine and navigation node receives the total system context, including the fused pose, goal information, and any detected fault or obstacle condition. It determines the next commanded motion and sends drive commands through a motor interface. This pathway closes the loop between high-level autonomy and the lower-level actuator controllers.

In an idealized flight-ready system, High Level Controls runs on the top-level compute node and coordinates autonomous extension, alignment, and docking. Low-level controllers remain responsible for motor control, encoder acquisition, and actuator safety logic, while the HLC software determines which motion should occur and when it is safe to proceed.

- **Inputs:** User goal information from the GUI; camera-based AprilTag pose; wheel encoder and IMU odometry; LiDAR obstacle detection; motor status and fault feedback.
- **Localization:** An EKF produces a fused relative pose estimate by combining intermittent AprilTag updates with continuous odometry data.
- **Autonomous Control:** A state machine moves the system through deployment, coarse motion, fine motion, and docking based on the estimated pose and system status.
- **Safety and Operator Control:** Any fault condition may interrupt the nominal autonomous sequence and enter a fault state. A teleoperation mode is available for operator override or manual recovery.
- **Outputs:** Motion goals and drive commands are sent to the embedded control layer through the motor interface. Current state, pose, progress, and fault information are returned to the GUI for crew awareness.

3.4.1 HLC Architecture

The HLC architecture separates sensing, operator interaction, localization, decision making, and actuation into clearly defined pathways. The central context node receives obstacle status, AprilTag pose, odometry, fused pose, and GUI goal information. State machine/navigation reads this context and issues drive commands through the MotorInterface. This separation allows individual nodes to be replaced or tested without rewriting the entire autonomy system.

GUI Pathway: The user sends a desired goal over a serial interface, which starts a ROS2 action request. A central context node receives this goal, as well as other state information, and starts the state machine and autonomous drive pathway. Throughout the process, status updates and fault monitoring information are sent for user viewing. Upon completion, a result is sent back to the GUI, ending the ROS2 action for this user request.

Sensing Pathway: The purpose of the sensing pathway is to understand where the tunnel is located at the present moment, and ideally, what is around the tunnel. LiDAR (implemented in software but not hardware), camera, and odometry data from the CAN bridge is published to their associated ROS2 topics. The AprilTag and odometry topics are then merged using an Extended Kalman Filter to provide a fused pose.

Drive Pathway: The state machine receives all tunnel state information from the context node. Based on the goal pose and its current pose, it will determine what commands to send to the motors. The drive pathway will first issue commands to turn the tunnel about its yaw, then elevate it, and finally move it forwards, until the goal position is reached.

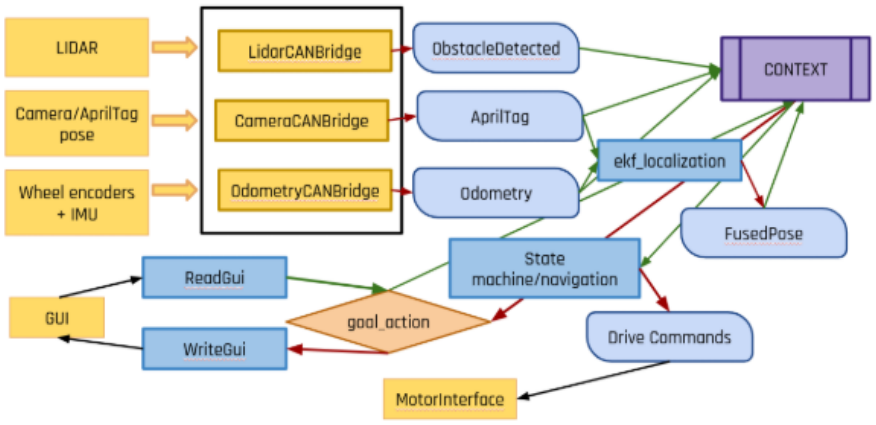

Figure 18: HLC Architecture

3.4.2 State Machine + Navigation

The state machine determines which portion of autonomous operation is active and prevents commands from being issued without the required context. There are two nominal processes: the nominal autonomous process and the nominal teleoperated process.

The nominal autonomous process begins in Idle, which waits for a goal request from the GUI. Upon receiving one, it progresses through DeployInit, which initializes states and conducts preliminary checks. CoarseMotion is used to move the tunnel toward the connecting surface element until an AprilTag is in sight, whereas FineMotion is used for more accurate alignment, until docking

structure is within a tolerable range. When within this range, Dock is an empty skeleton node to provide software extensibility whenever a docking mechanism is provided, and Complete finishes the ROS2 action by sending a successful response back to the GUI.

The nominal teleoperated process is a far simpler sequence that allows an operator to directly control the system, and transition to complete when successfully navigated within range to the provided docking interface.

The fault process provides a defined response when sensor feedback, state information, or actuator status indicates that nominal operation should not continue. The system can therefore stop or transfer control rather than continuing an unsafe motion sequence.

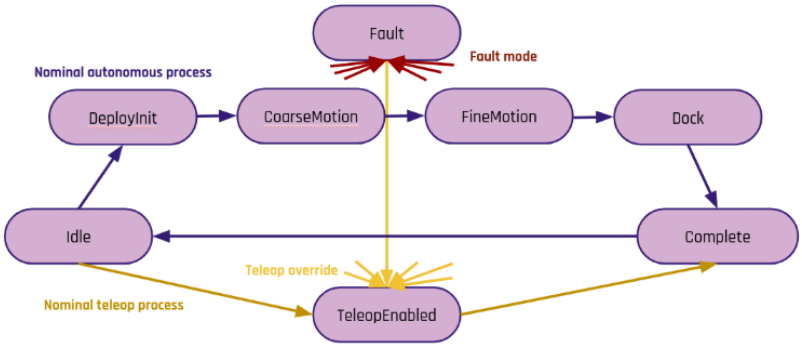

Figure 19: HLC Architecture

3.4.3 Localization

Localization estimates the relative position and orientation of the tunnel with respect to the connecting surface element. The selected approach is a custom Extended Kalman Filter that fuses AprilTag pose with odometry data. The AprilTag measurement provides a direct relative pose correction when the tag is visible. Encoder and IMU odometry provide continued motion information when the tag is partially obscured or leaves the camera frame.

The EKF structure consists of a prediction step based on the motion model and odometry input, followed by an update step when AprilTag measurements are available. This method was selected instead of AprilTag-only localization because the system cannot assume a tag remains continuously visible during extension and alignment. It was selected instead of dead reckoning alone because odometry error accumulates over motion and would not independently correct the final docking alignment.

3.4.4 Gazebo + RViz Simulation

A Gazebo and RViz simulation was developed to exercise the entire HLC software stack before a complete physical tunnel system was available. Gazebo represents the moving tunnel geometry and commanded motion, while RViz provides visualization of the model state and ROS2 data. To keep the test environment consistent, the Gazebo and RViz demo kinematics were separated into a C++ MobileKinematicsModel.

Python scripts were used to test full goal-reaching autonomy. At the joint-state level, pitch cases of 0 deg, 5 deg, 10 deg, and 15 deg were exercised. At the simulation level, yaw cases of 0 deg, 5 deg, 10 deg, and 15 deg were exercised. Each test checks the intermediate software levels needed to support autonomous alignment, including joint states, odometry, and current state information.

3.4.5 Controls System Architecture

The Power subsystem serves as the electrical backbone of the LATCH tunnel system. Its purpose is to receive 120V habitat power, convert it to the multiple voltage levels required by the tunnel's actuators, controllers, and sensors, and distribute that power reliably across both the left and right tunnel control systems.

The subsystem must power three primary mechanical functions — drive, elevation, and end-positioning — along with the perception and peripherals systems that enable autonomous operation. Specifically, this encompasses:

- **8 NEMA 23 Brushless DC Motors** (drive system) operating on a 24V rail, providing the torque necessary to traverse Martian surface inclines of up to 15°
- **8 NEMA 23 Stepper Motors** (elevation system) operating on a 48V rail, driving lead screw actuation to accommodate up to 0.4 m of relative elevation difference between habitats
- **NEMA 23 stepper and pancake motors** (end-positioning mechanism) enabling the docking platform to align with and latch onto the connecting surface element
- **Perception hardware** (Raspberry Pis and cameras) and embedded controllers (STM32 Nucleo boards) operating on 5V rails, along with CAN bus, IMUs, and limit switches on 5/12V rails

The total system power draw is 2,434.4 W, well within the RE-05 requirement of 6,000 W maximum. A central DC-DC converter steps the 120V habitat input down to 48V, 24V, 12V, and 5V distribution buses feeding both the left and right tunnel control assemblies in a mirrored architecture, with a Jetson compute module serving as the top-level controller coordinating all subsystems.

Component	Rail	Power	Current
8 NEMA 23 Stepper Motors	48 V	1,075.2 W W	22.4 A
8 Brushless DC Motors	24 V	1,344 W	56 A
2 Raspberry Pis + Cameras	5 V	8 W	1.6 A
8 STM32 Nucleos	5 V	0.01 W	0.002 A
CAN + IMUs + Misc	5/12 V	7.2 W	0.6 A
Total	-	2,434.4 W	-

Table 3: Power Budget

In a flight-ready scenario, the LATCH Controls and Power Architecture operates as a highly redundant, tightly integrated, and environmentally shielded network. The architecture is broadly divided into two primary networks: the Power Distribution Architecture and the Controls/Communication Architecture.

3.4.6 Power Distribution Architecture

As determined in the trade studies, the system must conform to the habitat's maximum power limits (RE-05.02). The idealized power architecture utilizes a central Primary DC-DC Converter to step down the habitat's raw 120V supply into four isolated, highly regulated continuous voltage buses, strategically routed to minimize voltage drop across the tunnel's span:

- **48V Bus:** Dedicated entirely to the Elevation subsystem. This high-voltage rail supplies the four NEMA 23 Stepper motors, providing the necessary overhead to deliver 17.1 kN of combined lifting force.
- **24V Bus:** Dedicated to the Drive and Platform (End-Positioning) subsystems, as well as the electromagnetic power-off brakes. This rail supplies the eight NEMA 23 BLDC drive motors and the precision pancake/stepper platform motors.
- **12V Bus:** Utilized for mid-level sensors and intermediate control hardware.
- **5V Bus:** Dedicated to logic-level components, including the primary compute nodes, perception modules (cameras), and system peripherals.

3.4.7 Controls and Communication Architecture

To manage the complex sequence of extending, aligning, and latching within a 30-minute window (RE-02), the system employs a hierarchical, multi-node control topology.

- **Top-Level Compute (Autonomy and Vision):** An overarching compute node (represented by an NVIDIA Jetson in the trade studies) serves as the "brain" of the LATCH system. In an idealized flight scenario, this would be a radiation-hardened equivalent capable of high-speed tensor operations. It is responsible for processing incoming video feeds from the perception system, calculating trajectory and alignment offsets for the docking interface, and orchestrating the high-level state machine.
- **Distributed Control Nodes:** To minimize wiring mass and signal degradation, low-level execution is decentralized into two mirrored hubs: **Left Tunnel Controls** and **Right Tunnel Controls.** Each hub contains dedicated embedded microcontrollers (flight-rated STM32 equivalents) that handle the real-time execution of the Drive, Platform, and Elevation mechanical sub-assemblies.
- **Intra-System Communication:** The central Jetson, the Left/Right tunnel controllers, and the Peripherals all communicate via a centralized CAN (Controller Area Network) bus. As established in the trade studies, CAN bus provides the differential signaling necessary to maintain perfect data integrity and reject the severe electromagnetic interference (EMI) generated by the 24V and 48V motor operations.
- **Perception and Peripherals:** Independent perception nodes feed spatial awareness data into the Left and Right control hubs, ensuring the system can perform real-time localized adjustments as the tunnel accommodates angular differences of up to 15°(CT-08.02) and height differences up to 0.4 meters (CT-08.01). The hardware selection of this system can be any high resolution camera that would be able to sense April Tags with accuracy as they are the main means of localization of the LATCH system.

4 System Prototyping

4.1 Prototype Breakdown

This section details the prototype versions adapted from the flight systems that were built and used for testing. These prototypes were used to test design decisions, characterize the system, and conduct functionality testing. Table 4 breaks down the different prototypes and what they were used for. Table 5 shows the key differences between the idealized design and the structural prototype. The following sections will go into more detail based on the subsystem.

Prototype Name	**Description and Reasoning**	**Included Design Elements**
Top-Half	A full scale model that consists of the passive elements that make up the structure of the tunnel. Used as a proof of concept and visualization of the design. Helps verify the extension requirements.	Rings, scissor mechanism, handrails, tarp
Bottom-Half	A scaled down model that consists of the active elements that extend, contract, raise, and position the tunnel. This prototype was scaled down by a factor of three. Helps verify the mobility requirements.	Treads, linear actuators, lazy susan, end positioning mechanism
User Interface	Demonstrates the UI and its functionality. Helps verify the UI requirements.	User Interface
Walkway	A semi-full scale model that demonstrates the functionality and size of the walkway. The model is full scale in terms of width but not length. Used for ergonomic testing.	Floor

Table 4: System Prototype Breakdown

Component	Flight Design	Prototype Design
Handrails	Telescoping handrails constructed out of aluminum 6061, attached via linear ball bearing, attached at each ring	Segmented cardboard tubing with built-in telescoping mechanism, attached only on the end rings
Ring Structure	Rectangle topped with a half-circle, made out of aluminum 6061	Rectangular frame made out of 80/20, attached to separate ring platforms
Scissor Mechanism	Accordion lattice made from aluminum 6061, sectioned between each ring	Made from modified steel extendable gates, using only the extension mechanism
Shell	2 layers of Vectran Fabric with Silicone coating	Plastic tarp attached between every two rings, large enough to be taut during extension
End Positioning Mechanism	Pancake motor mounted with large bearing to allow for yaw change; stepper motor mounted along axis for variable pitch	Servo motor mounted on top of lazy-susan bearing for yaw; two servo systems mounted along axis for pitch
Elevation	Lead screw stepper motors extending metal poles, holding the frame.	Lead screw stepper motor, extending cardboard tube material.
Drive	Two tank tread drive systems operating with two motors each, attached to bearing systems to allow drives to turn separately from the tunnel.	Two tank tread drive systems operating with high torque motors, attached to lazy-susan bearing systems to allow for drives to swivel.

Table 5: Idealized vs. Prototype Similarities and Differences

4.2 Top-Half Prototype

4.2.1 Frame

In the Top-Half prototype, the tunnel rings are constructed using bars of 80/20 aluminum profiles, connected together with L-brackets. This forms a rectangle shape instead of a rounded shape used in the flight system. These rings are not designed to bear any significant load; instead, they demonstrate the full size of the tunnel, and allow for mounting of the other passive elements of the system.

Figure 20: Top-Half Prototype

4.2.2 Shell

The prototype softgoods shell is constructed from a plastic tarp that is connected to every other ring via nuts and screws. The tarp on the top of the rings is connected to the tarps on the side rings using zipties. The tarp was included in the prototype design for functionality testing, to ensure during extension and compression the tarp does not interfere with the scissor mechanism.

4.2.3 Passive Extension

In order to fulfill the requirements we had for the motion of the scissor mechanism, we purchased an expandable gate. To fit the extendable portion of the gate onto the frame, we modified it by removing the outer supports that the extendable portion was set between. Then, we unscrewed each strip of steel and attached them back together to have the scissor fit the correct extension length. These scissor mechanisms were then bracketed onto the frame, tightened at the top and left loosened at the bottom to allow them to extend and retract without falling off of the frame itself. Figure 21 shows the mechanism fully compressed on the left and at full system extension on the right.

Figure 21: Passive Extension Prototype

4.2.4 Handrail

While trying to keep consistent with the flight system, our final prototype design was tweaked to account for issues and limitations we discovered as we built the structure. One of the main changes is the material we used. Instead of using aluminum tubing, which proved hard to attach to the frame, we opted to use pre-made cardboard telescoping tubes. With this switch of material, we also decided against installing a linear ball bearing, as the sliding mechanism of the cardboard tubes would not fit with the linear ball bearing we had. The handrails are directly secured to the outer two rings and are able to extend and retract to the full extension and retraction of the scissor mechanisms between the rings.

Figure 22: Prototype Handrails Compressed and Extended

4.3 Bottom-Half Prototype

4.3.1 Active Extension

All components of the drive system's structure came from the YonPhsy Robot Track Tanked Car Chassis [3] and shown in Figure 23 below.

Figure or Table containing sensitive information, or possible unauthorized copyright information has been removed.

Figure 23: Drive Prototype

The prototype design was made to represent the functions of the idealized tunnel on a smaller scale. We worked under the assumption that the ideal system would have the load bearing capabilities to hold the system up and power the actuation. The prototype still uses the tank tread system with two sets of two treads working in parallel with each other. This allows us to still test the efficiency of the treads, as well as see if the treads can endure obstacles in the manner we expect them to.

Component	**Flight System**	**Prototype**
Tread	Bulky and powerful enough to support the weight of the tunnel and drive the actuation.	Light and maneuverable while still durable enough to undergo verification testing.
Body	Strong enough to bear the weight of the system with enough mounting room for the ideal electrical components.	Light and small but still enough size to hold the treads and all electrical components.

Table 6: Drive Flight Design vs Prototype Differences

The main component of the drive in the prototype is the tread system. These treads are held in place by 5 gears, which keep the treads tight. The prototype treads are roughly three times smaller than the flight treads.

In this prototype, the main body differs from the flight system in many aspects, so much as the system could not be used for load testing. The main body used came from the same drive system purchased from YonPhsy, so the system itself was able to be easily assembled.

This prototype system integrates into other systems by supporting the linear actuators as well as the end positioning platform mechanism. The different systems are not constrained by each other, so testing is all independent. For the sake of validation, having integrated systems helped to see how wiring and attachment could work for all the different systems.

For the flight system, the drive system would have the same functionality as the prototype with the addition of being the actuator that drives the extension and retraction of the tunnel as a whole.

To achieve this, the tractive force generated between the drive treads and the Martian regolith must overcome the static and dynamic inertia of the tunnel's total mass. Consequently, the flight-model treads must be scaled dimensionally so they may overcome any obstacles on the Martian surface and coupled to a high-torque motor assembly to prevent stalling, ensuring continuous operational reliability under Martian environmental constraints.

4.3.2 End Positioning

The end positioning mechanism prototype is a scaled down version of our flight design with some slight changes. The platform of our end positioning mechanism is connected by two servo motors holding it in place on either side; these servo motors account for the pitch change. On the platform we have placed a lazy Susan bearing and in the middle there is another servo motor. This motor attaches directly to the secondary platform, which is also attached to the lazy Susan via spacers. The secondary platform thus has the ability to change in yaw. Additionally, our prototype is mounted in a way to give our basic function of being able to move up and down, as well as side to side.

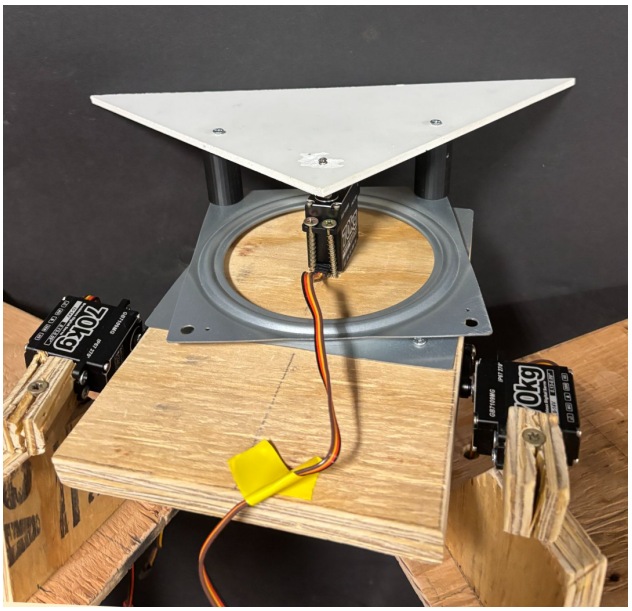

Figure 24: End Positioning Mechanism Prototype

Figure 24 displays the connection between our end position mechanism platform and the secondary platform that moves with variable yaw. You can see in the center our servo motor in the middle, our lazy Susan connected to the upper secondary platform, which is also held up by our cylindrical spacers.

4.3.3 Elevation Change

The material for the shell of the linear actuator was made from the extra cardboard tubes ordered for the handrails. This tube was cut to fit the motorized lead and attached in such a way that allowed for vertical actuation when run with the power of NEMA 17 stepper motors. The bolt itself had a lead of 2 millimeters and a length of 330 millimeters, allowing us to demonstrate the lead screw based elevation change effectively.

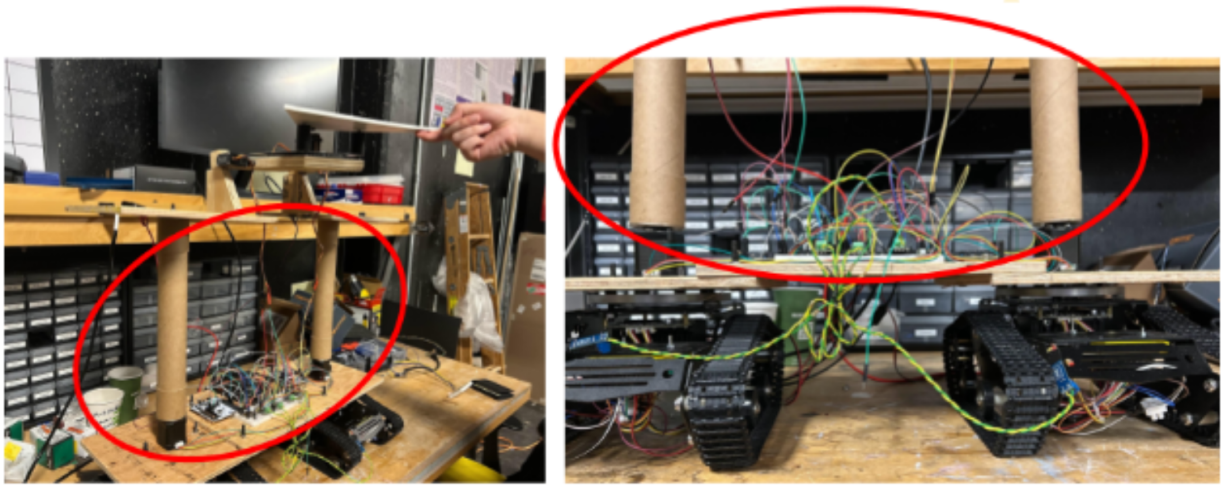

Figure 25: Bottom-Half Prototype Showing Linear Actuators

4.3.4 Suspension

No prototype of the suspension subsystem was fabricated. The suspension architecture was developed late in the project timeline in response to the identification of a terrain-compliance failure mode in the original rigid tread-to-actuator mount. Because of this timing, the team was unable to complete detailed component sizing, fabrication, or integration with the full-system prototype before the end of the project cycle.

4.3.5 System Architecture

As seen in the figure above, the bottom-half prototype consists of two tread assemblies with lead screw elevation systems mounted on top, extending with cardboard tube columns. There is a servo-actuated end positioning platform as well. Four different STM32 Nucleo board act as the embedded microcontrollers, communicating over a CAN bus through CAN transceivers. The STM32 boards were a trade decision, communicating alongside miscellaneous peripherals, preserving the specifications of the idealized design. Power is distributed amongst three different rails: a 24V for the drive motors on the treads, 14V for the stepper and servo motors, and 5V for the control logic such as the STM32 boards and other peripherals.

Table 6 below summarizes the primary differences between the prototype and the full idealized system. The substitutions were driven by cost and timeline.

Component	Flight System Design	Prototype Design
End-Positioning Mechanism	Pancake motor mounted with large bearing to allow for yaw change; stepper motor mounted along axis for variable pitch.	Servo motor mounted on top of lazy-susan bearing for yaw; two servo systems mounted along axis for pitch.
Elevation	Lead screw stepper motors extending metal poles, holding the frame.	Lead screw stepper motor, extending cardboard tube material.
Drive	Two tank tread drive systems operating with two motors each, attached to bearing systems to allow drives to turn separately from the tunnel.	Two tank tread drive systems operating with high torque motors, attached to lazy-susan bearing systems to allow for drives to swivel.

Table 7: Drive Flight Design vs Prototype Differences

Prototype Power Budget The prototype's power architecture has a total steady-state draw of about 301.7 W. Compared to the idealized system, this lower number reflects the reduced motor count and lower voltage rails used for prototyping. Power is supplied via a nominal voltage 22.2V (up to 25.2V) LiPo 6s battery, with buck converters stepping down for each voltage rail. Rail current draws are 10.8 A on the 24V rail, 3.95 A on the 14V rail, and 0.07 A on the 5V rail. Table 2 below details the component-level power budget.

Component	Rail	Power	Current
4 Brushed DC Motors	24 V	259.2 W	10.8 A
2 Stepper Motors	14 V	47.04 W	3.36 A
2 Servo Motors	14 V	13.2 W	0.59 A
4 STM32 Nucleos	5 V	0.005 W	0.001 A
CAN + IMUs + Misc	5 V	1.5 W	0.07 A
Total	-	301.7 W	-

Table 8: Prototype Power Budget

4.4 Walkway Prototype

The walkway prototype is a commercially-purchased rollable floor made from aluminum and plastic. This prototype is used only to simulate what the rolling may look like, and to be used as a means of testing walkway usability. This prototype is not designed to be weight-bearing or connected to another prototype.

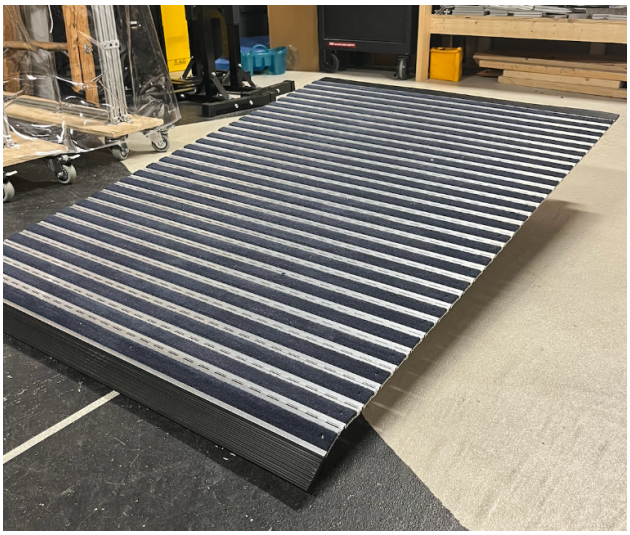

Figure 26: Walkway Prototype

The floor beams that lay under the walkway were not prototyped. Instead, we built a ramp out of wood to support the walkway for testing.

4.5 High Level Controls Design Prototype

The prototype HLC design was implemented as a ROS2 software architecture and tested using Gazebo and RViz. Due to time constraints, the software prototype allowed us to exercise the command, localization, state transition, and visualization pathways using simulated tunnel motion and generated sensor feedback, without requiring mechanical and embedded hardware to be available.

The prototype retained the same major interfaces as the idealized system: goal information entered through the GUI/action pathway; simulated or generated AprilTag and odometry data entered through sensing topics; the EKF produces a fused pose; and the state machine/navigation module generates drive commands. The primary difference is that the actuator and sensor behavior are represented in simulation rather than being produced by flight-like hardware.

Area	Idealized Design	Prototype Design
Sensors	Cameras, AprilTags, encoder/IMU, odometry, and LiDAR hardware Connection to full fault monitoring sensing capabilities (e.g. current draw, degraded sensors, damage, etc)	AprilTag and odometry feedback generated or represented in software; response to LiDAR data represented in software Limited software checks regarding camera, AprilTag, and odometry faults, but not the full range of possible faults
Actuators	Commands executed by drive, elevation, and docking mechanism	Commands move a Gazebo/RViz tunnel model through a C++MobileKinematicsModel
Verification	Hardware-in-the-loop, environmental, and mission-duration testing	GTests and goal-reaching Gazebo/RViz integration tests

Table 9: HLC Flight Design vs Prototype Differences

4.6 User Interface Prototype

Through the designed prototype, the major considerations identified in the trade studies were incorporated as effectively as possible. Ergonomic factors, such as button size, were considered to accommodate variations in astronauts' finger sizes and to ensure ease of use during operation. Based on these considerations, it was concluded that in an idealized real-life design, the UI screens would be adapted for tablet displays located outside the tunnels. The design also assumes that users would interact with the interface through direct touchscreen input rather than using a mouse or external pointing device.

Overall, the UI subsystem is intended to integrate effectively with the other subsystems. In particular, it should reflect the digital system architecture developed by the controls team, ensuring that key system functions, commands, and status information can be clearly visualized and accessed through the user interface.

The current UI prototype is divided into three distinct stages, each representing a different operational state of the tunnel system.

In the first stage, the prototype tests the basic functionality of the UI under the assumption that there are no active alarms or alerts and that the system is operating as intended. As previously described, the interface includes three primary display sections. One display provides a diagrammatic view of the tunnel, showing its alignment and attachment status relative to the hatches of nearby habitats. The other two displays show camera feeds from both inside and outside the tunnel. In addition, the UI includes an overview of key system metrics, reflecting data collected through the sensors integrated with the controls subsystem.

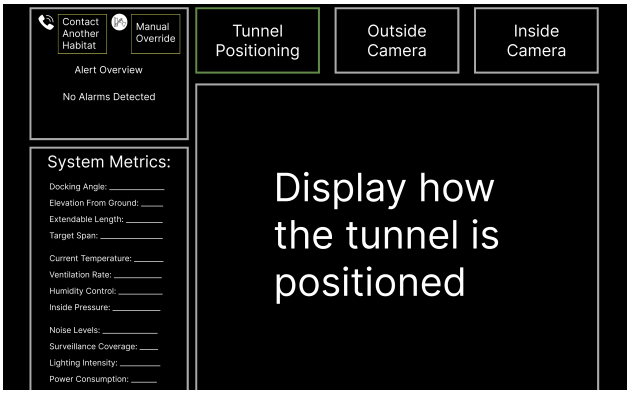

Figure 27: UI Prototype Start Page

The top-left corner of the interface includes interactive features for astronaut use. These include a Contact Another Habitat function, which allows the crew to establish communication before docking, and a Manual Override function, which provides access to manual control of tunnel movement and docking adjustments. The exact form of the manual control system may vary, but the UI is designed to support direct crew interaction with these critical tunnel operations.

Figure 28: Contact Another Habitat Page

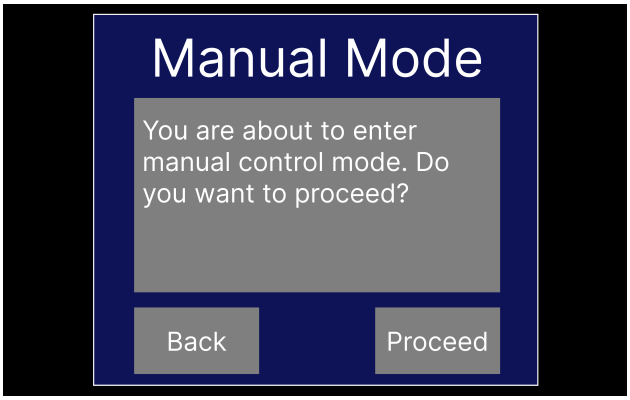

Figure 29: Manual Override Page

In the second stage, the prototype introduces an active pressurization issue. Under this sce-

nario, an alert immediately appears, indicating a critical pressurization level within the tunnel. The alert message gives the astronaut the option to either dismiss the issue temporarily or resolve it immediately. If the astronaut chooses to resolve the issue, a resolution procedure appears, outlining the required steps for addressing that specific alarm. If the astronaut dismisses the alert, it is moved to the Alert Overview menu, where it remains accessible. The astronaut can then select the alert from this menu at any time to open the corresponding resolution procedure.

It is also important to note that the System Metrics display adjusts depending on whether the resolution procedure is open or closed. This design choice helps minimize cognitive overload by using progressive disclosure, allowing the interface to present only the most relevant information at a given time while still keeping essential system data accessible.

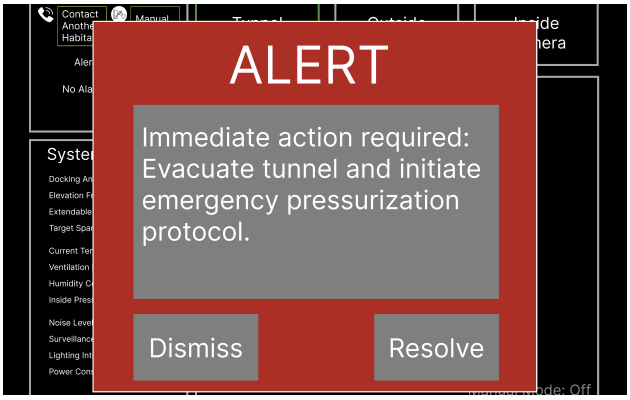

Figure 30: Alert Popup

Figure 31: Alert Resolution Procedure

In the final stage of the UI interaction journey, the user is presented with multiple items in the Alert Overview menu. At this stage, the system distinguishes between different levels of concern, including both alerts and warnings. Alerts are marked with a red triangular indicator, while warnings are marked with a yellow triangular indicator. This visual distinction allows the astronaut to quickly identify the severity of each issue and prioritize responses accordingly.

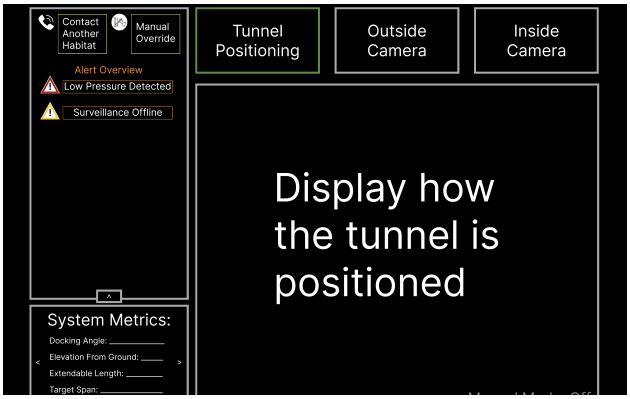

Figure 32: Alert Overview

The user can navigate between multiple resolution procedures, with each procedure corresponding to a specific alert or warning. In the assumed warning scenario, the surveillance system is offline. When the user selects this warning, the UI presents a procedure for restoring camera functionality. To accommodate multiple active alerts and warnings, the Alert Overview menu expands when more than two items are present, ensuring that the interface remains organized and usable even during more complex emergency scenarios.

5 Trade Studies

5.1 Mechanical

5.1.1 Frame

A trade study was performed to select the material for the structural rings. When choosing a material for the structural rings, we wanted to ensure that astronauts rely on the material not to fail during operation, and ensure that the rings contribute only as much mass as needed for operation (high strength-to-weight ratio). The main stresses experienced during operation come from pressurization cycles, crewmembers walking, and wind. For this study, failure is defined by the yield strength limit, as any permanent plastic deformation could impede the tunnel's mechanical extension and retraction mechanisms.

In low Martian temperatures (ranging as low as -120°C near the equator), diffusion-based creep was not a major concern for materials due to insufficient activation energy. Fatigue and stress corrosion cracking were considered due to cyclic loading from pressurization, walking, and wind. Therefore, materials that exhibit high fracture toughness and resistance to stress-corrosion cracking were favorable. A critical factor was avoiding the Ductile-to-Brittle Transition (DBT). Additionally, materials that retain high impact resistance at -120°C were favored.

The materials analyzed were Aluminum 7075 and 6061, Titanium Ti-6Al-2Nb-1Ta-0.8Mo, Magnesium AZ31B, and Stainless Steel 405. While composites like carbon fiber offer high performance, composites were not analyzed for complexity and manufacturing reasons. However, their uses for structural applications in Martian environments should not be overlooked for the final design decisions. Based on material properties like strength-to-weight, cost, tensile yield strength, and toughness at low temperatures, Aluminum 6061 was chosen.

5.1.2 Shell

A trade study was performed for the inflatable softgoods shell which analyzed shell materials and coatings. The shell material is based largely on material strength, pliability, and weight, as this layer would be the most load-bearing. Some of the options for the materials included Kevlar, Vectran, and polyethylene fabric. Based on superior material properties and previous testing by NASA, Vectran was chosen as the main shell material.

Material coatings were chosen on their ability to insulate, protect from radiation, and ability to provide an air barrier. Some of these options were urethane, silicone, or boron nitride nanotubes. Based on the material properties and its ability to withstand the Martian environment, silicone was chosen as the fabric coating.

5.1.3 Passive Extension

A trade study was performed to determine the passive extension method which will be responsible for maintaining the alignment of the rings during compression and extension. The Martian surface conditions present three main issues for an extension mechanism. First, despite seals, abrasive Martian dust will likely enter the tunnel. In sliding joints, this dust causes friction and potential jamming; in revolute joints, it can lead to accelerated wear. Second, the extreme temperature swings cause expansion and contraction, which may lead to jamming. Lastly, the cold surface

temperatures may lead to brittleness of the material, which may lead to increased sensitivity to expected vertical and radial loads. Other factors that were important in making our decision were the cost of the mechanism and the mass and volume of the component.

We considered using a cascading elevator mechanism, in which nested stages extend sequentially through passive linkages or guided members. Cascading systems have high structural stiffness and predictable linear motion, but they require tight manufacturing tolerances and multiple sliding interfaces, making them highly sensitive to dust contamination, thermal expansion, and misalignment.

We also considered using a telescopic rod mechanism, in which adjacent tunnel rings are connected through sliding rods or tubes that extend and retract as the tunnel changes length. Telescopic rod systems minimize interference with internal subsystems like handrails and flooring with their compactness. However, telescopic rod systems are highly sensitive to side loading, manufacturing tolerances, and angular misalignment between rings, all of which may cause binding or jamming during deployment. Martian dust contamination and thermal expansion may further increase friction within the sliding interfaces, potentially reducing reliability over repeated deployment cycles.

We also traded scissor mechanisms, which offer many advantages in the realm of designing and manufacturing the extendable tunnel. They offer high extension ratios, are well analyzed, and easily transition between compression and extension with variable length options. However, the scissor mechanisms can suffer from "force amplification" at high extension angles, making controlling the maximum extension imperative.

Ultimately, we chose to use the scissor mechanisms due to their high extension-to-compression ratios, higher margin-of-error for misalignment caused by thermal expansion, low storage volume and mass, and ability to support radial loads placed on the tunnel.

5.1.4 Handrail

The trade decisions were evaluated based on what would provide the most support if the astronauts were to put their full weight onto the apparatus. Once we determined options that fit this requirement, we pivoted to looking into designs that would allow for smooth extension and retraction, minimal maintenance, ease of material sourcing, and weight considerations.

After deliberation, the extension mechanisms and minimal maintenance were the key factors in our decision. We concluded that having something require heavy maintenance was not feasible, as this structure was expected to be a long-term installment.

Our considerations for handrail design included vertical handrail bars, a tightly wound suspension cable, and a horizontal telescoping tube. We decided to not continue with the vertical handrails as the jump in between handrail units proved to be dangerous and ineffective for if an astronaut unexpectedly fell in the tunnel. We did not continue with the cable design as the small diameter of the cable proved to be uncomfortable for individuals walking through the tunnel, and the mechanism through which tension seemed to interfere with other moving parts of the tunnel.

One of the concerns that was brought up when looking for tubes was the role of friction in the extension and retraction mechanisms. This led to a discussion of potential materials that could

be utilized. The top contenders suggested were plastic, titanium, aluminum, and steel. Plastic was ruled out as a contender as it lacks the structural integrity to withstand the expected forces. Under sudden impact, the handrail would be likely to deform, or even break under the pressure. Additionally, due to the brittle nature of plastic, the likelihood of breaking and thermal expansion of the plastic would lead to frequent changes and repairs.

Titanium alloys, often used by NASA, seemed like an appealing choice. Titanium is just as strong as steel, but around 45% lighter than steel. Additionally, titanium has a low thermal conductivity, while steel has a high thermal conductivity, making titanium appealing for temperature varying environments where user interaction is required. Both steel, titanium, and aluminum have a high modulus of elasticity. Steel has a modulus of elasticity of about 200 GPa compared to titanium's 116 GPa and Aluminum 6061's of 68.9 GPa. The advantage of being stiffer reduces the likelihood of the handrails to undergo plastic deformation or fracture under heavy amounts of pressure. However, titanium is largely more expensive than steel and aluminum. Furthermore, aluminum and steel are both easier to fabricate and manufacture, allowing for easier tweaks to the apparatus. Aluminum 6061 was ultimately chosen, as it would lessen the weight of the component. Additionally, aluminum was chosen to conform to the material selected for the rest of the system.

The next thing to consider was how to address consequent friction from the telescoping mechanism. Discussion of potential solutions led to the usage of a linear bearing to facilitate the horizontal motion of extension and contraction. We decided on two options for the mechanism, the first being a polymer bearing. The benefits of this bearing are that the bearing itself is self-lubricating, not requiring routine maintenance, and would not require housing in the telescoping rods. The other option was a linear ball bearing, and ultimately the linear ball bearing proved to be the optimal choice. The linear ball bearing is able to withstand higher speeds than the polymer one, allowing more flexibility in the deployment time of the tunnel. Additionally, the linear ball bearing relies on rolling friction instead of sliding friction, leading to a lower coefficient of friction of roughly 0.005, as opposed to that of a polymer bearing: roughly 0.1.

Figure 33: Polymer Sleeve Bearing

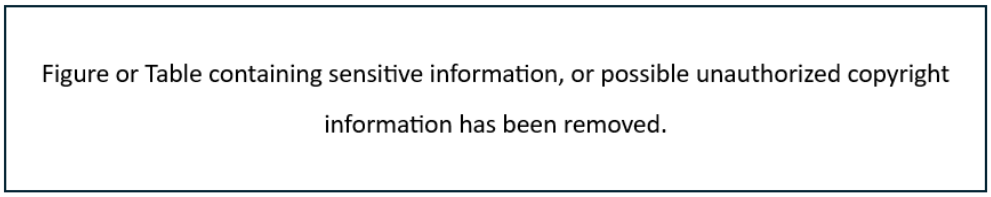

Figure 34: Linear Ball Bearing

5.1.5 Active Extension

The key trade decision focused on selecting which actuated wheel system should be chosen. The primary evaluation criteria included the maximum structural load capacity of each configuration, material composition, obstacle traversal capabilities, and projected maintenance lifecycles under extreme environmental conditions.

The assumptions we made also informed the final decision of the trade study. We assumed the Tunnel will always be securely connected to the initial habitat on its closest end segment, removing a large amount of the load placed on the wheels of the farther end segment. We also assumed the friction between the wheels and surface will be sufficient enough for the wheel to not slip as the system goes to full extension.

For trade options, different types of passive caster wheels and bearings were considered as more standard wheels. We also considered the NiTiNOL wheel and tank treads for their resistive properties. In searching for an ideal solution, we looked for a tire that can withstand the weight of our crew members passing through the stagnant tunnel, as well as the weight of the tunnel. This is an important consideration because we don't want the wheels to fail, but we also don't want to have too many wheels, which could impede upon the system's ability to retract and introduce parasitical friction. Stronger wheels would directly correlate to needing fewer wheels for active extension.

We also looked for a material that can withstand the thermal and cyclic fatigue from the environment and tunnel. Lastly, we looked for a wheel capable of traveling over smaller obstacles such as rocks on the lunar surface. We considered the ability to withstand force as the most important factor as there will always be force applied, but there will not always be obstacles to the tire's movement.

The decision for the ideal design for this system was selected to be a tank tread system. The conclusion was made based on needing an active drive system to actuate the tunnel's extension

while still needing maneuverability and endurance to get past any obstacles on the Martian surface.

5.1.6 Walkway

During the initial stages of design, there were multiple different ideas generated about what the walkway should look like. Some of these ideas included a rolling "sushi-mat" design, telescoping sheets, or a tarp-like design that would be held taut. Based on the perceived low weight and simplicity of the rolling design, the "sushi-mat" was chosen for the ideal system. Originally, the floor slats were planned to be held together using a fabric, but it was later decided to use hinge joints instead because these joints would be significantly more rigid and strong compared to a fabric.

Some factors to consider when selecting materials are the high temperature swings (-120°C to 20° near the equator), corrosion resistance from dust entering the tunnel, and most importantly the ability to survive cyclic loading from crew members walking across the tunnel. These actions contribute the most to the stresses within the material. For this study, failure is defined by the yield strength limit, as any permanent plastic deformation could jeopardize the walkways rollout mechanism.

The two main materials analyzed for the walkway were aluminum 7075-T6 and titanium Ti-6Al-4V. These materials were chosen for their high strength-to-weight ratios, common use in aerospace applications, and manufacturability. Figures 35, 36, and 39 show hand calculations that went into the material decision.

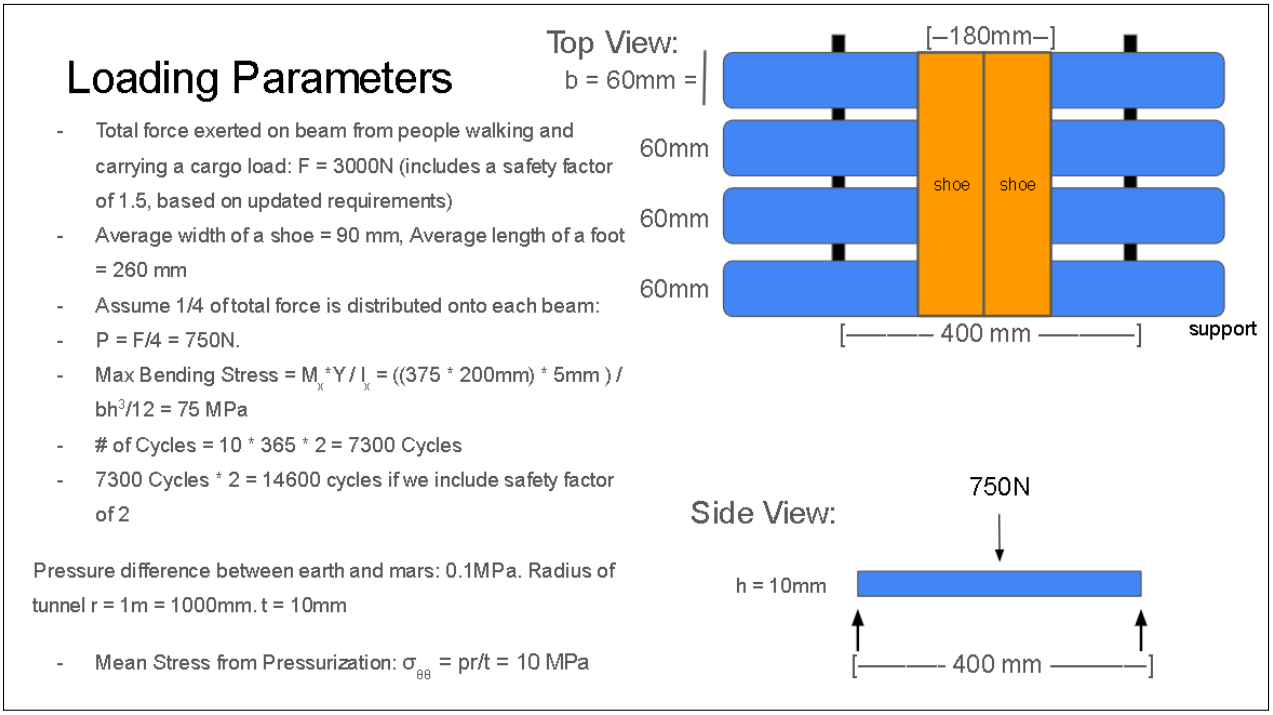

Figure 35: Floor Loading Parameters Hand Calculations

Fatigue Analysis for Ti-6Al-4V

Can a Ti-6Al-4V beam last the full 10 years?

σ_y = 880 MPa, σ_{UTS} = 950 MPa, σ_m = 10MPa, σ_a = 75MPa

Check for yield: 75.4MPa < 880MPa

$$\frac{\sigma_a}{\sigma_{ar}} + \frac{\sigma_m}{\sigma_u} = 1$$

$$\sigma_{ar} N_f^a = C_1$$

Stress Ratio = $\sigma_{min}/\sigma_{max}$

σ_{max} = 85MPa = 12.33ksi

→ R <<1, and R >0, so we use the curve corresponding to R = 0.10

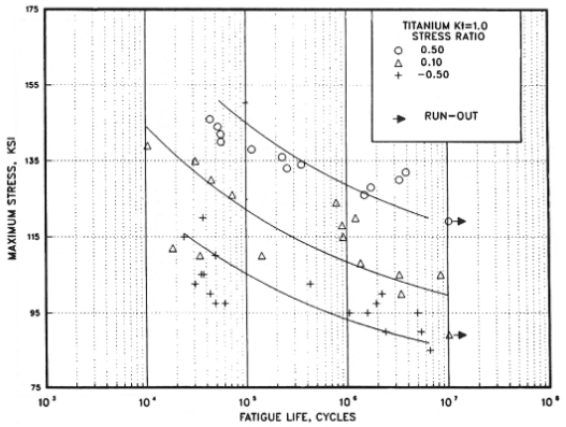

Figure 5.4.1.1.8(f). Best-fit S/N curves for unnotched Ti-6Al-4V annealed sheet, long transverse direction.

https://materialsdata.nist.gov/bitstream/handle/11115/177/Mecnanical%20Properties%20Data.pdf?sequence=3

According to the S/N Curve, material will survive more than 14600 Cycles, and therefore the duration of the mission

Figure 36: Titanium Floor Fatigue Analysis

Fatigue Analysis for Aluminum 7075-T6

Can a Al 7075-T6 beam last the full 10 years?

σ_y = 503 MPa, σ_{UTS} = 572 MPa, σ_m = 10MPa, σ_a = 75MPa

Check for yield: 75.4MPa < 503MPa

$$\frac{\sigma_a}{\sigma_{ar}} + \frac{\sigma_m}{\sigma_u} = 1 \quad \sigma_{ar} = [(1 - \frac{\sigma_m}{\sigma_u}) / \sigma_a]^{-1}$$

$$\sigma_{ar} N_f^a = C_1$$

σ_{ar} = 76.3MPa

C_1 = 1000, a = 0.12

$N_f = (C_1/\sigma_{ar})^{1/a}$ = $2.05*10^9$ Cycles > 14600 Cycles

Material Will Survive According to Basquin's Law

Aluminum alloys	Major addition	Minor additions	Yield strength (MPa)
1xxx	none	none	25-125
2xxx	4% Cu	Mg, Mn, Si	30-165
3xxx	Mn	Mg, Cu	50-250
Cast 4xxx	Si	none	50-150
5xxx	Mg	Mn, Cr	200-500
6xxx	Mg, Si	Cu, Mn	40-300
7xxx	Zn	Mg, Cu, Cr	350-600

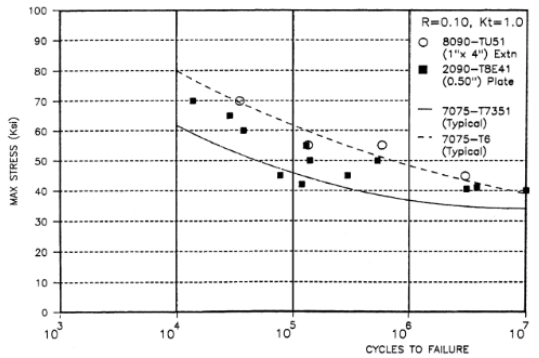

'.9 Comparison of *S-N* curves for 8090-TU51 extrusion with 2090-T8E41 plate and typical 7075-T6/T7351 0.1, K_t = 1. Source: Ref A7.11

https://materialsdata.nist.gov/bitstream/handle/11115/177/Mecnanical%20Properties%20Data.pdf?sequence=3

Stress Ratio = $\sigma_{min}/\sigma_{max}$ → R <<1, and R >0, so we use the curve corresponding to R = 0.10

σ_{max} = 85MPa = 12.33 ksi

According to the S/N Curve, material will survive more than 14600 Cycles

Figure 37: Aluminum Floor Fatigue Analysis

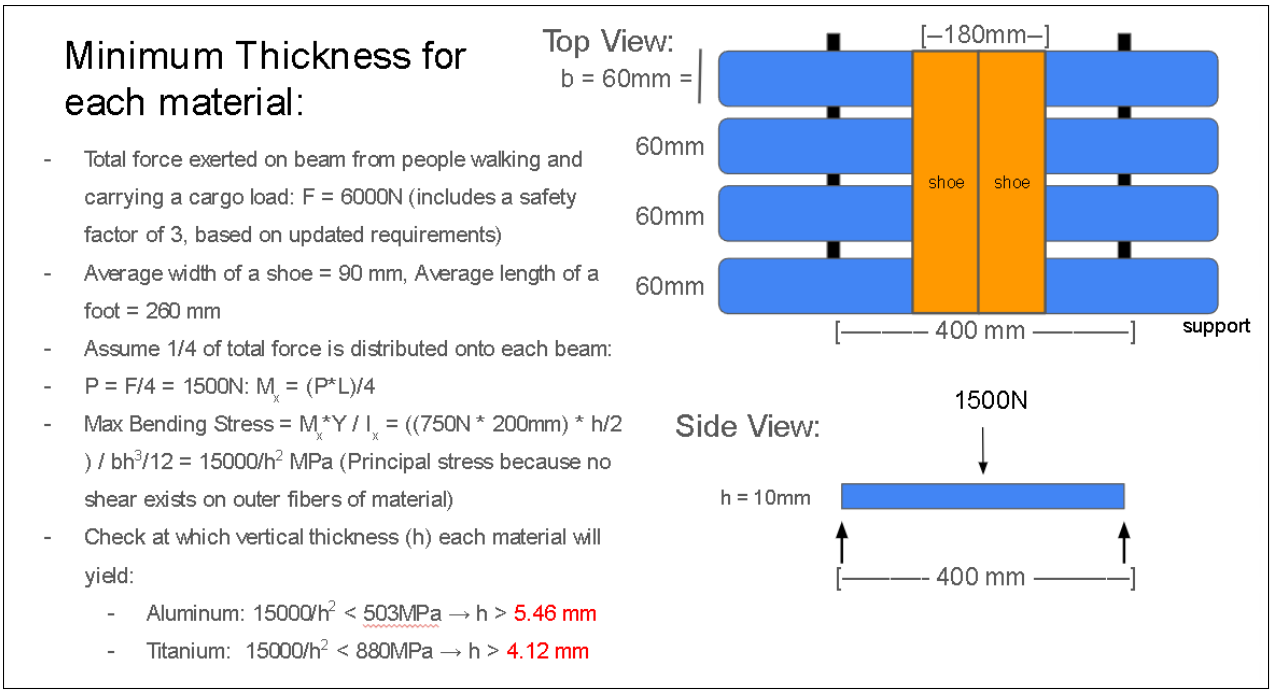

Figure 38: Aluminum and Titanium Floor Thickness Analysis

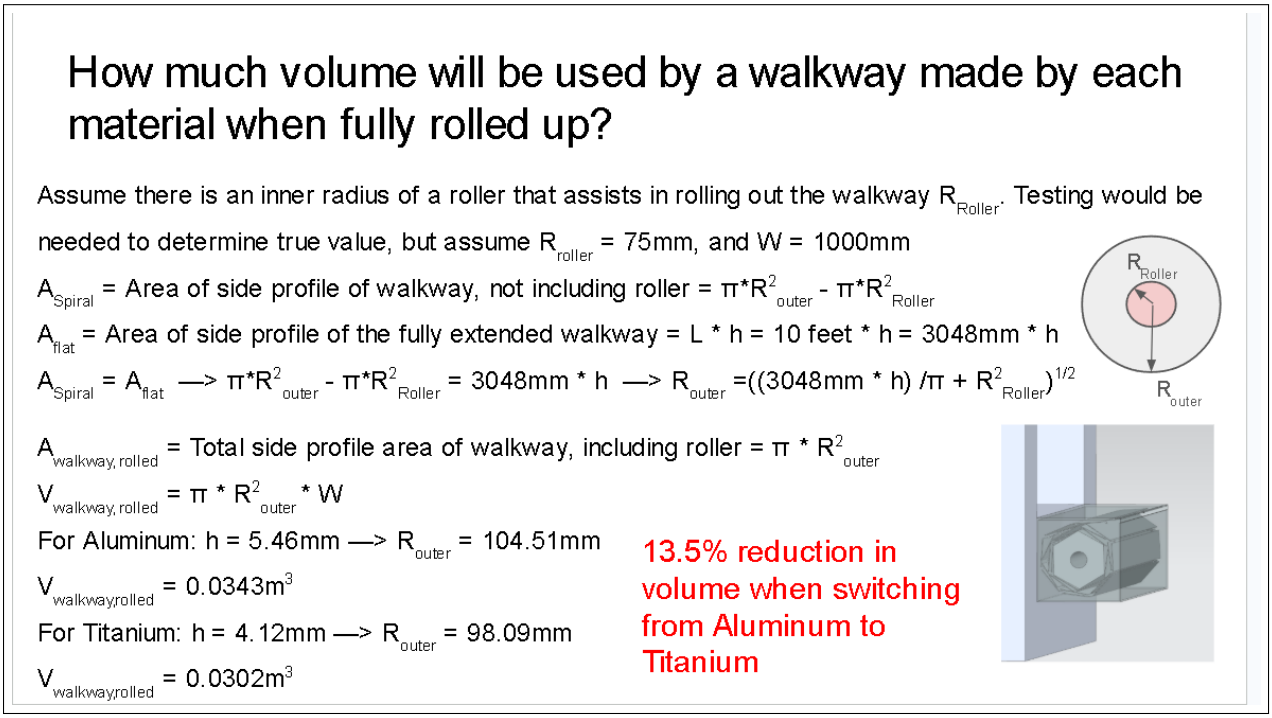

Figure 39: Aluminum and Titanium Floor Volume Analysis

Titanium is significantly more expensive than aluminum, but its material properties are superior in comparison. For example, its resistance to corrosion and fatigue is superior to that of aluminum, which is an important property in a dust filled environment. Additionally, titanium is

stiffer, increasing the stability of the walkway as it is traversed. The above calculations show that the titanium floor will take up 13.5% less volume. A rolled up walkway made up of aluminum will take up 0.0343 m^3 of volume, compared to titanium which will take up 0.0302 m^3 of volume. Based on the high strength-to-weight ratio of titanium relative to aluminum, along with its exceptional corrosion resistance, Ti-6Al-4V was selected as the optimal material for the floor slats.

There are also telescoping floor beams below the floor slats to provide support for the walkway. They help reduce the stress in the walkway during loading, while also providing support and stabilization for the rings. There were no other design ideas for the floor beams besides telescoping based on the geometry of the floor slats. These floor beams will also be made of titanium for the same reasons as the floor slats.

5.1.7 End Positioning

A trade study was conducted to determine the optimal system for an end positioning mechanism.. The decisions were evaluated based on the safety, complexity, usability, and mass. We made the assumption that NASA wanted us to get the end of the tunnel parallel to the hatch of the targeted habitat. Therefore, we took that as part of our scope that requires this end positioning mechanism to have ample Degrees of Freedom (DOF) to correctly position the end segment. We also made the assumption that hatches on different surface assets will be facing the same general area. That is, the tunnel will not need to significantly bend around a surface asset to reach a hatch.

Three different options for how to operate the end positioning mechanism were evaluated. The first was a two part system of a motor drive shaft to give lateral movement and a servo to give pitch movement which allowed for 2 DOF, not including elevation change. The second was a Stewart platform system, which allowed for 6 DOF. The third was a system similar to a jet catwalk used for connecting to planes, which could have a range of DOF.

We ultimately decided on the motor drive shaft and servo system because the stewart platform allowed more freedom of movement than needed, which added unnecessary complexity and mass to the end positioning mechanism. The jet catwalk system is effective and safe for earth systems, but we decided it would not be safe for Lunar or Mars surfaces because the jet catwalk would not provide a safely airtight environment in the tunnel. The motor drive shaft and servo system provides the freedom that we need and we can ensure a rigid and safe connection to the habitat.

5.1.8 Elevation Change

The primary trade decision was the selection of a drive mechanism to provide the vertical motion under load. Three candidate mechanisms were evaluated. The first was a lead screw driven by an electric motor, a threaded screw rotated by a motor driving a follower nut attached to the translating element. The second was a rack and pinion design: a motor-driven pinion engaging a linear rack to produce vertical translation. Lastly, a pneumatic or hydraulic cylinder providing direct linear actuation.

These options were compared qualitatively against four criteria relevant to the tunnel's operating environment and functional requirements. First, compatibility with the Martian environment: the mechanism must survive the Martian thermal environment, thermal cycling, low atmospheric

pressure, and abrasive regolith. Next, self-locking under load: the subsystem must hold the tunnel at a commanded height indefinitely without continuous power input or drift, back-driving under load is unacceptable. Also, load capacity: the mechanism must support the full static weight of the tunnel plus dynamic loads transmitted through the suspension. Finally, precision of height control: height must be precisely adjusted enough to achieve a sealed connection at the habitat/airlock interface. Environmental compatibility was treated as the most heavily weighted criterion, since a mechanism that cannot survive transit and surface operation is disqualified regardless of how well it performs on the other criteria.

The lead screw driven by an electric motor was selected. An electromechanical drive has no working fluid, no pressurized lines, and no dynamic seals exposed to the environment as pneumatic or hydraulic systems do. On the surface, seal leakage under thermal cycling and low atmospheric pressure is a known failure mode for fluid systems, and any leak is a permanent loss of a non-replenishable consumable. While the rack and pinion design is electromechanical and avoids the fluid-related issues, its toothed interface is susceptible to Martian dust. Additionally, a rack and pinion system is not self-locking and would require a brake. Finally, pneumatic and hydraulic systems hold position only as long as pressure is maintained, and bleed-down is a known failure mode. Ultimately, lead screws are well-suited to high-load, low-speed vertical applications and scale well to the expected tunnel mass.

5.1.9 Suspension

The main trade decision was the selection of a suspension type to mount the treads to the linear actuators, the three types evaluated were: double wishbone, MacPherson strut, and trailing arm. These were then evaluated qualitatively against three main criteria: terrain adaptability, complexity, and compatibility with existing tunnel systems. As the suspension system was incorporated late in the project, compatibility with the existing tunnel was given the highest weight. The double wishbone suspension type was selected as it allowed well controlled vertical wheel travel and clear compatibility with the linear actuators. The increased complexity was offset by ease of integration into the design. A spiral torsional spring was added into the knuckle to add pitch capabilities to the treads which the other suspension types could not account for easily.

5.2 Ergonomics

5.2.1 Handrail Height

A trade study was conducted to determine various different handrail heights that would be useful to test during Ergonomic Testing. Several different sources had different recommendations, ranging from as low as 76.2 cm and as high as 106.7 cm. The handrail height options for testing were evaluated based on how much stability those heights provided members of their respective studies, how accessible the handrails are/would be for prospective astronauts, how useful they might be in Martian gravity, and how much they minimized torso flexion. Ultimately, we decided to conduct our Optimal Handrail Height Test with the handrail heights of 90, 100, and 110 cm based on preliminary results from the trade studies.

5.2.2 Handrail Shape and Dimensions

Trade studies were conducted to determine the optimal handrail shape and dimensions that should be employed in the tunnel. The trade options were evaluated based on their ability to

adhere to the criteria that the handrail must extend the entire length of the tunnel, and that the handrails must extend/contract with the tunnel. Thus, the shape must not hinder the extension mechanism of the tunnel. In combination with trade studies from the mechanical team, a telescoping method of extension was decided on for the handrails. From here, the ergonomics team debated the following trade options: floating dog-bone, non-circular cross-section, and circular cross-section handrails. Further evaluation of the trade options included if the shape would allow the handrails to structurally support a load of 370 N, were practical for our testing (meaning were they parts we could obtain or manufacture), and if the dimensions were suitable for the wide range of prospective astronauts - from the 1st percentile female to 99th percentile male. Based on these evaluations and the need to adhere to requirements, we ultimately decided upon using a circular cross-section handrail with a diameter of 5.08 cm (2 in), as it is at the upper end of OSHA's 3.175-5.08 cm (1.25-2 in) handrail thickness guideline, and because we already had a 5.08 cm diameter metal pipe in the lab for testing. However, in an idealized version of the telescoping handrail system, we suggest each segment of handrails extend in 3 parts with diameters of 3.175, 3.81, 4.445 cm, respectively (1.25, 1.5, 1.75 in). This is so that the handrails can have less variation in diameters across shrinking telescoping sections, and the dimensions are more closely aligned with the lower end of the dimension spectrum outlined by OSHA, and with the 3.81 cm thickness of ISS IVA handrails.

5.2.3 Walkway Width

A trade study was conducted to determine the optimal walkway width inside the tunnel. The trade options were evaluated based on their ability to fit the shoulder width of a 99th percentile male with a safety factor of 2, if they met standards set by previous NASA projects, ensured there was enough clearance for two crew members to potentially transfer cargo through the tunnel via the walkway, and met the requirement that the walkway system must have a minimum internal width of 0.61 meters. The options traded included: 1.0, 1.2, and 1.4 meter walkway widths. Ultimately, 1.0 meter was chosen based on the 99th percentile male shoulder width being 46.2 cm; with a safety factor of 2 this measurement becomes 92.4 cm. In addition, officials at Johnson Space Center determined the optimal internal architecture of a habitat and its hatch sizing to be 1.05 meters. Based on these two data points, 1.0 meter was determined to be optimal.

5.2.4 Tunnel Shape

A trade study was conducted to determine the optimal cross-sectional tunnel shape. The trade options were evaluated based on their ability to allow two astronauts to move through the tunnel while transporting cargo, ease of incorporating handrails into the design, and structural integrity. It is assumed that the tunnel shape must support a design that can accommodate a relative angular difference of up to 15 degrees (pitch and yaw) between surface habitats, have an extension ratio of at least 1:2, have an internal height of at least 2.01 meters, and have an internal width of at least 0.61 meters. The options traded were a cylindrical cros-section tunnel and a rounded rectangle cross-section tunnel. Ultimately, the rounded rectangular tunnel was chosen due to its design allowing for more consistent overhead clearance and more ease in mounting handrails and other equipment.

5.2.5 User Interface

For this subsystem, most of the trade studies focused on identifying an appropriate alert system. It was determined that an alert system is a critical feature to include in the UI mainframe, as it must effectively notify users of emergencies within or around the tunnel and assist them in

navigating safely through the tunnel, including with support from camera feeds. Alert systems are essential to this project because they significantly enhance the overall safety of the end user. For example, one assumed emergency scenario involves an earthquake, during which the user must be immediately alerted and guided out of the tunnel to ensure their safety.

Several trade options were considered, including:

- **New color-coding system vs. conventional color-coding system:** Evaluating whether to implement a redesigned color-coding scheme or use a more traditional system, such as the one applied to tunnel lighting.
- **Video feed with connected audio controls:** Using internal tunnel camera feeds and audio communication systems to monitor conditions inside the tunnel and inform users of potential dangers during an emergency.
- **Multi-tiered alarm system:** Implementing alarms based on emergency severity, where different alarm classes are activated depending on the level of risk.

The trade decisions were evaluated by conducting trade studies to identify the critical elements of alarm systems that could be incorporated into the UI. These studies led to several key conclusions. First, designing the alert system to be consistent with existing spaceflight programs would reduce crew training requirements and contribute to a safer operating environment. Second, the alarm system must comply with established sound-level limits; specifically, the alarm signal's A-weighted sound level should not exceed 95 dBA at the intended receiver's location. Finally, the effective masked threshold was considered, defined as the level at which an alarm signal is just audible over ambient noise. Therefore, the alarm must remain within acceptable sound limits to avoid disorienting the user while still being effective in notifying them of issues related to the tunnel system.

At the conclusion of the trade study analysis, several features were selected for inclusion in the final design. First, a conventional color-coding scheme was chosen for the alarm system because it leverages the end users' familiarity with established alert conventions, reducing the need for additional training and improving response time. This scheme will be tested in conjunction with the proposed alarm systems.

Second, the design will include video feeds with connected audio controls to help monitor the interior of the tunnel and alert users to potential hazards during an emergency. This feature will support situational awareness and provide users with real-time information about conditions inside the tunnel.

Third, a multi-tiered alarm system will be implemented. Depending on the severity of the emergency, an alarm from the appropriate class will be activated. This is especially important for controlling the amplitude of the alarm sound, ensuring that the alert is noticeable without being disorienting or exceeding acceptable sound-level limits.

Additionally, if the necessary technology is available, augmented reality (AR) could be integrated with the alert system in future development to further improve user guidance and emergency response.

5.3 High Level Controls

To determine a controls architecture that can support autonomous alignment, while remaining testable in a prototype environment, the following decisions were evaluated:

- **High Level Controls Architecture:** Selecting the overarching architecture, framework, and middleware that would be used to translate input and sensor information into actionable motor commands.
- **Localization Method:** Selecting the sensor inputs and estimation method used to determine the tunnel's current position and orientation relative to the connecting surface element.
- **Autonomous Behavior Structure:** Selecting how the system organizes the sequence of extension, alignment, completion, and fault-handling behaviors required for autonomous operation.
- **Software Verification Environment:** Selecting how software will be validated.

Decisions were evaluated using the following criteria: Reliability and Fault Tolerance, or the ability of the software to detect unexpected conditions and prevent incorrect motion; Robustness, or the ability to maintain usefulness when under noisy conditions; Performance and Responsiveness, or the ability to complete the task quickly and to the highest extent feasible; and Integration and Verification Complexity, or the ability to connect the controls software with the GUI, embedded motor controllers, perception system, and prototype simulation without requiring a complete physical tunnel.

These criteria reflect the primary role of the HLC subsystem: it must produce safe and correct autonomous movement, continue operating when sensor availability changes, and be testable before full mechanical and electrical integration. Because the available prototype did not include a complete flight-like hardware implementation, verification complexity was especially important for ensuring that the autonomy logic could still be meaningfully tested through software simulation and generated sensor feedback.

5.3.1 High Level Controls Architecture

Selected: Modular ROS2 Architecture

Trade: A monolithic controls program versus a modular ROS2-based architecture with separate nodes for GUI communication, sensor interfaces, localization, state machine/navigation behavior, and motor command output.

Justification: A modular ROS2 architecture was selected because the HLC system requires several functions to operate together while remaining independently testable. In the selected design, GUI commands begin an autonomous goal request, sensor interface nodes publish odometry and AprilTag information, the localization node produces a fused pose estimate, and the state machine/navigation node generates drive commands through the motor interface. Separating these functions allows individual portions of the system to be tested without requiring the entire tunnel hardware assembly to be operational.

This architecture also improves reliability during integration. Sensor measurements, fused pose, state transitions, drive commands, and fault conditions can be observed as separate ROS2 topics

or actions rather than remaining hidden within a single program. As the design progresses toward flight hardware, the simulated interfaces can be replaced by CAN-connected embedded controllers and physical perception hardware without requiring the overall software structure to be redesigned.

5.3.2 Localization Method

Selected: Extended Kalman Filter Combining Odometry and AprilTag Pose Measurements

Trade: Dead reckoning using wheel encoder and IMU odometry only; direct localization from AprilTag measurements only; a Kalman Filter combining odometry and AprilTag measurements; or an Extended Kalman Filter combining odometry and AprilTag measurements.

Justification: An Extended Kalman Filter was selected because neither odometry nor AprilTag sensing is sufficient by itself for reliable autonomous alignment. Odometry provides continuous position updates as the tunnel moves, but error accumulates over time due to wheel slip, terrain variation, and measurement noise. AprilTag measurements provide a direct estimate of position relative to the docking interface, but the tag may be partially obscured or leave the camera's field of view during motion.

The selected EKF combines the strengths of both measurements. Odometry is used to continuously predict the tunnel's position while moving, and AprilTag pose measurements are used to correct this estimate whenever the docking target is visible. An EKF is preferable to a basic Kalman Filter because the relationship between tunnel motion, orientation, and measured pose is not strictly linear during combined extension and angular alignment. This approach provides a more robust pose estimate for the navigation and state machine logic, especially during periods when AprilTag feedback is temporarily unavailable.

5.3.3 Autonomous Behavior Structure

Selected: State Machine with Navigation Command Generation

Trade: Direct motor command generation from user input; a continuous behavior-based controller; or a state machine that sequences autonomous navigation, alignment, completion, and fault-handling behaviors.

Justification: A state machine was selected because deployment and alignment of the LATCH tunnel occur as an ordered sequence of actions rather than as a single continuous motion. The system must accept a goal, begin movement, monitor localization feedback, adjust its commands as alignment changes, recognize completion, and enter a fault condition when required. Organizing these behaviors as explicit states makes the expected software response clear at each stage of operation.

This structure also supports safer autonomous motion. State transitions can be conditioned on the fused pose estimate, sensor validity, goal completion, and fault inputs rather than allowing drive commands to continue without confirmation of system status. The state machine can therefore stop or redirect the autonomy sequence when AprilTag measurements become unreliable, when an injected fault occurs, or when the requested goal has been reached. For the prototype, this structure was also straightforward to validate through generated goals and simulated sensor

feedback.

5.3.4 Software Verification Environment

Selected: Gazebo and RViz Simulation with GoogleTest Unit Testing

Trade: Testing only on physical hardware; testing only individual software functions through unit tests; or combining unit tests with a Gazebo and RViz simulation of the complete HLC software pathway.

Justification: A combined simulation and unit testing environment was selected because complete flight-like tunnel hardware was not available during prototype development. GoogleTest provided a repeatable method for validating lower-level autonomy behavior, including command generation and state transitions under different setpoints, partially obscured AprilTag measurements, and injected fault conditions. These tests allowed errors in the software logic to be isolated before running a complete autonomy sequence.

Gazebo and RViz were then used to validate integration across the full controls pathway. The simulation provided a visual and kinematic representation of tunnel movement, while the software could be evaluated using the same types of goals, pose updates, odometry outputs, and state transitions expected during physical operation. This approach allowed the HLC design to be tested for pitch and yaw alignment cases up to 15 degrees without requiring the complete mechanical tunnel or embedded motor hardware. Together, GoogleTest and Gazebo/RViz provide both repeatability at the component level and system-level validation of autonomous alignment behavior.

5.4 Controls System Architecture

To ensure the LATCH tunnel system meets its operational requirements within the 6,000 W power limit and operates reliably in a Martian environment, trade studies were conducted for the following critical subsystems and components:

- **Motor Selection** (Drive, Elevation, and End-Positioning): Determining the optimal motor topology for high-torque mobility, high-precision actuation, and alignment.
- **Power Buffering/Battery Selection:** Evaluating onboard energy storage for peak load leveling.
- **Low-Level Microcontrollers:** Selecting the embedded architecture for real-time motor and sensor control.
- **Top-Level Compute Node:** Choosing the processing unit for autonomy, vision, and system orchestration.
- **Communication Protocol:** Selecting the data bus for intra-system telemetry and control.

Decisions were evaluated using a weighted trade matrix focusing on four primary criteria: Power Efficiency/Density (minimizing draw on the 120V habitat line), Reliability/Noise Immunity (vital for an environment with heavy EMI from the motors), Performance/Compute Headroom (torque for motors, processing speed for controllers), and Integration Complexity (software support, wiring

mass).

It was assumed that Martian gravity (3.72 m/s^2) would lessen the static loads compared to Earth testing, but the system must still be designed with a factor of safety to handle dynamic loads during 15-degree incline traversal. The total system mass is calculated at 1,530 kg. It is also assumed that the habitat's 120V power supply is generally stable, but subject to minor voltage dips under heavy transient loads.

Below is the detailed breakdown of the selected components and their derivations.

5.4.1 Motor Selection & Derivation

Distinct motor profiles were required for the three primary mechanical functions based on their torque and precision needs.

Drive System (Selected: NEMA 23 Brushless DC Motors - 24V)

Trade: BLDC vs. Brushed DC vs. Stepper Motors.

Justification: BLDCs were chosen over Steppers for the drive system due to their superior torque-at-speed characteristics, higher power efficiency, and better thermal dissipation.

Derivation: To traverse a 15-degree incline, the system must overcome the parallel component of Martian gravity. With a total system mass of 1,530 kg and Martian gravity of 3.72 m/s^2, the force acting against the system is roughly 1,473 N. The drive system utilizes 8 NEMA 23 BLDC motors, each with a 25:1 gear reduction, allowing for 56.25 Nm of output torque per motor. This provides a total of 450 Nm of torque spread across the 8 motors, which yields a safety factor of $\sim$ 3.2x to overcome the elevation requirement (CT-08.02).

Elevation System (Selected: NEMA 23 Stepper Motors - 48V)

Trade: Stepper Motors vs. Servo Motors.

Justification: Steppers provide maximum holding torque at zero RPM. Because the elevation system must maintain a static height for prolonged periods without back-driving, steppers are ideal. A 24V electromagnetic power-off brake was also recommended to lock the position.

Derivation: The elevation system uses 4 NEMA 23 stepper motors (no gear reduction) driving M6 titanium bolts with 2 mm fine pitch to accommodate the 0.4 m height compensation (CT-08.01). The total resting weight of the 1,530 kg system on Mars is approximately 5.69 kN. The 4 stepper-based actuation systems provide 17.1 kN of combined lifting force, giving the system a robust safety factor of $\sim$ 3x.

End-Positioning Mechanism (Selected: NEMA 23 Stepper and Pancake Motors)

Trade: Standard Steppers vs. Flat/Pancake Steppers for spatial constraints.

Justification: The end-effector requires precise manipulation of the docking interface (CT-08). A standard NEMA 23 stepper with a 5:1 gear reduction (11.25 Nm of output torque) was selected for vertical actuation. For the horizontal pivot, space constraints dictated a high-torque NEMA 23 pancake (flat) motor with a 100:1 gear reduction, providing a massive 127.5 Nm of output torque.

Derivation: Because the end-effector only manipulates the docking interface and does not bear the 1,530 kg load of the tunnel, the selected output torques provide a safety factor of $\sim$ 3x for the required alignment forces.

5.4.2 Embedded Controllers

Selected: STM32 Nucleo Boards

Trade: STM32 (ARM Cortex-M) vs. Arduino (AVR) vs. ESP32.

Justification: Generating precise, synchronized step pulses for the elevation steppers and closed-loop PWM control for the BLDCs requires strict hardware determinism. STM32s feature advanced hardware timers with dedicated motor control features.

5.4.3 Top-Level Controller

Selected: NVIDIA Jetson Compute Module

Trade: Jetson vs. Raspberry Pi 4 vs. Industrial PC.

Justification: The perception system relies on camera data to autonomously identify the docking interface and align the end-positioning mechanism. The Jetson platform features dedicated CUDA cores for hardware-accelerated tensor operations, processing visual data at frames-per-second rates that standard microprocessors cannot achieve.

5.4.4 Communication Protocol

Selected: Controller Area Network (CAN)

Trade: CAN bus vs. I2C/SPI vs. Ethernet.

Justification: The LATCH system features a distributed architecture spanning significant physical distances, passing near heavy EMI sources (motors). CAN bus utilizes differential signaling, making it highly immune to electromagnetic noise. Its multi-master architecture ensures that the Jetson, STM32s, and motor drivers can broadcast telemetry and receive commands reliably with guaranteed latency.

6 Testing and Results

6.1 Verification

L1 Requirements						
Requirement ID	**Literature Review**	**Hand Calculation**	**CAD/Simulations**	**Testing**	**Verified?**	**Verification Notes**
Crew Transportation						
CT-01				X	Yes	Inspection
CT-02				X	Yes	Handrail testing was performed for varying heights, distances apart, and inclines
CT-03			X		Yes	Sims run for 530 N shock load, 3000 N static load over two footprints, and 142 kPa dynamic load (to simulate walking)
CT-04			X		Yes	Sims run for 5000 N load applied on scissor mechanisms
CT-05			X		Yes	Inspection
CT-06			X		Yes	Inspection
CT-07				X	Yes	Top-half prototype confirmed extension and retraction of two tunnel segments
CT-08				X	Yes	Bottom-half prototype confirmed pitch, yaw, and elevation change
CT-09			X		Yes	Sims run for 5000 N load on scissor mechanisms for collapsed, partially-extended, and fully-extended cases
CT-10			X		Yes	Gazebo modeling of course motion
CT-11				X	Yes	Pitch, yaw, roll, right-left, and elevation degrees modeled on bottom-half prototype; back-forward degree modeled on top-half prototype
Environmental Control						
EC-01	X				Yes	Vectran fabric picked used by NASA for space applications
EC-02	X				No	No specific method of temperature regulation picked out
EC-03	X				No	Not all components necessary for space system were picked out and thus not all could be confirmed to stay below 60 dB noise level
EC-04	X				No	Dust tolerance was not researched to pick out a material or specific application of a "dust door"
EC-05	X				Yes	Vectran fabric picked used by NASA for space applications
EC-06				X	Yes	Bottom-half prototype was run over simulated rocky Martian terrain
EC-07	X				No	Due to the lack of hatch specifications, seal estimation, simulation or testing was performed
Operational Capability						
OC-01	X				No	Not all components necessary for space system were picked out and thus not all could be confirmed to be operational for the 30 sol minimum
OC-02	X				Yes	Vectran fabric picked used by NASA for repeated inflatable space applications
Resource Efficiency						
RE-01			X		No	System mass, estimated with CAD, exceeded the 230 kg requirement
RE-02		X			Yes	Motor selected has a high enough torque output to extended the tunnel within a couple of minutes
RE-03			X		Yes	Inspection
RE-04				X	Yes	User interface requires only one crew member to operate it
RE-05	X				Yes	Power budget from space-relevant system was found to be under 6000 Watts
RE-06				X	Yes	User interface allows for teleoperation

Figure 40: Level 1 Requirement Verification

L2 Requirements						
Requirement ID	**Literature Review**	**Hand Calculation**	**CAD/Simulations**	**Testing**	**Verified?**	**Verification Notes**
Crew Transportation						
CT-01.01				X	Yes	User interface testing
CT-01.02				X	Yes	User interface testing
CT-01.03				X	Yes	User interface testing
CT-01.04				X	Yes	Inspection
CT-01.05				X	Yes	Inspection
CT-01.06				X	Yes	User interface testing
CT-02.01				X	Yes	Handrail testing
CT-02.02			X		Yes	Inspection
CT-02.03			X		Yes	Inspection
CT-02.04				X	Yes	User interface testing
CT-02.05				X	Yes	Walkway and handrail testing
CT-02.06			X		Yes	Sims run on handrails in collapsed, partially-extended, and fully-extended cases with a with a 370 N uniaxial load
CT-02.07				X	Yes	Walkway testing
CT-02.08				X	Yes	Bottom-half prototype testing
CT-03.01			X		No	We did not have enough time for appropriate wind testing or simulations
CT-03.02			X		Yes	Sims run for 142 kPa dynamic load to simulate walking on floor beams and roll-up floor
CT-03.03				X	Yes	Sims run for 530 N shock load
CT-07.01			X		Yes	Inspection
CT-07.02			X		Yes	Inspection
CT-07.03				X	Yes	Inplemented by high level controls code
CT-08.01				X	Yes	Bottom-half prototype testing for pitch angle
CT-08.02				X	Yes	Bottom-half prototype testing
CT-08.03				X	Yes	Inplemented by high level controls code
CT-08.04			X		Yes	Gazebo confirmed autonomous deployment sequence
CT-08.05				X	Yes	Bottom-half prototype testing
CT-08.06				X	Yes	User interface testing
CT-09.01			X		Yes	Sims run for 5000 N load on scissor mechanisms for collapsed, partially-extended, and fully-extended cases
CT-10.01				X	Yes	Gazebo confirmed system tracking
Environmental Control						
EC-02.01	X				Yes	Vectran fabric picked used by NASA for space applications
EC-04.01			X		No	We did not have enough to implement this idea past the conceptual phase
EC-05.01	X				Yes	Vectran fabric picked used by NASA for space applications
Operational Capability						
OC-01.01	X				Yes	Materials and mechanisms selected were found to have a long lfie cycle
OC-01.02	X				Yes	Materials and mechanisms selected were found to have a long lfie cycle
Resource Efficiency						
RE-05.01	X				Yes	Selected components were found to require less than 4.5 kW hours to power
RE-05.02	X				Yes	Buck converter selected to convert 120 V to lesser voltage

Figure 41: Level 2 Requirement Verification

Top-level system and subsystem requirements were verified through literature review, hand calculations, CAD/simulations, and physical testing.

6.2 Top-Half Prototype

In order to test the designed capabilities of the rack, validation testing was performed on the full-system prototype. All tests are outlined in this section, and are broken down by subsystem.

6.2.1 Frame

Unit testing of the structural rings can be found in the “passive extension” section of the report. Verification and validation of the structural rings can be found in the “passive extension” section

of the report.

6.2.2 Shell

Unit Testing was not performed on the softgoods shell due to complex geometry and material properties that cannot be simulated easily with our software. Verification and validation of the shell was done through literature review.

6.2.3 Passive Extension

Test 1: Scissor Mechanism Simulation

Purpose This is a verification test to evaluate the structural integrity of the scissor mechanism during operation. The goal is to verify that the scissor mechanism can safely withstand operational loads and repeated cycling without exceeding material limits or experiencing premature fatigue failure.

Test Requirements

- CT-03.02: The tunnel shall be able to support a load of 2000 N from two people walking at a speed between 1.11 m/s and 1.39 m/s.
- CT-03.03: The tunnel shall be able to withstand a maximum force of 530 N, dropped from a maximum height of 1 meter.
- CT-09.01: The tunnel shall support 2000 N of force at any of its deployed lengths.

Test Materials The materials used for testing were as follows:

- CAD Software (Siemens NX)
- Tunnel CAD
- Simulation Software with CAD (Solidworks FEA)

Test Procedure The following test procedure was used to fulfill the test objectives:

1. Define material properties for all scissor components.
   (a) Titanium Ti-5Al-2.5Sn
2. Apply boundary conditions:
   (a) Define 4 pin connections
   (b) Define 2 slider interfaces
   (c) Fix on structural ring
   (d) Apply force at linear actuator connection point. 5000 newtons at each connection point estimated with Martian gravity.

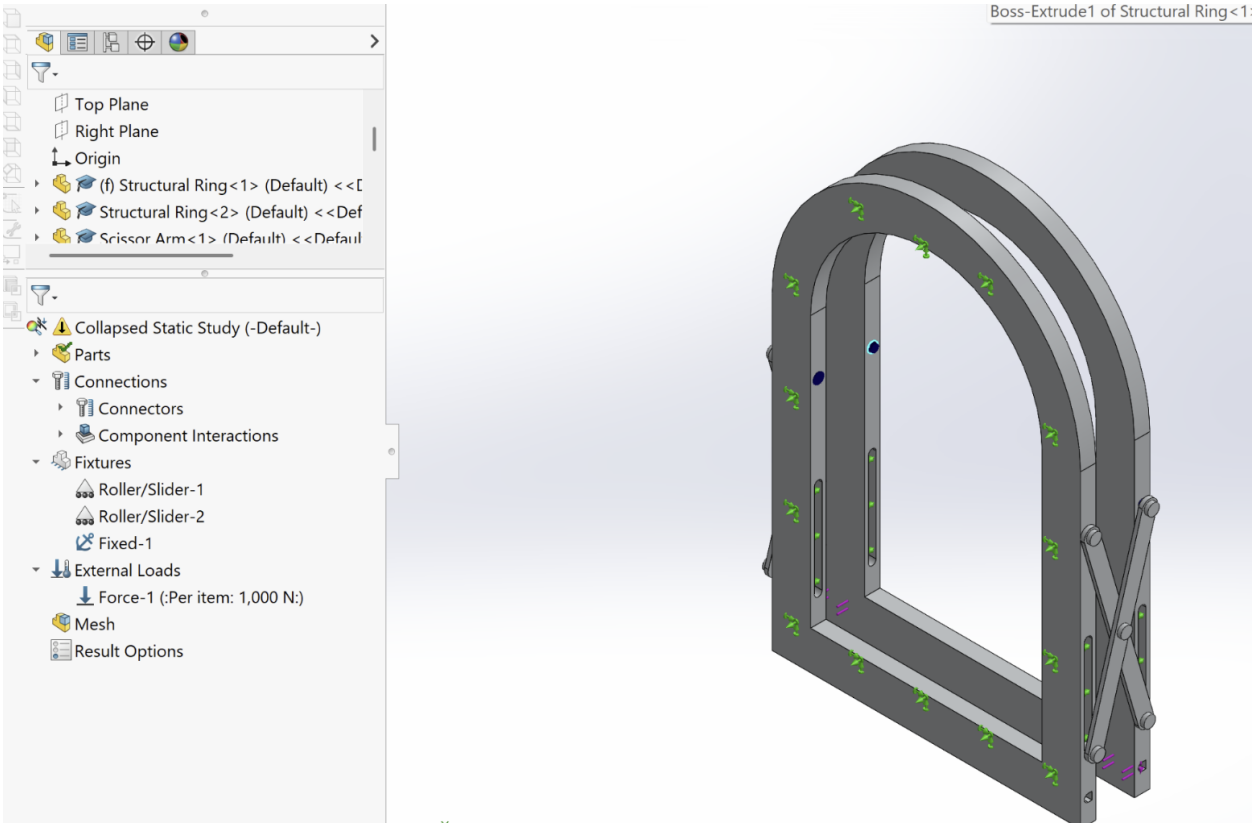

Figure 42: Passive Extension Simulation Applied Forces

3. Run static FEA for each position. Record Von Mises stress, displacement, factor of safety, and contact pressures at pivot joints.
4. Set up a fatigue study using the static results as the loading input. Define the cyclic loading profile (fully reversed or zero-to-max per the operational duty cycle).

Variable	**Maximum Value**	**Yield Strength**
Von Misses Stress	$1.282\times10^{7}\ N/m^2$	$8.270\times10^{8}\ N/m^2$
Displacement	9.238×10^{-2} mm	-
Strain	6.352×10^{-5}	-

Table 10: Collapsed Static Simulation Results

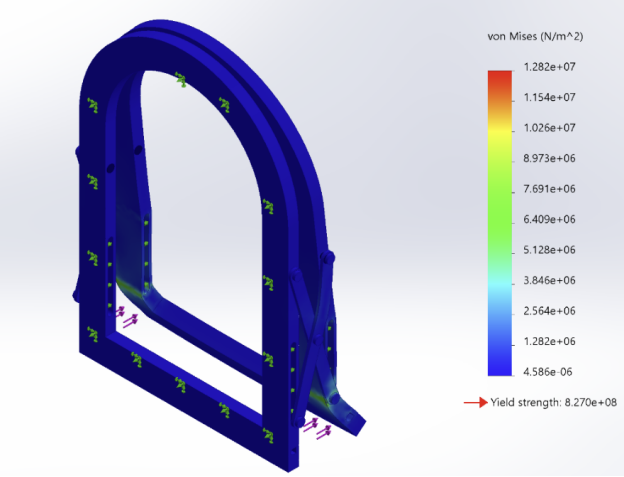

Figure 43: Compressed Simulation Result

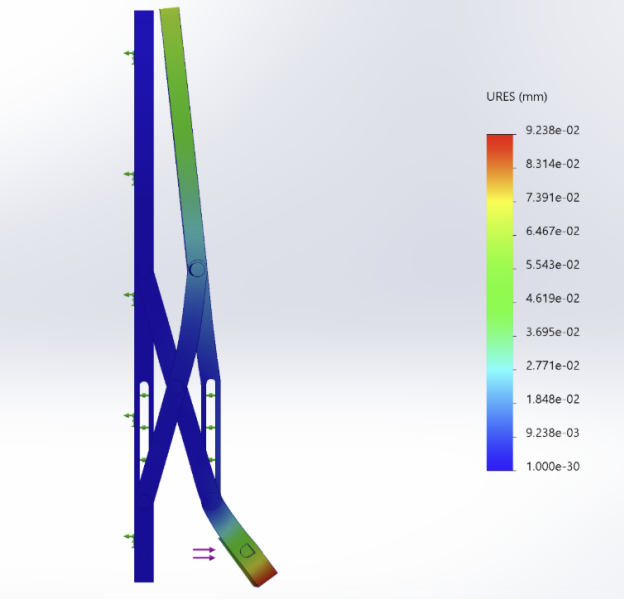

Figure 44: Compressed Simulation Strain Result

Variable	**Maximum Value**	**Yield Strength**
Von Misses Stress	$10^7\ N/m^2$	$8.270\times10^8\ N/m^2$
Displacement	10^{-2} mm	-
Strain	10^{-5}	-

Table 11: Extended Static Simulation Results

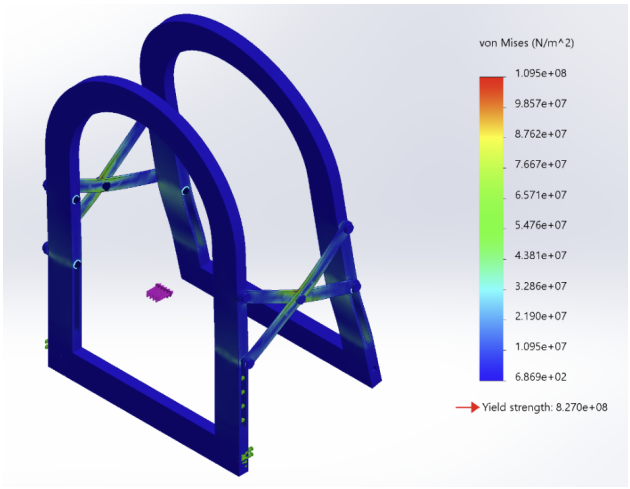

Figure 45: Extended Simulation Result

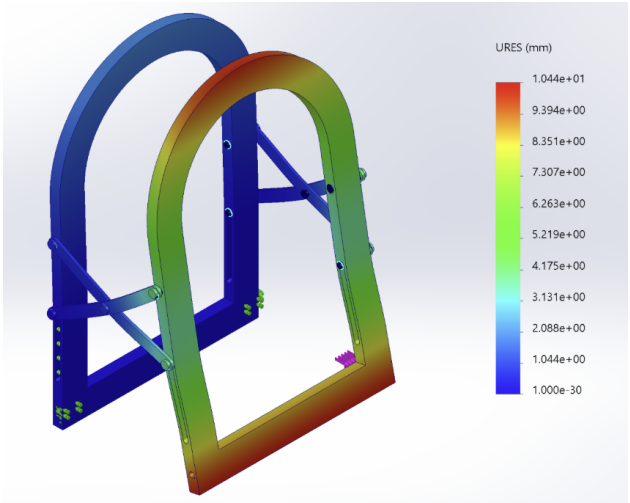

Figure 46: Extended Simulation Strain Result

Test Results and Analysis The results from the two different simulations above show that the scissor mechanism is structurally capable of withstanding the operational loads. Across all extension states, the Von Mises Stress is well below the yield strength of Aluminum 6061 which indicates a low risk of structural failure. The minimal deformation and stress shows that the mechanism is able to keep its structural integrity during operational use. These results support the feasibility of the current design.

Test 2: Top-Half Prototype Scissor Mechanism Extension

Purpose This is a verification that the scissor mechanism is able to smoothly extend and retract with the tunnel.

Test Requirements

- RE-03: The system shall have an extension ratio of at least 1:2.

Test Materials The materials used for testing were as follows:

- Top-Half Prototype with the scissor mechanisms attached.

Test Procedure

1. Start with the scissor mechanism fully retracted.
2. Extend the rings in random increments to check if the the scissor mechanisms are stable stopping at any point.
3. Extend the scissor mechanism to their full length.
4. Repeat steps 1-3 at for at least three cycles to confirm the extension and retraction works.

Test Results and Analysis Upon completing this test we were able to observe the smooth extension and retraction of the scissor mechanism. This test was completed on the physical prototype, which is made of a different material than the idealized design (steel vs aluminum), meaning the extension mechanism is similar, but factors such as friction and weight could change the results of this test in practice. With the steel scissor mechanism we were able to successfully fulfill RE-03, as the tunnel was able to extend and retract with a 1:3 ratio with no interference from the scissor mechanism.

6.2.4 Handrail

In order to test the designed capabilities of the handrail subsystem, unit testing and validation testing were performed. Unit testing was used in tandem with rapid-prototyping to iteratively finalize the system designs. All verification and validation testing was performed on the Top-Half prototype. All tests are outlined in this section.

Test 1: Handrail Simulation

Purpose This is a verification plan to ensure that the handrail components of the top half maintain stability during operation, and that the handrails can withstand the expected loads.

Test Requirements

- CT-02.01: The tunnel shall have mobility assistance surfaces that aid in walking.
- CT-02.06: The mobility assistance surfaces shall be able to bear a minimum of 370 N of force in any direction.

Test Materials The materials used for testing were as follows:

- CAD Software (Siemens NX)
- Tunnel CAD
- Simulation Software with CAD (ANSYS Mechanical)

Test Procedure The following test procedure was used to fulfill the test objectives:

1. Import and assemble handrail assembly in Ansys Mechanical.
2. Set applicable constraints into Ansys to specify connections and fixed points. Use sketches to simulate the point where the handrail is connected to the frame and where the hand is putting force.
3. Set the component material to Titanium Ti-6Al-4V.
4. Generate the component mesh, setting the mesh grain size to 0.01 meter.
5. Insert load condition:
   (a) A 370 N distributed load in the center of the handrail (worst case scenario).
      i. 10s constant load
6. Run each load condition in Ansys.

Component	**Stress (Pa)**	**Strain**	**Deformation (μm)**	**Safety Factor**
Large Handrail	1.77×10^{7}	1.60×10^{-4}	140	15
Middle Handrail	6.10×10^{6}	6.50×10^{-5}	5.4	15
Large Handrail	6.30×10^{7}	6.60×10^{-4}	450	15

Table 12: Handrail Test Results and Analysis

Test Results and Analysis Siemens NX was used to model the handrails, and ANSYS Mechanical was used to test the handrails. The results are listed in Table 4. Before running any simulations, the fixed support locations were assigned based on the fullscale model of the tunnel. Additionally, downward stress was applied at 3 different points to model the use case of the handrail. Lastly, ANSYS' stress, strain, and deformation tools were used to perform the analysis.

The handrail with the smallest cross section experienced the most stress, which was expected as there is the smallest area moment of inertia, making the geometry unfavorable. The middle handrail was the most stable, which follows as it is supported by the ball bearings as well as the two handrails attached to it. Simulations found that the maximum stress fell below the yield strength of Titanium Ti-6Al-4V for all 3 load tests. The deflection found for each handrail section was found to be very small as well. In conclusion, the handrails were able to maintain structural integrity under the expected loads.

Test 2: Top-Half Handrail Extension

Purpose This is a verification that the handrails are able to smoothly extend and retract with the scissor mechanisms of the tunnel.

Test Requirements

- RE-03: The system shall have an extension ratio of at least 1:2.

Test Materials The materials used for testing were as follows:

- Top-Half Prototype with the scissor mechanisms and handrails attached.

Test Procedure The following test procedure was used to fulfill the test objectives:

1. Start with the handrails fully retracted.
2. Extend the handrail in random increments to check if the handrails are stable at every point in the extension.
3. Extend the handrails to their full length.
4. Repeat steps 1-3 at for at least three cycles to confirm the extension and retraction works.

Test Results and Analysis Upon completing this test we were able to observe the smooth extension and retraction of the handrails. This test was completed on the physical prototype, which is made of a different material than the flight design (cardboard vs aluminum), meaning the extension mechanism is similar, but factors such as friction and weight could change the results of this test in practice. With the cardboard tubes we were able to successfully fulfill our relevant requirement, as the tunnel was able to extend and retract with a 1:3 ratio with no interference from the handrails.

6.3 Bottom-Half Prototype

6.3.1 Active Extension

In order to test the designed capabilities of the drive subsystem, unit testing and validation testing were performed. Unit testing was used in tandem with rapid-prototyping to iteratively finalize the system designs. All tests are outlined in this section.

Test 1: Rock Traversal

Purpose The purpose of this test is to verify that the bottom half prototype of the proposed tunnel can successfully navigate through Martian terrain.

Test Requirements

- EC-06: The system shall allow for travel across rough Martian terrain.

Test Materials The materials used for testing were as follows:

- Rocks 1-9 centimeters in diameter.
- Assembled drive system (treads, body, motors).

Test Procedure The following test procedure was used to fulfill the test objectives:

1. Set up an environment for testing by setting up a playing field covered in rocks.
2. Place the prototype into the environment.
3. Step away from the environment and allow the prototype to traverse the environment.

4. Stop the prototype at the end of the test from afar.
5. Retrieve prototype and assess any damage incurred.
6. Record observations.

Trial 1 Damage	Trial 1 Success	Trial 2 Damage	Trial 2 Success	Trial 3 Damage	Trial 3 Success
none	yes	none	yes	Moderate damage to end position structure (separated)	Moderate (Reached end point with damage)

Table 13: Active Extension Rocky Terrain Testing Results

Test Results and Analysis

6.3.2 End Positioning

In order to test the designed capabilities of the end positioning subsystem, validation testing was performed. All verification and validation testing was performed on the Bottom-Half prototype, and all tests are outlined in this section.

Test 1: Pitch Angle Control

Purpose The purpose of this test is to verify the system can accommodate a pitch difference of up to 15 degrees relative to the connecting habitat.

Test Requirements

- CT-08.02: The tunnel shall accommodate relative angular difference of up to 15 degrees (pitch and yaw) between surface habitats.

Test Materials The materials used for testing were as follows:

- Bottom-Half prototype assembly.
- Adjustable platforms/blocks to raise the target mockup.
- 2x GOTECK 70KG Brushless Digital Servo.
- Complete wiring/power setup.

Test Procedure The following test procedure was used to fulfill the test objectives:

1. Set up the target docking mockup in a fixed, level position.
2. Initialize the tunnel system at a standard level resting state.
3. Angle the target mockup up/down by 15 degrees (pitch).
4. Command the system to adjust its platform/tunnel to match the angle.
5. Record visual evidence.

Test Results and Analysis The test proved to be a success, as the mechanism was fully capable of moving to the exact specified angle. The rest position (0°) was determined to be at the level position, positive was an upward angle, and negative was a downward angle. Shown in the figures below are the mechanism at rest, a downward angle, and upward angle.

Test 2: Yaw Angle Control

Purpose The purpose of this test is to verify the system can accommodate a pitch difference of up to 15 degrees relative to the connecting habitat.

Test Requirements

- CT-08.02: The tunnel shall accommodate relative angular difference of up to 15 degrees (pitch and yaw) between surface habitats.

Test Materials The materials used for testing were as follows:

- Bottom-Half prototype assembly.
- 1x lazy susan for angular freedom.
- 1x GOTECK 70KG Brushless Digital Servo.
- 2x Spacers for structural support.
- Complete wiring/power setup.

Test Procedure The following test procedure was used to fulfill the test objectives:

1. Set up the target docking mockup in a fixed, forward position.
2. Initialize the tunnel system at a standard forward resting state.
3. Angle the target mockup left/right by 15 degrees (yaw).
4. Command the system to adjust its platform/tunnel to match the angle.
5. Record visual evidence.

Test Results and Analysis This test also proved to be a success, as the mechanism was fully capable of moving to specified angles in a 180°range. The rest position (0°) was facing straight ahead, and the mechanism could move 90°both ways. Shown in the figures below is the mechanism at various positions in its 180°range.

Based on both of these tests, we can conclude the objectives were met and can verify that this mechanism meets the specified requirements. The biggest takeaway from this testing is that the system's physical structure can constrain the angular movement slightly when both pitch and yaw are controlled at the same time, so if the mechanism was to be redesigned, those constraints would be something to take note of.

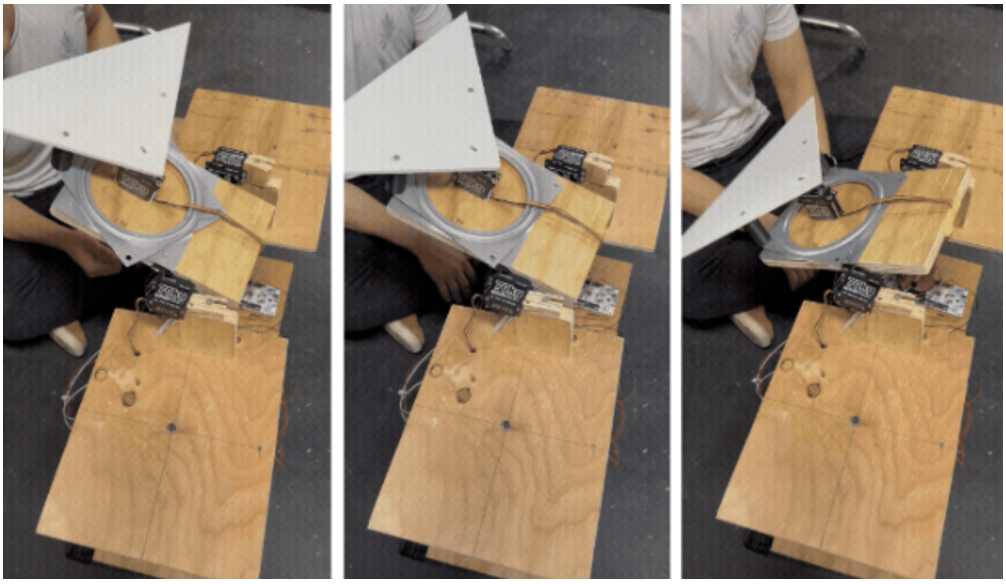

Figure 47: End Positioning Mechanism Testing

6.3.3 Elevation Change

The following outlines the full system verification and validation testing that was performed for the elevation change subsystem.

Test 1: Elevation Height Control

Purpose The purpose of this test is to verify that the prototype's nested lead screw mechanism can successfully execute smooth vertical translation and reliably achieve up-and-down motion to validate the elevation change architecture.

Test Requirements

- CT-08.01: The tunnel system shall accommodate a relative elevation difference of up to 0.4 meters between surface habitats.

Test Materials The materials used for testing were as follows:

- Bottom-Half prototype assembly.
- 2x NEMA 17 stepper motors.
- 2x 330 mm lead screws (2 mm thread pitch) with matching follower nuts.
- Embedded microcontroller (STM32 Nucleo) and motor drivers.
- Complete wiring/power setup.

Test Procedure The following test procedure was used to fulfill the test objectives:

1. Secure the bottom-half prototype frame on a level testing surface in its fully lowered resting position.

2. Initialize the microcontroller and supply logic and motor power to the NEMA 17 stepper motor drivers.
3. Command the stepper motors to rotate in a forward direction to drive the internal 330 mm lead screws.
4. Observe the vertical translation of the nested inner tubes as they extend upward to their maximum stroke length.
5. Command the stepper motors to reverse direction to return the actuators to their baseline position.
6. Verify smooth mechanical clearance, checking for any binding or stalling during the extension and retraction cycles.

Test Results and Analysis This test successfully validated the fundamental mechanics of the lead-screw elevation design. When commanded, the NEMA 17 stepper motors effectively translated rotational torque into linear vertical motion, driving the nested tubes smoothly through their entire 330 mm structural stroke length.

Because this bottom-half prototype was scaled down by a factor of three, demonstrating a clean 330 mm (0.33 m) structural stroke successfully confirms that the full-scale design can comfortably accommodate the required 0.4-meter elevation difference. Additionally, the 2 mm fine pitch of the threads natively provided an exceptional self-locking capability, maintaining the platform's height perfectly when the motors were unpowered.

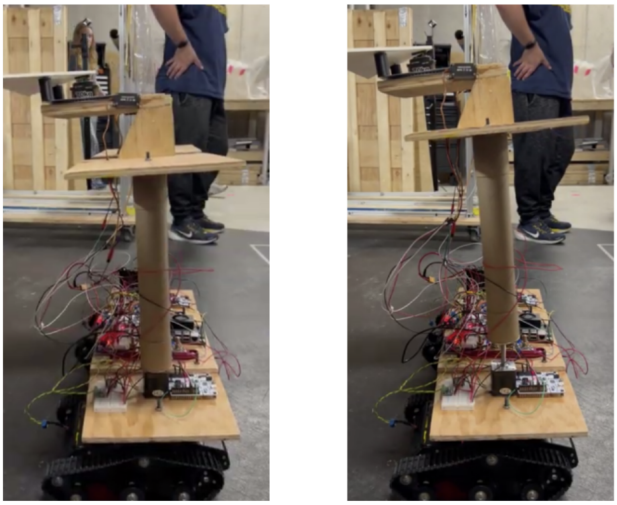

Figure 48: Elevation Change Testing

6.3.4 Suspension

No unit, verification, or validation testing was performed on the suspension subsystem. The subsystem was designed in response to a late-stage identification of a rigid-mount failure mode, and the remaining project timeline did not permit fabrication of a prototype or execution of a test plan.

6.4 User Interface

In order to test the designed capabilities of the User Interface subsystem, unit testing and validation testing were performed. Unit testing was used in tandem with rapid-prototyping to iteratively finalize the system designs. All verification and validation testing was performed on a full-system prototype. All tests are outlined in this section.

Test 1: Verification of Functional Requirements

Purpose This test verifies that the GUI meets the core functional requirements mandated for the LATCH system, specifically regarding emergency communication, system monitoring, and manual control.

Test Requirements

- CT-01.02: The graphical user interface shall aid with emergency communication between crew members.
- CT-01.05: The graphical user interface shall display the internal conditions within the tunnel.
- CT-01.06: The graphical user interface shall allow a crew member to manually override the system.

Test Materials A functional UI prototype was used alongside a stopwatch and NASA-TLX feedback forms, all within a standardized testing environment supplied with randomized task sheets.

Test Procedure The following test procedure was used to fulfill the test objectives:

1. Initiate the UI prototype at the primary entry screen.
2. Observe the tester as they attempt to locate the Internal Pressure and Power Consumption metrics as required by Procedure 2.
3. Trigger a multiple alert state and record the time taken for the user to navigate to the resolution procedure for both high and low severity alerts.
4. Direct the user to enter manual override mode and verify that the system successfully hands over control from the autonomous state machine.
5. Verify that all interactive buttons are responsive and reachable within the digital interface.

Test Results and Analysis The UI met all validation criteria for L1 and L2 requirements. All testers successfully located internal pressure and power metrics during Procedure 2, satisfying CT-01.05. Manual override functionality was verified, though testing revealed that a confirmation pop-up screen is needed upon exiting manual mode to prevent unintentional handovers to the autonomous system (CT-01.06). For CT-01.02, testers resolved alerts within an average of 8.07 seconds as novices and 5.28 seconds after training, satisfying the requirement for rapid emergency communication.

Test 2: User Interface Intuitiveness and Expert Benchmarking

Purpose The purpose of this test was to evaluate the intuitiveness of the graphical user interface (GUI) for an untrained user and to measure the learning curve associated with specialized tunnel operations. By comparing walk-up-and-use performance against expert benchmarks and post-training trials, the team was able to determine whether the UI design facilitates rapid operation during both nominal and emergency scenarios.

Test Objectives

- Measure the time required for a first-time user to complete sequential tasks without prior training.
- Quantify the "Multiple of Expert" (MoE) ratio by comparing tester times against a 1.0x expert benchmark.
- Assess the proficiency gain after a single training session to determine the learning curve.
- Identify specific UI elements that impede navigation or successful task completion.

Test Materials A functional UI prototype was hosted on a high-resolution display to simulate the tunnel control terminal. Procedure timing was recorded to the millisecond using a digital performance timer for Time-on-Task (ToT) measurement, recording how long a user takes to complete a given performance from start to finish. Mental demand, physical demand, and frustration were assessed through the NASA-TLX Subjective Workload Scale. Completion status, error counts, and timestamp data were logged in real time using a tracking spreadsheet. Finally, randomized Standardized Task Instruction Sheets were provided to testers to maintain test integrity.

Test Procedure Testing utilized a within-subjects design in which testers performed three distinct procedures, with the order randomized to mitigate learning bias.

1. An expert user established the "Gold Standard" time for each procedure.
2. Trial A (Novice): Untrained testers were asked to complete the three procedures with zero prior exposure to the UI layout.
3. A two-minute training session was provided to familiarize testers with the UI information.
4. Trial B (Trained): Testers repeated the procedures to measure proficiency gains.
5. For each trial, the team recorded the time to complete, any "mis-clicks" or navigational errors, and the NASA-TLX workload scores.

Test Results and Analysis The interface demonstrated high intuitiveness, with novice testers able to navigate to critical telemetry without prior assistance.

Metric	Procedure 1	Procedure 2	Procedure 3
Expert Benchmark (sec)	10.51	12.43	4.56
Trial A: Novice Avg (sec)	24.07	26.57	8.07
Trial B: Trained Avg (sec)	14.26	15.86	5.28
Initial MoE (Novice/Expert)	2.29x	2.21x	1.79x
Proficiency Gain (%)	40.76	40.31	34.57

Table 14: User Interface Testing Results

Across the three procedures, the data shows an average proficiency gain of 38.5%, indicating that the UI layout is quickly memorized and the operational logic is easy to internalize. While novice users initially performed at roughly 2.1x the expert benchmark, a single training session allowed them to close that gap significantly. Procedure 3 participants, for example, reached a trained completion time within 0.72 seconds of the expert gold standard.

6.5 Controls Testing

6.5.1 High Level Controls

Testing for High Level Controls was performed at the software unit-test and software-integration levels. The prototype did not represent complete flight hardware or environmental behavior; instead, testing focused on verifying command generation, state transitions, pose-estimation pathways, and simulated goal-reaching behavior.

Test 1: Command Generation (GTests)

Purpose To verify that the HLC command generation software produces appropriate motion commands for a defined relative alignment goal.

Test Objectives

- Exercise command generation for representative extension and alignment cases, including the maximum pitch and yaw alignment conditions represented by the software prototype.

Test Procedure:

1. Twelve automated tests feed generated goals into the command generation logic.
2. The cases include 0 deg pitch/0 deg yaw full extension, 0 deg pitch/15 deg yaw, 15 deg pitch/0 deg yaw, and 15 deg pitch/15 deg yaw, with additional intermediate cases used to complete the test set.

Test Results and Analysis: The tested command generation logic correctly executed commands to reach the provided goals. This verifies the command-generation portion of the autonomous drive pathway for the tested software cases.

Test 2: State Machine Logic (GTests)

Purpose To verify that system state transitions occur correctly as localization feedback, goal progress, teleoperation requests, and fault conditions change.

Test Objectives

- Validate nominal autonomous transitions and confirm that non-nominal inputs can enter the intended teleoperation or fault behavior.

Test Procedure:

1. Ten automated tests feed sequences of fake AprilTag and odometry feedback into the state machine.
2. Cases include partially obscured AprilTag information, injected faults, and different setpoints.

Test Results and Analysis: The state machine correctly transitioned on all tested state events. The test results support the use of explicit states for autonomous sequencing and error handling within the prototype software.

Test 3: Gazebo + RViz End-to-End Autonomy Simulation

Purpose To test the integrated HLC software pathway from a relative alignment goal through state machine behavior, motion commands, simulated movement, and reported feedback.

Test Requirements

- CT-08: The system shall provide a means of aligning with the connecting surface element.
- CT-08.04: The alignment method shall be autonomous.

Test Procedure:

1. The ROS2 HLC nodes are launched with the Gazebo and RViz tunnel model.
2. Python scripts issue goal-reaching scenarios. Pitch behavior is exercised at 0°, 5°, 10°, and 15°at the joint-state level, and yaw behavior is exercised at 0°, 5°, 10°, and 15°at the simulation level.
3. The scripts assert intermediate outputs such as joint states, odometry, and state progression.

Test Results and Analysis: The simulation exercised the full software stack and demonstrated the intended prototype pathway for autonomous alignment. This provides verification of the software architecture and testability of the alignment sequence in simulation. It does not by itself validate final motor sizing, sensor performance in the Martian environment, or hardware fault response.

Test 4: Localization Pathway Verification

Purpose To verify that the localization architecture accepts odometry and AprilTag pose information and produces the fused pose used by state machine/navigation.

Test Requirements

- CT-08.03: The sensors shall measure the relative X, Y, and Z location of the connecting surface elements.

Test Procedure

1. AprilTag pose and odometry inputs are published through their associated prototype topics, passed to the EKF localization node, and observed at the fused-pose output consumed by the central context and state machine/navigation logic.
2. Cases with reduced AprilTag availability are represented in state machine testing through partially obscured tag input.

Test Results and Analysis The software architecture establishes the required localization data path and supports use of odometry when AprilTag information is reduced. Quantitative accuracy, covariance tuning, and camera-range performance require further validation using hardware sensor data and a representative docking target.

The High Level Controls design provides a clear software pathway between operator goals, sensor information, localization, autonomous decision making, and motor commands. The selected modular ROS2 architecture allows the major functions of the system to be tested separately while still operating together through the context and action pathways. The state machine gives the autonomous process a defined sequence and includes teleoperation and fault paths instead of relying on unrestricted command execution.

Software testing verified command generation and state transition logic for the tested cases. The Gazebo and RViz simulation provided a system-level environment for exercising goal-reaching autonomy over representative pitch and yaw alignment cases. The EKF localization approach is appropriate for the system because it combines the direct pose information of AprilTags with continued odometry when the visual target is unavailable.

The HLC prototype therefore demonstrates that the proposed autonomy architecture can support software-level extension and alignment behavior. The design is not yet flight ready: the remaining work is primarily integration with physical sensors and actuators, quantitative localization validation, fault-response validation, and environmental and reliability testing.

6.5.2 Controls System Architecture

Due to project timeline constraints and the absence of physical, full-scale hardware, validation of the System Architecture, Power Subsystem, and Actuation Mechanisms was performed purely analytically. Rather than physical testing or software simulation, mathematical hand calculations were utilized to verify that the recommended components meet the mission requirements under theoretical Martian conditions.

Test 1: Drive System Torque Verification (Hand Calculation)

Purpose To analytically verify that the selected NEMA 23 Brushless DC motors and gearboxes provide sufficient torque to propel the 1,530 kg system up the required incline.

Test Objectives Calculate the theoretical dynamic load on a 15° incline in Martian gravity. Verify that the selected motors meet this load with an adequate safety factor.

Test Materials Free-body diagram kinematic equations. Motor and gearbox manufacturer specification sheets.

Test Procedure

1. Input system constants: System Mass = 1,530 kg; Martian Gravity = 3.72 m/s^2; Max Incline = 15°.
2. Calculate the parallel component of gravity acting against the system using fundamental trigonometry.
3. Compare the required force against the combined theoretical continuous output torque of the 8 BLDC motors with 25:1 gear reductions.

Test Results and Analysis Hand calculations confirmed that the parallel force of Martian gravity acting on the system at a 15° incline is approximately 1,473 N. The 8 selected NEMA 23 BLDC motors, with their gear reductions, produce a combined theoretical maximum of 450 Nm of torque. Calculations prove that this architecture provides a minimum safety factor of $\tilde{3}$.2x under static loads. This provides sufficient theoretical overhead for dynamic friction and regolith resistance. The objective was met.

Test 2: Elevation System Load Verification (Hand Calculation)

Purpose To analytically verify the lifting capabilities of the NEMA 23 Stepper motors and lead screw mechanisms in the elevation subsystem.

Test Objectives Verify that the 4 stepper-driven lead screws can theoretically lift the resting mass of the system without back-driving.

Test Materials

- Linear actuation and mechanical advantage equations.
- Stepper motor holding torque specifications.

Test Procedure

1. Calculate the total resting weight of the system in Martian gravity.
2. Calculate the mechanical advantage provided by M6 titanium bolts with a 2 mm fine pitch.
3. Determine the total theoretical lifting force generated by the 4 NEMA 23 Steppers.

Test Results and Analysis Calculations determined the resting weight of the system on Mars is approximately 5.69 kN. By factoring in the mechanical advantage of the 2 mm pitch lead screws, the 4 stepper motors generate a theoretical lifting force of 17.1 kN. This yields a robust $\tilde{3}$x safety factor. The mathematical analysis verifies the components are appropriately sized for the elevation requirements. The objective was met.

Test 3: Platform End-Positioning Mechanism Torque Verification (Hand Calculation)

Purpose To analytically verify that the chosen standard stepper and flat pancake motors provide sufficient torque for the vertical and horizontal alignment of the docking platform.

Test Objectives Validate that the selected gearing and motor topologies can overcome mating/docking resistances with a safety factor of at least 3.

Test Materials

- Rigid body rotational torque equations.
- NEMA 23 stepper and pancake motor specification sheets.

Test Procedure

1. Isolate the mass properties of the docking interface (noting it is mechanically decoupled from the main 1,530 kg tunnel load).
2. Calculate the output torque for the vertical axis using a standard NEMA 23 stepper with a 5:1 gear reduction.
3. Calculate the output torque for the horizontal pivot axis using a high-torque NEMA 23 pancake motor with a 100:1 gear reduction.
4. Compare calculated outputs against the estimated alignment and latching resistance forces.

Test Results and Analysis Hand calculations showed that the vertical stepper configuration outputs 11.25 Nm of torque, and the tightly packaged horizontal pancake motor outputs 127.5 Nm of torque. Because the end-effector exclusively manipulates the docking interface structure rather than bearing the tunnel's weight, these high torque outputs yield a calculated safety factor of 3 for the required alignment and latching forces. The objective was met.

Test 3: System Power Budget Verification (Hand Calculation)

Purpose: To verify that the idealized power architecture and all selected components will not exceed the habitat's maximum allowable power allocation.

Test Requirements

- RE-05: The system shall operate within a maximum power draw of 6,000 W.

Test Materials

- Power budget spreadsheet.
- Electrical datasheets for all selected motors, compute nodes, and sensors.

Test Procedure

1. Tabulate the maximum continuous power draw (Voltage x Current) of all components across the 48V (Elevation), 24V (Drive and Platform), 12V, and 5V buses.
2. Sum the values to find the theoretical maximum steady-state system power draw.
3. Compare the total sum against the 6,000 W requirement limit.

Test Results and Analysis The hand-calculated power budget yielded a steady-state continuous draw of exactly 2,434.4 W when all subsystems (Drive, Elevation, End-Positioning Platform, Compute, and Sensors) are fully powered. Even when accounting for theoretical DC-DC conversion inefficiencies and worst-case transient motor spikes, the calculated power draw remains well below the 6,000 W limit imposed by the habitat. Requirement RE-05 is successfully validated by analysis.

The system architecture defined and validated the electrical specifications required to deploy a tunnel autonomously between two surface habitats on Mars. Through trade studies, the system had a well-defined controls topology, consisting of a Jetson node, distributed amongst multiple STM32-based controllers. This is all alongside a centralized DC-DC power distribution supplying voltage rails to all hardware. Analytical validation confirmed that the chosen motors met mechanical and electrical requirements with safety factors of around 3, and the total idealized system power draw of 2,434.4 remains withing the habitat's limit of 6,000 W. The prototype provided confidence that the overall system architecture, inclusive of the drive, elevation, and end-positioning mechanisms, is well-suited to scale towards a more flight-ready system.

6.6 Ergonomic Testing

Test 1: Optimal Handrail Height

Purpose The purpose of this test was to determine the optimal handrail height based on participant feedback regarding the comfort level of its placement.

Test Objectives

- Determine optimal handrail height within a to-size prototype section based on participant feedback and collected data.
  - Obtain a comfort rating from participants based on the handrail placement (1-10; 1 is low, 10 is high).
- Observe walking speed(s), number of slips/stumbles, and torso flexion of participants in a simulated tunnel environment.

Test Materials

- 2x 10ft by 2in diameter PVC pipes.
- 2x ZenStyle 550 Lb Pair of Adjustable 40 In. - 66 In. Rack Sturdy Steel Squat Barbell Free Bench Press Stands Gym/Home.
- 1x roll masking tape.
- Zip ties.

Test Procedure The following test procedure was used to fulfill the test objectives:

1. Set up racks in 3 meter by 1 meter rectangle and attach the PVC pipes using zip ties.
    - Note that the handrails should be 1 meter apart, not the bases of the squat racks.
    - PVC pipes can be attached via zip tie due to holes drilled on their ends
2. Adjust handrail height by trial: 90 cm, 100 cm, 110 cm.
3. Have 20-30 participants run trials for 3 heights.
    (a) Collect participant height information.
    (b) Record video data, time the participant during each trial.
    (c) Instruct participants to actively use the handrails throughout their traversal of the simulated tunnel.
4. Issue post testing feedback forms for participants to fill out.
    - Forms include questions about comfortability of each trial (1-10 scale), if participants felt they had to bend over to access the handrail, their preferred handrail height, and any other feedback they may have had.

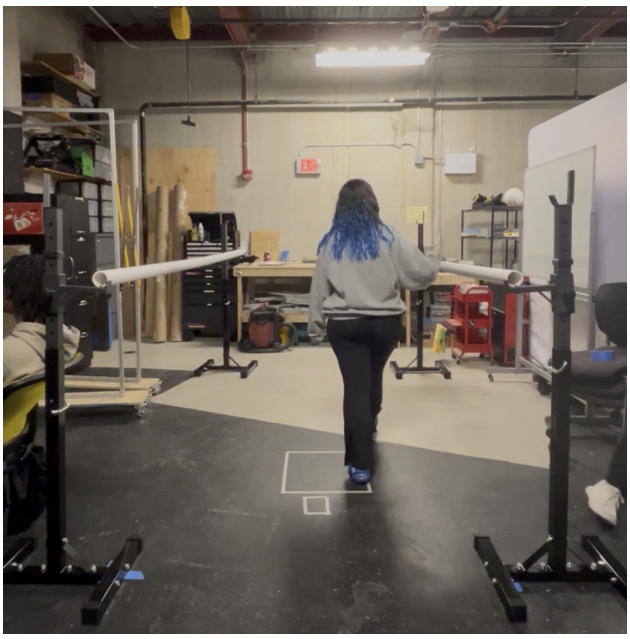

Figure 49: Participant Completing a Trial for the Optimal Handrail Height Test

Test Results and Analysis Overall, a majority of participants selected the 90 cm height as the most comfortable out of the 3 heights. The 110 cm height was only preferred by an individual in the tallest height group (180-189.9 cm). Results show there is a slight correlation between participant height and handrail height preference for the 100 cm and 110 cm height, but there is no correlation between participant height and the 90 cm handrail height. This suggests that the 90 cm handrail height was comfortable and preferred by a majority of participants, regardless of the participants height.

Figure 50 shows the data points for 90 cm, 100 cm, and 110 cm comfort ratings in comparison to participant heights along with trend lines. There was no correlation between preference for the 90 cm comfort rating and participant height. There were weak correlations between comfort ratings for the 100 cm height (R2 = 0.119) and 110 cm height (R2 = 0.184) in comparison to participant height.

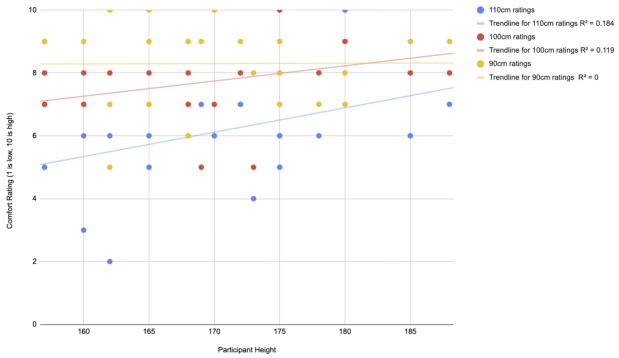

Figure 50: Correlations Between Handrail Height Comfort Ratings and Participant Height

Figure 51 displays the number of participants in height bins of 160-169.9 cm, 170-179.9 cm, and 180-189.9 cm that preferred 90 cm, 100 cm, or 110 cm handrails. The most preferred handrail height overall was the 90 cm rail, but there is a positive relationship between lower participant height and preference for lower handrail height. Middle height participants generally preferred the 100 cm rail, suggesting the average user may prefer this height. 110 cm is rarely preferred, and only by tall participants.

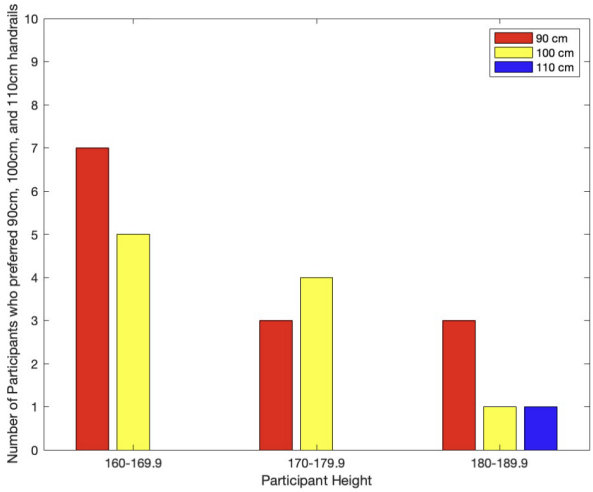

Figure 51: Preferred Handrail Height vs. Participant Height

Based on the results of this test being that 13 out of 24 participants (54%) prefer the 90 cm handrail, we recommend that this be the handrail height utilized in an idealized version of the tunnel. Participants report that this height felt the most natural, was accessible, minimized torso flexion, and was overall what they expected when they thought of a handrail. This aligns with current guidelines and our trade studies. Furthermore, NASA criteria indicate astronauts can be anywhere from a 1st percentile female to a 99th percentile male; these heights range from 148 cm to 192.7 cm [4]. Our testing population had heights ranging from 157 cm to 188 cm; this range of heights almost represents the entirety of NASA's indicated range, with the exception of lower percentile females, hence we believe our testing population well represents prospective astronauts overall.

Test 2: Fall Recovery

Purpose The purpose of this test is to help determine the optimal handrail height based on the ease with which participants are able to return to an upright position from kneeling. For safety reasons, this test was conducted instead of instructing participants to fall and attempt to catch themselves with the handrails.

Test Objectives

- Determine which handrail height is optimal based off of:
  - How quickly participants can recover to a standing position.
  - How comfortable/uncomfortable participants rank each handrail height while using the rail to return to standing position.
  - How participants rank their level of perceived exertion for each trial/height.

6	No exertion
7	Very, very light
8	
9	Very light
10	
11	Fairly light
12	
13	Somewhat hard
14	
15	Hard
16	
17	Very hard
18	
19	Very, very hard
20	Maximal exertion

Figure 52: The Ranking of Perceived Exertion Scale Employed During Testing

Test Materials

- 1x 2 in x 3 ft x 0.25 in thick aluminum pipe.
- 2x ZenStyle 550 Lb Pair of Adjustable 40 In. - 66 In. Rack Sturdy Steel Squat Barbell Free Bench Press Stands Gym/Home.
- 2x Hose Clamps.
- 2x 25kg weights.

Test Procedure The following test procedure was used to fulfill the test objectives:

1. Set up squat racks 3 ft apart, secure pipe to racks with hose clamps.
2. Adjust handrail height by trial: 80, 90, or 100 cm.
3. Have 20-30 participants run trials for each height.
    - Note: have each participant do each height twice.
4. Record the following data during each trial:
    (a) Time to return to standing.
    (b) Video

5. Issue post testing feedback form to record RPE and perceived comfort rating.

Figure 53: Participant executing the Fall Recovery Test

Test Results and Analysis Overall, data shows that there was not a significant difference in the average time to return to standing between different handrail heights, with the average time to return to standing for the 80 cm and 100 cm trials being around 1.60 seconds, and the average time to return to standing for the 90 cm trials being roughly 1.54 seconds. However, there were notable differences in comfort rankings and rankings of perceived exertion. Figure 54 shows a histogram of comfort rankings for the Fall Recovery Test. Data shows that 80 cm and 90 cm trials were consistently ranked as more comfortable than 100 cm. This suggests higher handrails reduce usability in fall recovery.

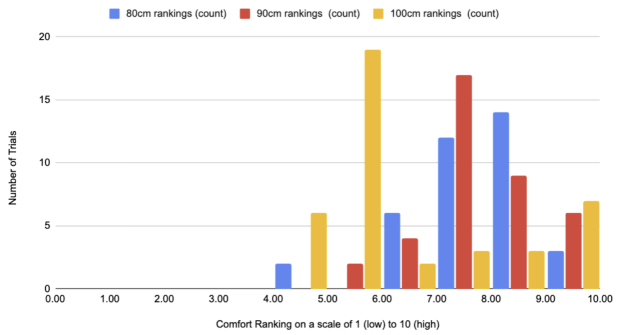

Figure 54: Fall Recovery Trials Comfort Rankings

Figure 55 shows that the average ranking of perceived exertion ranked higher as handrail heights increased: 8.475 for 80 cm, 9.2 for 90 cm, and 10.8 for 100 cm.

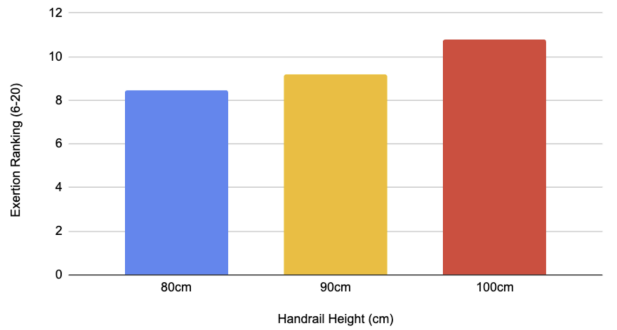

Figure 55: Handrail Height vs. Average Exertion

From our collected data, we had a decision to make between the 80 cm and 90 cm handrail heights; 90 cm had already been noted as most comfortable during Optimal Handrail Height Testing, but 80 cm performed similarly to the 90 cm height in Fall Recovery Testing. 100 cm was ruled out due to its high ranking of perceived exertion, low comfort rankings, and participant feedback including that their leverage was significantly reduced and their arms, elbows, and shoulders were put in uncomfortable positions. Ultimately, we determined that 90 cm would be most optimal for NASA's prospective astronauts. This is due to the fact that 80 cm is below waist height for even the 1st percentile female. Furthermore, in reduced gravity, astronauts' centers of gravity will be different from their centers of gravity on Earth; with this in mind, a higher handrail will better support the minimization of torso flexion and further instability.

Test 3: Inclination

Purpose The purpose of this test is to evaluate the usability, safety, and human interaction of users with the roll-out floor and handrails when used at various angles of inclination.

Test Requirements

- CT-08.02 : The tunnel shall accommodate relative angular difference of up to 15 degrees (pitch and yaw) between surface habitats.

Test Materials

- 2 x 10 ft by 2 in PVC pipes.
- 2x ZenStyle 550 Lb Pair of Adjustable 40 In. - 66 In. Rack Sturdy Steel Squat Barbell Free Bench Press Stands Gym/Home.
- Zip ties.
- 1.524 meter x 1 meter roll-out industrial floor.
- 1.524 meter x 1 meter plywood reinforced platform.
- Stacking items to prop up the ramp (i.e. wooden slabs).

Test Procedure The following test procedure was used to fulfill the test objectives:

1. Set up racks to encompass the roll-out floor.
2. Secure pvc pipes to the racks using zip ties.
3. Adjust height of the handrails to be 90 cm above the floor height throughout the entire distance of the flooring.
4. Have 20-30 participants complete the following:
   (a) Walk up and down the ramp at a normal pace at 7.5°and 15°.
5. During step 4, record the following data:
   (a) Traversal time.
   (b) Number of slips, stumbles, foot catches.
   (c) Handrail engagement.
   (d) Video.
6. After each trial survey the participants about:
   (a) Their perceived stability.
   (b) Their perceived exertion (RPE scale).

RATE OF PERCEIVED STABILITY		
Completely stable	Standing undisturbed on solid ground	1
Steady	Balance does not feel challenged, but may have some body movements	2
		3
Unsteady	Feels like work to keep balance, but still do not need to step OR reach	4
		5
Mildly Unbalanced	Feels like I might/could have to take a step OR reach for support to maintain balance	6
Moderately Unbalanced		7
Unbalanced	Feel that even the smallest or sudden movements will cause a fall	8
Very Unbalanced		9
About to Fall	Extremely challenged; have to step AND/OR grab support to keep balance	10

Figure 56: Rate of Perceived Stability Scale

Figure 57: Participant Executing the Inclination Verification Test

Test Results and Analysis Across all trials, no slips, trips, or stumbles occurred. In addition, the highest level of instability recorded was a level 3, which corresponds to a steady ranking. These data points suggest that the 7.5°and 15°levels of inclination do not pose a problem for the stability of participants and that the roll out floor does not impose a tripping hazard for participants . It is noted that there were slightly higher levels of instability on down trials than up trials. In addition, handrails were used in 53% of trials despite participants not explicitly being instructed to use them in every trial; rather, participants were instructed to use them if they felt more comfortable doing so. Because of this, it can be inferred that the handrails are accessible and effective. In conclusion, our test requirements were verified.

7 Risks and Mitigation

Risk management is a critical aspect of any project, particularly in endeavors as complex and multifaceted as ours. A comprehensive risk matrix has been developed to identify and assess potential hazards that could impact the success of our mission. Each risk item has been meticulously analyzed, considering its likelihood of occurrence and the severity of its consequences on a scale of 1-5. Through this process, we have identified various technical, schedule, cost, and safety-related risks that could impede our progress or compromise the functionality and safety of our system. Appendix B includes the missions and human risk matrices along with their respective fever charts for detailed documentation of risks. Fever charts are a visual representation of how application of mitigation strategies has a positive impact on the risks associated with the design.

One notable technical risk involves the possibility of the structure yielding while the astronauts are inside, leading to injury or death. Mitigation strategies have been proposed for each risk item to minimize their potential impact. For instance, in response to concerns about yield strength, additional floor beams were added to the design to support extra load. Finite element analysis was run on these extra beams, as well as the roll-out floor itself, indicating that they are strong enough to withstand up to three times the expected loads from two astronauts walking through the tunnel with cargo. Both distributed and shock load cases were tested in order to encapsulate the extra force from walking or dropped cargo.

Similarly, measures were taken to mitigate risks related to inaccurate berthing or docking outcomes that could render the system unusable. By implementing a multi-sensor fusion approach using LiDAR and computer vision, we are able to ensure that the system supports course and fine motion with cross-validation. Additionally, we have implemented a human-in-the-loop override that can be used by the astronauts or ground control throughout the docking sequence to confirm alignment and enable takeover in the event of a technical failure.

In addition to technical risks, human-level risks have also been identified and addressed in our risk management approach and evaluated on a logarithmic scale for their likelihoods of occurrences. These include risks such as user injury due to electrification on improperly housed electronics, harm caused by failed alerts, or abrasion on sharp surfaces. Mitigation strategies for these risks focus on providing proper training, instructions, and incorporating safety features to minimize the likelihood of accidents or injuries during manual tunnel operation.

Overall, our risk management strategy is aimed at proactively identifying and mitigating potential hazards to ensure the successful and safe execution of our mission. By implementing robust mitigation measures and continuously monitoring and reassessing risks throughout the project life cycle, we aim to minimize disruptions and maximize the effectiveness of our tunnel system in supporting crew transportation between surface assets during space missions.

8 Project Management

8.1 Work Breakdown Structure

The work breakdown structure (WBS) for the LATCH project is roughly illustrated in Figure 58.

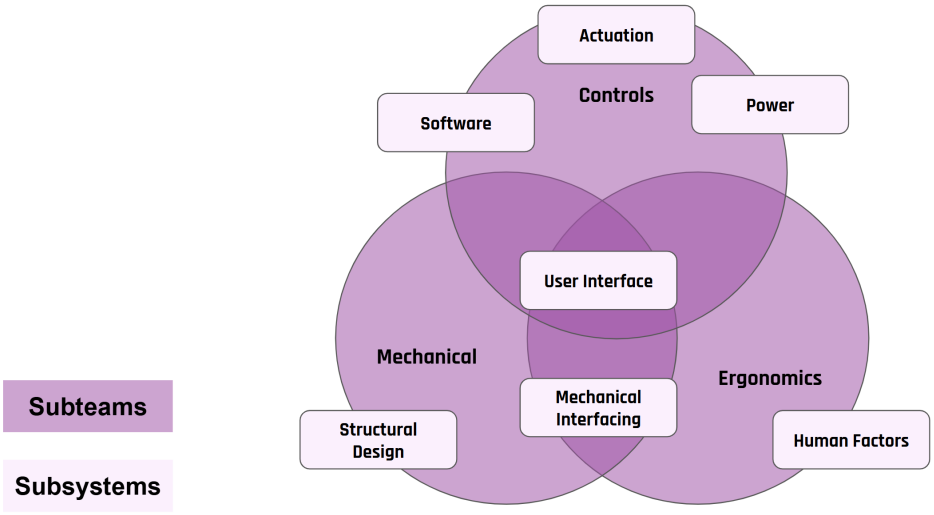

Figure 58: Work Breakdown Structure.

8.2 Project Schedule

With a complex project, such as this one, an important aspect that needs to be accounted for is the project schedule. The success of this project will be dependent on the ability of our team to stay on course with the project schedule that has been predetermined.

The key dates that our team ensured to abide by are listed below:

- **October 21, 2025:** System Definition Review
- **December 9, 2025:** Preliminary Design Review
- **February 20, 2026:** Critical Design Review
- **April 10, 2026:** Progress Checkpoint Review
- **May 7, 2026:** Project Completion and Evaluation

Our team designed a Gantt chart so that we could have the key milestones and dates depicted in an easy-to-view manner as shown in Figure 59.

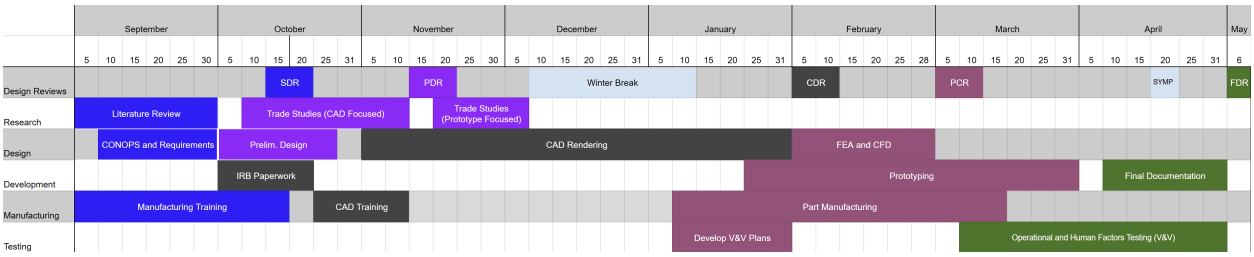

Figure 59: Year-Long Gantt Chart

To note, winter break was scheduled into the Gantt chart due to the majority of project team members being unable to meet in person and work on the project during that time.

8.3 Project Cost

The budget allocation for this project was $(removed). The budget breakdown is depicted in Figure 60.

Figure or Table containing sensitive information, or possible unauthorized copyright information has been removed.

Figure 60: Budget Allocation

Our final cost breakdown is shown in Figure 61.

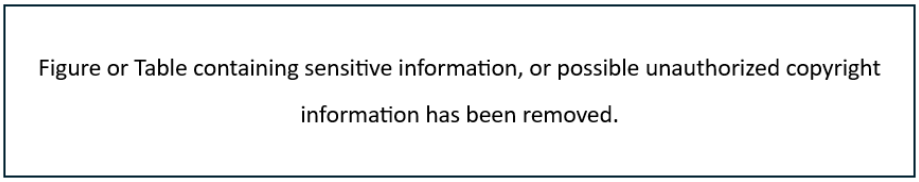

Figure 61: Project Costs

To note, our team decided to go with a 10% cost margin.

9 Suggestions For Future Exploration

9.1 Mechanical

With more time and resources, we would continue to build a fully integrated and functional prototype of the tunnel and expand all of our testing on the components and the full system to include shock testing, load testing, functionality testing, and environmental testing. If given more time, the design would be changed as needed to allow for it to be adapted more easily for different use cases. Additional work could focus on enabling modular tunnel sections capable of connecting surface elements separated by greater distances than our current tunnel accommodates for. This design was also made with the use case being on Mars, but ensuring that it could easily be adapted to a Lunar use case is important. Future work should evaluate how the design would need to change for lunar environmental and operational conditions. The following sections will outline future work for each subsystem in more detail.

9.1.1 Frame

Based on simulations, the rings have a very high factor of safety while experiencing the harshest loads, meaning that the rings could be optimized through reduced thickness and revised geometry. In other words, the rings can be more mass-efficient. Additionally, more materials could be compared to see which combination yields the best use of mass, strength, and cost for the mission. Some limited testing would be required, including load and fatigue tests to ensure the optimized design will last the lifetime of the mission. The frame may also be able to be created using 3D printing of martian (or lunar) regolith. This could significantly reduce the launch mass and volume that the rings consume.

9.1.2 Shell

While a similar softgoods shell has been developed and tested by NASA, more testing using our specific geometry and material selection would be necessary before the system can be flown. Some of these tests would include simulated pressurization cycles, tears, punctures, thermal strains, or other damages. It would also be helpful to test the shell in a simulated Martian environment to see how environmental conditions (i.e. temperature, dust storms, etc.) may affect the material properties.

9.1.3 Passive Extension

Based on the simulations and FEA run on the scissor mechanism, our design is able to withstand all expected loads. However, further simulations and FEA, such as load and fatigue simulations and testing, should be done in order to ensure the design is ready for flight. In the event that the scissor mechanisms are unable to support the load of the rings, adjusting the geometry of the links, so there is more mass towards the center, could mitigate this stress. Additionally, the number of scissor mechanisms on each side of the tunnel could potentially be doubled to further reduce stress. Finally, the material of the mechanism's joints and the shape of each link in the scissor could be adapted to distribute mass in a more favorable manner.

Changes should also be made to reduce the mass, protect against shearing of the tarp, and ensure reliability throughout the mission. Mass reduction will mainly stem from geometry changes. Loads perpendicular to the plane the scissor mechanisms are extending in can be

minimized with a "rib cage" that prevents the tarp, which surrounds the scissor mechanism and bears loads from the environment, from interacting or touching the scissor mechanism.

Bearings and seals may also be introduced into the scissor mechanism with the purpose of reducing friction and mitigating the entry of dust into the joints.

9.1.4 Handrail

Based on testing, the handrails could be improved upon in multiple ways. Notably, the addition of more segments should be explored to minimize the compressed length of the handrails, possibly allowing the extension ratio of the entire tunnel to improve. Having smaller segments to extend might also decrease the chances of tubes getting caught in each other, which could impede the extension of the entire tunnel. However, having fewer segments will decrease the number of joints, parts, and entry points for dust. This tradeoff should be considered when finalizing the design of the handrails.

Although we were able to model the effects of sudden impacts on the handrail, it would be beneficial to assess the extension and retraction of the handrails more comprehensively, including testing with rotational forces.

9.1.5 Active Extension

A flight-ready system would require additional tests to be run on the capabilities of the active extension system, especially with a full prototype as opposed to a separated bottom half. The treads we selected are capable of traversing over small obstacles, but we weren't able to test if they can drive the extension of the system, which certainly needs to be tested before the system could be implemented. This full prototype would also be ideal for testing the traversal ability of the treads. Testing or simulating the impact of Martian winds on the system is an important next step to ensure that the tunnel can withstand the frequent winds experienced on the planet.

Future work should refine drivetrain force, traction, and power modeling using higher-fidelity simulations and full-scale testing. More simulations should be run to have a better idea of the number of cycles the wheels can withstand before any potential fatigue failures.

9.1.6 End Positioning

If given more time and resources, this system could be further designed to optimize the use of resources and minimize weight. As it stands, the bearing and motor system is heavy, and the pitch angle control we designed for the prototype is not nearly as strong as the actual system would need. More in-depth calculations and design planning can be performed to ensure the platform can withstand the forces of dropped cargo and walking, connect to all possible docking hatches, and not become jammed by dust.

The testing could also be greatly improved, as the system was not made as one complete prototype but instead as part of a separate bottom half. A full model could be built with a target for the end mechanism to attempt to attach onto. We also were unable to load test the end mechanism, as we did not have the time nor resources.

9.1.7 Elevation Change

If given more time and resources, this system would be scaled up from the bottom-half prototype to a full flight-ready model to verify its actual load-bearing and force producing capabilities. Future design work would focus on optimizing the square extrusion dimensions to minimize weight while ensuring tight tolerances to prevent any friction-induced binding. This becomes especially complicated with thermal expansion being introduced, as accounting for the changing diameters is highly difficult.

Testing would need to be expanded significantly to include structural load and fatigue testing on the fine-pitch lead screws over its expected operational cycles. Crucially, the recommended 24 Volt electromagnetic power-off brake must undergo rigorous physical testing. This is necessary to confirm its holding capacity, ensure it completely prevents back-driving under full structural loads, and verify its electrical reliability during emergency power losses in extreme Martian temperatures.

9.1.8 Suspension

The suspension system was not prototyped or tested and so no empirical claim can be made that the design works as intended. Significant additional development would be required to bring this system to becoming flight-ready. Starting with design refinement which includes complete detailed component sizing, arm geometry, spring rate, bushing and rod-end selection, and material selection. Kinematic analysis to confirm camber, toe, and tread-footprint behavior through the full travel range should be performed. Additionally, the torsion spring geometry should be refined to achieve target angular travel and fatigue life.

Along with this, more modeling and analysis should be performed, including FEA on all load-bearing components under expected static, dynamic, and shock loads. Multibody dynamic simulations of the full tunnel traversing representative Mars terrain can be used to characterize loads and articulation demands. Thermal analysis across the Mars surface temperature range, including effects on spring rate and bushing behavior should be performed.

Full-system testing on a prototype system should target obstacle traversal, incline traversal, height adjustment under load, and endurance cycling. Finally, dust tolerance and seal design for all bearings, bushings, and pivot points should be incorporated, as well as general vibration and shock qualification and redundancy analysis and implementation for single-point failures.

9.1.9 Walkway

Since simulations revealed a very large factor of safety, it is possible that the walkway design could be optimized to be more mass-efficient. Specifically, the thickness of each segment within the walkway could be decreased, or the shape of each segment could reflect that of an I-Beam. Joint and rail geometry would need to be defined for a flight model, and lubrication, as well as dust mitigation, would need to be analyzed more in-depth. The rolling mechanism of the floor would need to be greatly optimized to allow the floor to take as little volume as possible. The walkway would also need to undergo significant testing to ensure it can withstand numerous loading conditions as well as fatigue under the conditions expected in the Martian environment. Additional materials could be analyzed to compare material properties, strengths, and costs, and surface coatings could be chosen to make the surface non-slip.

9.2 Controls

9.2.1 High Level Controls

To transition from the current prototype to a flight-ready High Level Controls subsystem, the following development and qualification work would be required:

- **Hardware integration:** Integrate the HLC software with flight-representative cameras, IMUs, wheel encoders, LiDAR hardware if retained, embedded motor controllers, and the complete CAN communication architecture
- **Localization validation:** Calibrate cameras and AprilTags, characterize sensor noise and tag visibility limits, tune EKF covariances using measured data, and measure pose-estimation accuracy during full alignment and docking motion
- **Autonomy and fault handling:** Expand fault monitoring to include sensor dropout, CAN communication loss, actuator non-response, unexpected obstacles, and localization uncertainty. Verify safe stop, manual override, and recovery behavior for each fault case
- **Hardware-in-the-loop and full-scale testing:** Run the state machine and navigation software against embedded controllers and actuators, followed by tests on a full-scale mechanical system with representative terrain, habitat interfaces, and docking tolerances
- **Flight qualification:** Port the HLC design to radiation-tolerant compute and sensors, verify thermal and power behavior, perform electromagnetic compatibility and communication-reliability testing, and establish redundancy and crew-operable contingency procedures for long-duration surface operation

9.2.2 Controls System Architecture

If given unlimited time, funding, and resources, getting this system to be flight-ready would require work across a few different areas. First, all components would need to be replaced with flight-qualified substitutes. This includes parts that can withstand environmental testing such as thermal vacuum chamber (TVAC) testing throughout a full lifecycle (60 deployments). Custom PCBs replacing the STM32 Nucleo boards and motor drivers would be essential for packaging reasons, as multiple development boards carry significant overhead in size and mass that is unnecessary and unacceptable for a flight system. These custom boards would integrate essential and dedicated circuitry protection. This includes overcurrent, overvoltage, and reverse polarity protection, automatic emergency stops, power sequencing, and thermal monitoring.

The CAN bus communication protocol would likely be replaced by SpaceWire, given its heritage in space applications and its ability to handle higher data rates with predictable latency over different cable lengths. Electromagnetic Interference (EMI) mitigation could be done through Faraday cages, such as lining components in a metal mesh like copper, ensuring that component functions are not disrupted. Electronic heaters would also need to be incorporated to maintain component operating temperatures on Mars. Taken together, these steps would bring the entire system from a functional prototype on Earth to qualified, flight-ready architecture.

9.3 Ergonomics

9.3.1 User Interface

With infinite funding and resources, the UI would be transitioned off a 2D screen entirely, whether through a heads-up display (HUD) or a haptic feedback glove interface, to enable true hands-free operation. Testing would also be conducted in high-vibration environments and under simulated background noise to ensure alerts remain salient in high-stress situations. On the logging side, more robust error tracking would be implemented to capture every individual mis-click occurring during flight qualification. Additional improvements already under consideration include a larger hit radius for the small arrows, a digital scroll wheel for habitat contact selection, and a safety confirmation pop-up upon exiting manual override mode. It is also recommended that the art style and display placement of the UI be integrated with whichever habitat(s) it will be interfacing with.

9.3.2 Physical Interfaces

To advance this system toward flight qualification, we recommend the following design opportunities be approached: create a full-scale ergonomic prototype, identify proper lighting placements, and incorporate an active alert system in conjunction with the UI. From there, we suggest that our previously conducted ergonomic testing be validated on the full-scale prototype. Furthermore, we recommend long-term usability testing be conducted, cargo transportation verification, stability testing of the roll-out floor using IVA suit boots, and verification of the telescoping handrail mechanism. Finally, a complete system assessment in Martian gravity should be conducted.

10 Acknowledgments

This project would not have been possible without the hard work of the members of the LATCH team listed here:

- Project Leads: Max Swartz, Lowen Walter
- Mechanical
  - Subteam Lead: Elisabeth Bassin
  - Angel Saul Andrade
  - Avanti Ganesan
  - Manan Gupta
  - Lucas Hamlin
  - Kalista Kollmansberger
  - Elizabeth Kooistra
  - Nicholas Lopez
  - Olivia Miller
  - Aasha Patel
  - Reid Schmaltz
  - Darren Sheinberg
  - Ronja Stargala
  - Nguyen Tran
  - Lukas Zahuranic
- Controls
  - Subteam Lead: Nicholas DaSilva
  - Alice Chen
  - Adrian Corrales
  - Joban Guron
  - David Jackson Jr.
  - Amanda Juvera
  - Vanya Krishna
  - Katherine Snowdon
  - Joshua Walker
- Ergonomics
  - Subteam Lead: Morgan Taege
  - Nava Abedinpour
  - Nicholas Demopoulos
  - Zachary Gammo

– Teagan Hollman
– Sophia Kersh
– Oleg Korobkov
– Kaycee Rasch

We would like to thank our industry sponsor, Dr. Tracie Prater, at NASA Marshall Space Center for her encouragement and invaluable feedback throughout this project. Dr. Prater, as well as other subject-matter experts at NASA Marshall, have played a pivotal role in empowering and supporting our project. We would also like to thank the X-Hab Program Office and the National Space Grant Foundation for providing the opportunity for the team to carry out this project.

We would also like to acknowledge our subject-matter experts from the University of Michigan, Drs. Leia Stirling, Jon Van Noord, and Evgueni Filipov, for connecting us with resources across the university to further advance our project. We would also like to thank Dr. Emily Matula at the Johnson Space Center for sharing her knowledge of EVAs and ISS operations, as well as BLiSS alums Ollie Paulus, Chad Cerruti, Christopher May, Ilyana Smith, Jakob Swilley, Tobi Farbstein, and Preston Withun for their guidance and mentorship throughout the project for both general members and project leadership. As our advisors, their help was instrumental in developing the design as it has been presented in this report.

Finally, we would like to thank Professor Nilton Rennó, Professor Steve Battel, Emily Bailey, Laura Hopkins, Stephanie Echavarria, Yvonna Olds, and the custodial staff at the Climate and Space Research Building for their help in managing the logistics of the project.

References

[1] *Moon to Mars eXploration Systems and Habitation (M2M X-Hab) Academic Innovation Challenge – FY25 Solicitation*. 2024. URL: https://spacegrant.org/wp-content/uploads/2025/03/M2M-X-Hab-Challenge-Solicitation-2026.pdf.

[2] Michelle A. Rucker et al. "Mars Surface Tunnel Element Concept". In: National Aeronautics and Space Administration, 2016. URL: https://ntrs.nasa.gov/api/citations/20160001028/downloads/20160001028.pdf.

[3] "Robot Tracked Tank Car Chassis, Shock Absorbing Robot Chassis Full-Metal Robotic Moving Platform Track for Raspberry Pi Arduino Jetson Microb DIY Maker Smart Car Learning Kit". In: Amazon, 2026. URL: https://www.amazon.com/YonPhsy-Absorbing-Full-Metal-Platform-RaspberryPi/dp/B0DRCS7RTF?ref_=ast_sto_dp&th=1.

[4] ARMY NATICK SOLDIER RESEARCH DEVELOPMENT and ENGINEERING CENTER MA. "2012 anthropometric survey of U.S. Army Personnel: Methods and summary statistics." In: National Aeronautics and Space Administration, 2014. URL: https://www.nasa.gov/organizations/ochmo/human-integration-design-handbook/.

APPENDICES

A Requirements

A.1 Level 1 Requirements

System Requirements - Level 1		
Requirement ID	**Description**	**Derived From**
Crew Transportation		
CT-01	The system shall provide graphical user interfaces.	R1
CT-02	The system shall provide crew interface devices to facilitate crew translation.	R1
CT-03	The system shall withstand variable forces acting on it.	R1
CT-04	The system shall remain aligned to the connecting habitat while crew members traverse to the next habitat.	R1
CT-05	The system shall have a minimum internal width of 0.61 meters.	R1
CT-06	The system shall have a minimum internal height of 2.01 meters.	R1
CT-07	The system shall be extendable and retractable along at least 1 axis.	R1
CT-08	The system shall provide a means of aligning with the connecting surface element.	R1
CT-09	The system shall maintain functionality at a variety of deployment lengths.	R1
CT-10	The system shall provide docking functionalities between surface elements.	R1
CT-11	The tunnel shall each have at least 3 degrees of freedom.	R1
Environmental Control		
EC-01	The system shall withstand temperature ranges from -70°C to 20°C.	R2
EC-02	The system shall thermally regulate its internal environment.	R2
EC-03	The system shall have a base noise level of at most 60 dB.	R2
EC-04	The system shall mitigate the entry of dust into the environment.	R2
EC-05	The system shall mitigate the entry of radiation into the tunnel.	R2
EC-06	The system shall allow for travel across rough martian terrain.	R2
EC-07	The system shall mitigate the loss of pressure with the environment.	R2
Operational Capability		
OC-01	The system shall provide base functionality for a minimum of 30 sols.	R3
OC-02	The system shall withstand a minimum of 60 pressurization cycles on its outermost layer.	R3
Resource Efficiency		
RE-01	The system shall have a mass less than 230 kg.	R4
RE-02	The system shall extend within 30 minutes.	R4

RE-03	The system shall have an extension ratio of at least 1:2.	R4
RE-04	The system shall be deployable by one crew member.	R4
RE-05	The system shall operate at a power level of at most 6000 Watts.	R4
RE-06	The system shall allow crew to manipulate the docking process.	R4

A.2 Level 2 Requirements

System Requirements - Level 2		
Requirement ID	**Description**	**Derived From**
Crew Transportation		
CT-01.01	The graphical user interface shall allow for crew members to initiate deployment of the tunnel.	CT-01
CT-01.02	The graphical user interface shall aid with emergency communication between crew members.	CT-01
CT-01.03	The graphical user interface shall be operable with one hand by a crew member wearing an IVA suit.	CT-01
CT-01.04	The graphical user interface shall be accessible from either end.	CT-01
CT-01.05	The graphical user interface shall display the internal conditions within the tunnel.	CT-01
CT-01.06	The graphical user interface shall allow a crew member to manually override the tunnel controls.	CT-01
CT-02.01	The tunnel shall have mobility assistance surfaces that aid in walking.	CT-02
CT-02.02	The tunnel shall have exterior lighting.	CT-02
CT-02.03	The tunnel shall have interior lighting.	CT-02
CT-02.04	The crew interface shall have an emergency system that can be triggered from both sides of the walkway.	CT-02
CT-02.05	The mobility assistance surfaces shall be free of sharp or jagged surfaces which could harm the user or their equipment.	CT-02
CT-02.06	The mobility assistance surfaces shall be able to bear a minimum of 370 N of force in any direction.	CT-02
CT-02.07	The walkway shall have a nonslip surface.	CT-02
CT-02.08	The tunnel shall have a means of distributing power to its components.	CT-02
CT-03.01	The tunnel shall withstand winds of up to 4.17 m/s.	CT-03
CT-03.02	The tunnel shall be able to support a load of 2000 N from two people walking at a speed between 1.11 m/s and 1.39 m/s.	CT-03
CT-03.03	The tunnel shall be able to withstand a maximum of 530 N, dropped from a maximum height of 1 meter.	CT-03
CT-07.01	The tunnel shall have a self contained electrical system.	CT-07

CT-07.02	The tunnel shall be extendable to a minimum of 1.524 meters (5 feet).	CT-07
CT-07.03	The tunnel shall measure its extension length and location.	CT-07
CT-08.01	The tunnel shall accommodate a relative elevation difference of at least 0.4 meters between surface habitats.	CT-08
CT-08.02	The tunnel shall accommodate relative angular difference of up to 15 degrees (pitch and yaw) between surface habitats.	CT-08
CT-08.03	The sensors shall measure the relative X, Y, and Z location of its connecting surface elements.	CT-08
CT-08.04	The tunnel alignment method shall be autonomous.	CT-08
CT-08.05	The tunnel shall have an override for a teleoperated alignment method.	CT-08
CT-08.06	The user interface device shall communicate if it experiences errors when connecting to a surface element.	CT-08
CT-09.01	The tunnel shall be able to support 2000 N of force at various lengths once deployed.	CT-09
CT-10.01	The tunnel shall be able to sense the docking state on either side of the tunnel.	CT-10
Environmental Control		
EC-02.01	The tunnel shall maintain an inner temp between 18.5°C and 25°C.	EC-02
EC-04.01	The tunnel shall contain a physical barrier that mitigates entry of dust into the tunnel during extension.	EC-04
EC-05.01	The tunnel exterior shall limit radiation exposure to crewmembers to below 50 mSv per year.	EC-05

Operational Capability		
OC-01.01	The tunnel's actuation mechanisms shall withstand at least 60 extensions.	OC-01
OC-01.02	The tunnel's actuation mechanisms shall withstand at least 60 retractions.	OC-01
Resource Efficiency		
RE-05.01	The power system shall have a minimum capacity of 4.5 Kilowatt hours.	RE-05
RE-05.02	The power system shall convert the habitat's voltage of 120 V to power components of lesser voltage.	RE-05

B Risk

B.1 Risk Matrices

		Fever Chart - After Mitigation				
Estimated Likelihood	80%-100%					
	60%-80%					
	40%-60%		2			
	20%-40%	10, 11	9	12		
	0%-20%	18	16	8, 14, 20, 25, 27	7, 13	5, 6
		Negligible	Minor	Moderate	Critical	Catastrophic

Figure 62: System Risk Matrix Before Mitigation

		Fever Chart - After Mitigation				
Estimated Likelihood	80%-100%					
	60%-80%					
	40%-60%		2			
	20%-40%	10, 11	9	12		
	0%-20%	18	16	8, 14, 20, 25, 27	7, 13	5, 6
		Negligible	Minor	Moderate	Critical	Catastrophic

Figure 63: System Risk Matrix After Mitigation

		Fever Chart - After Mitigation				
Estimated Likelihood	80%-100%					
	60%-80%					
	40%-60%		2			
	20%-40%	10, 11	9	12		
	0%-20%	18	16	8, 14, 20, 25, 27	7, 13	5, 6
		Negligible	Minor	Moderate	Critical	Catastrophic

Figure 64: Human Risk Matrix Before Mitigation

		Fever Chart - After Mitigation				
	80%-100%					
	60%-80%					
	40%-60%		2			
Estimated	20%-40%	10, 11	9	12		
Likelihood	0%-20%	18	16	8, 14, 20, 25, 27	7, 13	5, 6
		Negligible	Minor	Moderate	Critical	Catastrophic

Figure 65: Human Risk Matrix After Mitigation

B.2 Risks

Risk ID	Subsystem Risk ID	Risk Description	Human or System Risk?	Consequence	Likelihood	Risk Score	Justification	Mitigation Strategy	Consequence after Mitigation	Likelihood after Mitigation	Risk Score after Mitigation
1		If there is exposed wiring, then the crew could be harmed.	Human	5	2	10	Exposed wiring can shock, burn, or electrocute crew. This is unlikely to occur as proper wiring will occur when the control system is integrated, and safety testing will be conducted.	Implement industrial-grade wire looms and cable management, conduct continuity and insulation resistance testing before deployment, and use keyed connectors to prevent improper mating.	4	1	4
2		If the task scheduling system fails, then the tunnel may not dock or berth properly.	System	3	3	9	If one task occurs before / after necessary, then the tunnel could function inaccurately.	Implement a watchdog timer and redundant software fail-safes that trigger a "Safe Mode" dock if timing signals deviate beyond a specific millisecond threshold.	2	3	6
3		If there is a high voltage discharge, then the crew could be harmed.	Human	5	2	10	High voltage can lead to serious burns but it's unlikely to occur since our components will have shut-offs and proper insulation to prevent the wires from discharging it into the area where humans will operate	Enclose all high-voltage components in grounded Faraday cages, utilize automatic interlock switches that cut power when access panels are opened, and apply thick conformal coating to sensitive junctions.	4	1	4
4		If there is overamperage, then crew can be harmed.	Human	5	2	10	Overamperage can lead to overheating and a fire, causing burns or even death for crew. This is unlikely to occur as amperage will be monitored.	Install fast-acting digital circuit breakers and physical fuses rated at 125% of peak load, paired with real-time software alerts that throttle power if thermal thresholds are approached.	3	1	3
5		If the pressure seal fails then the system could be harmed.	System	5	3	15	We do not want foreign contents entering the system, nor do we want the contents of our system leaving the system.	We will create the sheath out of specific materials with high puncture resistance, which will reduce the likelihood.	5	1	5
6		If the tunnel experiences significant mass loads, the structure could yield.	System	5	1	5	It is unlikely the tunnel is overloaded by a mass load, but if the users do happen to introduce too much mass to the tunnel the structure could be at risk.	Monitor the loads being transported through the tunnel to ensure they do not exceed the 2000N of force requirement. Add extra floor supports to increase maximum supportable load.	5	1	5

Risk ID	Subsystem Risk ID	Risk Description	Human or System Risk?	Consequence	Likelihood	Risk Score	Justification	Mitigation Strategy	Consequence after Mitigation	Likelihood after Mitigation	Risk Score after Mitigation
7		If the tunnel experiences extreme weather conditions, the structure could yield.	System	5	1	5	The winds in strong martian storms tend to reach about less than half the speed of hurricanes on Earth, so dust storms might not be too concerning to the structural integrity. https://www.nasa.gov/solar-system/the-fact-and-fiction-of-martian-dust-storms/	We will select tunnel materials that are able to withstand the forces and strain from weather. Designing to be easily repaired can help mitigate consequence as well. This will reduce the consequence of extreme weather.	4	1	4
8		If the vertical actuation component fails, the tunnel cannot reach surface elements at varying elevations (critical requirement).	System	5	2	10	It is unlikely for the vertical actuation components to fail, but if this failure occurs the tunnel fails to meet a basic requirement for the mission, as well as most likely breaking.	We will incorporate redundant vertical actuation components and ensure the overall mechanism can be repaired/replaced, which will reduce the consequence and likelihood of the vertical actuation component failing	3	1	3
9		If foreign objects get caught in between rings/bubbles, the system may not extend/retract properly.	System	2	3	6	This could impede the extenstion/retraction mechanism of the tunnel. However, the object would likely be detected when deploying or bringing in the tunnel so there would likely not be a high risk of human injury, or large amounts of damage to the system.	We will implement a sensor that detects the addition of any objects between extension mechanisms/hinge points, which will reduce the impact of objects getting stuck	2	2	4
10		If the outer sheathe punctures then the pressure drop could lead to the system being harmed.	System	2	3	6	Sudden pressure drop, material rupture, dust accumulation inside the tunnel	Instead of using inflatable material for the cavas of our tunnel, we could prefer using thin metal sheet, just like the fuselage of an airplane. This would help in maintaining and stabilizing required pressure, as well as reducing the risk of potential hazards, mentioned in the justification.	1	2	2

Risk ID	Subsystem Risk ID	Risk Description	Human or System Risk?	Consequence	Likelihood	Risk Score	Justification	Mitigation Strategy	Consequence after Mitigation	Likelihood after Mitigation	Risk Score after Mitigation
11		If surface objects block the movement of the wheels, then the system could be prevented from moving.	System	2	3	6	With all of the rocks/debris on the surface of Mars, coupled with the powerful winds, it is likely there will be impediments to the movement of the wheels, whether they are passive or active.	There could be a sensor implemented for if the progress of the wheel ever stops that shuts the system down, allowing adjustment. The wheels could also be improved for better manueverability around obstacles.	1	2	2
12		If the perception system gives a false positive, the tunnel will inaccurately berth or dock.	System	3	3	9	Sensor noise, unexpected debris, or glare from the Martian sun could trick the computer vision or LiDAR into identifying a dock that isn't there.	Implement a multi-sensor fusion approach (LiDAR + Computer Vision) with cross-validation. A human-in-the-loop override should be required for the final 5 meters of the docking sequence to confirm alignment.	3	2	6
13		If a solar event bombards Mars with extreme levels of radiation then electronics can be harmed.	System	5	1	5	Solar events are more prevelant during solar maximum but low lilkelihood an severe event like CME occurss	We will expect Houston to track and warn crew members about solar events.	4	1	4
14		If there is exposed wiring, connections could become cut and the control system could stop functioning.	System	5	2	10	High likelihood due to the abrasive nature of Martian dust (regolith) and the physical wear and tear caused by the expansion/contraction of the tunnel.	All critical wiring should be routed through protective conduit or armored sheathing. Use redundant cable paths so that if one connection is severed, the control system maintains a secondary communication link.	3	1	3
15		If the floor is uneven, then crew could fall.	Human	3	2	6	If things shift around while the tunnel is being collapsed or expanded, then the floor could became uneven.	The floor will be constructed with precision to ensure that it is level. Handrails also reduce the risk of the crew falling.	2	1	2

Risk ID	Subsystem Risk ID	Risk Description	Human or System Risk?	Consequence	Likelihood	Risk Score	Justification	Mitigation Strategy	Consequence after Mitigation	Likelihood after Mitigation	Risk Score after Mitigation
16		If the tunnel fails to deploy, then astronauts cannot use the tunnel.	System	5	1	5	There is low to no risk to the human in this situation, as astronauts will not be traversing the tunnel when it is extending. However, the system could become damaged if it tries to deploy, and becomes jammed by debris or the enviornment in some way. If it is a controls error, it is likely fixable. If the system were to fail to deploy, that would mean a complete system failure making it a high consequence	Closely monitor tunnel deployment status during operation.	2	1	2
17		If the emergency alert system fails to trigger, then the crew will not be made aware of critical failures.	Human	5	1	5	Being unaware of potential health hazards or mission catastrophes while in the tunnel, could lead to injury, or death.	Emergency alert systems can be decentralized, so if one part fails the rest will trigger successfully. (ie. if the emergency lights fail to turn on, the PA system will still go off).	2	1	2
18		If the power goes out, then the alarm system will go offline.	System	3	1	3	There is a decent risk that, with the power going out, there will be no power supply for the alarm system within the tunnel.	Alarm systems can have their own reserve power source that will last before the issue with the main power source is resolved	1	1	1
19		If the lights inside the tunnel go out, then the crew could fall.	Human	3	2	6	There is a risk that the crew could fall if the light in the tunnel isn't working. Also, since the crew can't see, they could ruin other parts of the tunnel.	Implement emergency lights; they are NSTD mandated.	1	1	1
20		If a dense object is dropped in the tunnel, then it may damage the system.	System	3	3	9	Tools like hammers may be transported through the tunnel which if dropped or swung could dent handrails, or pierce the sheath. Heavy objects could also fall on the tunnel, puncturing the sheath and depressurizing the system.	Dense objects should be carried in bins or wagons to increase surface area upon drop impact so as to spread force over a greater area.	3	1	3
21		If a dense object is dropped in the tunnel, then it may damage the crew.	Human	5	4	20	Tools like hammers may be transported through the tunnel which if dropped or swung could dent handrails, or pierce the sheath. Heavy objects could also fall on the tunnel, puncturing the sheath and killing the crew.	Dense objects should be carried in bins or wagons to increase surface area upon drop impact so as to spread force over a greater area.	3	2	6
22		If the handrail fails to bear the force exerted upon it by the astronaut, then the astronaut could injure themself.	Human	2	1	2	It is extremely unlikely that the handrail will fail to bear 370N (see hand calc in handrail material trade study), and the astronaut would likely be only minorly injured.	Monitor handrail condition to ensure they are not damaged. Maintain the handrails by keeping them lubricated during use.	2	1	2

Risk ID	Subsystem Risk ID	Risk Description	Human or System Risk?	Consequence	Likelihood	Risk Score	Justification	Mitigation Strategy	Consequence after Mitigation	Likelihood after Mitigation	Risk Score after Mitigation
23		If the alerts of the alarm system are not salient, then important alerts could go unnoticed by the crew.	Human	5	1	5	If there is an extreme threat (ie. bad weather, fire, solar storm) and the astronauts in the tunnel are not notified or fail to see a notification, then the astronauts in the tunnel could die.	Make alerts salient; red in color, flashing lights, loud siren alerts, voice over alerts, etc.	2	1	2
24		If the walkway fails to bear the weight of the crew and cargo, then the crew could be harmed.	Human	5	1	5	It is extremely unlikely that the walkway will fail to bear 2000N based on the material it is made of, unless it is being used for loads it is not rated for. If this were the case, then the mission would fail and the astronauts would die due to the tunnel collapsing.	Monitor the loads being transported through the tunnel to ensure they do not exceed the 2000N of force requirement. Add extra floor supports to increase maximum supportable load.	5	1	5
25		If the handrail fails to bear the force exerted upon it by the astronaut, then the astronaut could puncture the tunnel sheath.	System	3	1	3	The system would fail if it were punctured during use, but this is a recoverable failure since the sheath can be patched.	Improve handrail design and use stronger materials to increase maximum load of handrails. Use stronger materials for tunnel sheath to prevent puncture.	3	1	3
26		If the pressure seal fails during traversal then the crew could asphyxiate.	Human	5	3	15	The crew will suffocate (and/or possibly implode) if the pressure seal fails, as they will not be wearing the appropriate suits.	Monitor sheath status and perform regular checks for weak spots in the sheath.	5	1	5
27		If the telescoping handrail jams during extension or retraction, then the handrail may not fully deploy and prevent proper tunnel operation.	System	3	2	6	Most likely wouldn't stop the system from fully deploying, would be something that could be fixed. Jamming is a possibility for any telescoping system, but isn't always common.	Place a linear ball bearings between the telescoping rods and keep the rods properly lubricated.	3	1	3